

Simulating South African Climate with a Super parameterized Community Atmosphere Model (SP-CAM)

Dissertation submitted in fulfillment of the requirement for the degree of Master of
Environmental Sciences

Department of Geography and Geo-Information Sciences

School of Environmental Sciences

University of Venda

Candidate: Nohlahla Dlamini
(11632101)

Supervisor: Dr H Chikoore

Co supervisor: Dr M.M Bopape (SAWS)

Co supervisor: Dr N.S Nethengwe

August 2019

Declaration

I Nohlahla Dlamini hereby declare, that this research dissertation submitted for the Masters of Environmental Sciences in the Department of Geography and Geo Information Sciences at the University of Venda is my own work and has not been previously submitted for any degree at this university or any other university; and that all sources that I have used or cited have been shown and acknowledge by means of complete references.

SIGNATURE

.....

DATE

.....

Acknowledgements

I would like to extend my gratitude to the Almighty God who gave me the strength to work on this research project.

I would also like to thank my Supervisors, Dr. H. Chikoore and Dr. N.S Nethengwe from the University of Venda and Dr. M.M. Bopape from the South African Weather Service (SAWS) for their major assistance, patience, encouragement and willingness to help throughout the period of the research project.

I would like to express my appreciation to the University of Venda and National Research Foundation (NRF) Research and Innovation for supporting this study through funding. A special Thanks to the SAWS for providing rainfall and temperature datasets used in the study and allowing us to use their environment in learning software (e.g GrADS and Fortran) used for analysis and visualization in the study.

Dynamic and thermodynamic fields used in the study were obtained from the National Centers for Environmental prediction (NCEP) NCEP reanalysis II. CAM and SPCAM datasets were obtained from Colorado State University (CSU) through the help of Dr Mark Branson. Model results are compared against several observation datasets. For precipitation the study used GPCP and SAWS rainfall data.

My appreciation also goes to Dr. Nkanyiso Mbatha from the University of Zululand for assisting with timeseries analysis, Mrs P Mulovhedzi from SAWS, Mr Offoro Kimambo for helping with GrADS. I would also like to appreciate Dr T.K Takalani and Dr George. P Nghonyama from Univen Innovative Growth company (UIGC) for their encouragement. My colleagues from the Department of Geography and Geo Information sciences, school of Environmental sciences are also appreciated. Mr Prince.N Njoku from the department of Ecology and Resource Management is also Acknowledge.



Dedication

This dissertation is dedicated to my entire family for encouraging, believing and supporting me throughout my study years.

Abstract

The process of cloud formation and distribution in the atmospheric circulation system is very important yet not easy to comprehend and forecast. Clouds affect the climate system by controlling the amount of solar radiation, precipitation and other climatic variables. Parameterised induced General Circulation Model (GCMs) are unable to represent clouds and aerosol particles explicitly and their influence on the climate and are thought to be responsible for most of the uncertainty in climate predictions. Therefore, the aim of the study is to investigate the climate of South Africa as simulated by Super Parameterised Community Atmosphere Model (SPCAM) for the period of 1987-2016. Community Atmosphere Model (CAM) and SPCAM datasets used in the study were obtained from Colorado State University (CSU), whilst dynamic and thermodynamic fields were obtained from the NCEP reanalysis II. The simulations were compared against rainfall and temperature observations obtained from the South African Weather Service (SAWS) database. The accuracy of the model output from CAM and SPCAM was tested in simulating rainfall and temperature at seasonal timescales using the Root Mean Square Error (RMSE). It was found that CAM overestimates rainfall over the interior of the subcontinent during December - February (DJF) season whilst SPCAM showed a high performance in depicting summer rainfall particularly in the central and eastern parts of South Africa. During June – August (JJA), both configurations (CAM and SPCAM) had a dry bias with simulating winter rainfall over the south Western Cape region in cases of little rainfall in the observations. CAM was also found to underestimate temperatures during DJF with SPCAM results closer to the reanalysis. The study further analyzed inter-annual variability of rainfall and temperature for different homogenous regions across the whole of South Africa using both configurations. It was found that SPCAM had a higher skill than CAM in simulating inter-annual variability of rainfall and temperature over the summer rainfall regions of South Africa for the period of 1987 to 2016. SPCAM also showed reasonable skill simulating (mean sea level pressure, geopotential height, omega etc) in contrast to the standard CAM for all seasons at the low and middle levels (850 hPa and 500 hPa). The study also focused on major El Niño Southern Oscillation (ENSO) events and found that SPCAM tended to compare better in general with the observations. Although both versions of the model still feature substantial biases in simulating South African climate variables (rainfall, temperature, etc), the magnitude of the biases are generally smaller in the super parameterized CAM than the default CAM, suggesting that the implementation of the super parameterization in CAM improves the model performance and therefore seasonal climate prediction.

Keywords: Cloud, Climate, Super Parameterised Community Atmosphere Model (SPCAM), Community Atmosphere Model (CAM), El Niño.

Table of Contents	
Acknowledgements.....	ii
Dedication.....	iii
Abstract.....	iv
Table of Contents.....	vi
List of Figures	xix
List of Acronyms.....	xvi
CHAPTER ONE.....	1
INTRODUCTION.....	1
1.1 Background to the study.....	1
1.2 Problem analysis and motivation	3
1.3 Research questions	4
1.4 Aim and Specific objectives.....	5
1.5 Description of the study area.....	5
1.6 Dissertation structure.....	6
CHAPTER TWO:.....	7
LITERATURE REVIEW	7
2.1 Introduction.....	7
2.2 Seasonal rainfall in southern Africa	7
2.3 Global remote influences	9
2.3.1 El Niño Southern Oscillation	9
2.3.2 Indian Ocean Dipole.....	10
2.3.3 Subtropical Indian Ocean Dipole	11
2.3.4 Other modes of variability	12
2.4 Seasonal forecasting	13
2.5 Challenges of Seasonal forecasting.....	14
2.6 Climate Models.....	14
2.6.1 Global Circulation Models.....	15
2.6.2 Dynamical downscaling.....	16
2.6.3 Statistical Downscaling.....	17
2.7 Convective clouds	18
2.8 Cloud microphysics.....	20
2.9 Methods of cloud processes in global circulation model.....	21

2.9.1	Convectonal parameterization.....	21
2.9.2	Cloud Resolving Models.....	22
2.9.3	Super parameterization	23
2.10	Summary.....	26
CHAPTER THREE.....		27
RESEARCH METHODOLOGY.....		27
3.1	Introduction.....	27
3.2	Observed data	27
3.2.1	Rainfall	27
3.2.2	Temperature.....	27
3.2.3	Sea surface temperatures.....	28
3.3	Reanalysis and derived variables	29
3.3.1	Vertical velocity.....	29
3.3.2	Mean Sea Level Pressure.....	29
3.3.3	Wind	29
3.3.4	Geopotential height.....	30
3.3.5	Relative humidity.....	30
3.3.5	Planetary boundary layer	30
3.4	Description of models	31
3.5	ENSO Indices	33
3.6	. Methods.....	33
3.6.1	Root Mean Square Error.....	33
3.6.2	Principal Component Analysis.....	34
3.6.3	Correlation analysis.....	34
3.6.4	Composite analysis.....	34
3.7	Analysis software.....	35
3.71	KNMI Climate Explorer	35
3.72	Grid Analysis and Display System version 2.0.2 oga.2.....	35
3.73	Geographic Information system	35
3.74	Summary	35
CHAPTER FOUR.....		37
THE CLIMATE OF SOUTH AFRICA FROM A SUPER PARAMETIRIZED COMMUNITY ATMOSPHERE MODEL (SPCAM)		37

4.1	Introduction.....	37
4.2	Rainfall climatology	37
4.2.1	Seasonal rainfall	37
4.2.2	Inter-annual variability.....	43
4.3	Temperature climatology.....	47
4.3.1	Seasonal temperature	47
4.3.2	Inter-annual variability.....	54
4.4	The mean circulation.....	57
4.4.1	Seasonal mean sea level pressure (MSLP).....	57
4.4.2	Seasonal planetary boundary layer height.....	60
4.4.3	Geopotential height and wind vectors (850 hPa and 500 hPa).....	63
4.4.4	Omega and specific humidity (500hPa and 850hPa)	68
4.4.5	Relative humidity (850 hPa and 500 hPa).....	73
4.5	Summary	78
CHAPTER FIVE		79
SIMULATED RESPONSE OF THE SOUTH AFRICAN CLIMATE TO DIFFERENT PHASES OF El Niño SOUTHERN OSCILLATION (ENSO) USING SUPER PARAMETERIZED COMMUNITY ATMOSPHERE MODEL (SPCAM).....		79
5.1	Introduction.....	79
5.2	Phases of El Niño Southern Oscillation	79
5.2.1	Evolution of Canonical El Niño and El Niño Modoki	79
5.3	Drought cases.....	83
5.3.1	Rainfall anomalies (1991/92; 1997/98; 2015/16).....	83
5.3.2	Geopotential height anomalies and wind vectors (1991/92; 1997/98; 2015/16)	84
5.3.3	Omega (500hPa) and Relative humidity % (1991/92; 1997/98 and 2015/16)....	85
5.4	Wet seasons	87
5.4.1	Rainfall anomalies (1999/00; 2010/11 and 2011/12).....	87
5.4.2	Geopotential height (500hPa) and wind anomalies (1999/00; 2010/11; 2011/12)	88
5.4.3	Omega (500 hPa) and Relative humidity (1999/00; 2010/1 and 2011/12).....	89
5.5	Summary	91
CHAPTER SIX:.....		92
DISCUSSION AND CONCLUSION		92
6.1	Introduction.....	92

6.2	Discussion and synthesis of key findings	92
6.2.1	South African climate as simulated by SPCAM.....	92
6.2.2	ENSO cases as simulated by SPCAM.....	93
6.3	Implications and future work.....	93
6.4	Conclusions.....	94
	References.....	95

List of Figures

Figure 1.1 : Schematic diagram of super-parameterization. Red colour shows a cloud resolving model (CRM) which is a 2D (x-z) (CRMs, horizontal grid length ~1km) embedded in a large-scale model with the horizontal grid length ~200 km and aligned along the x-axis (Source: Randall et al, 2003).....	3
Figure 1.2: Study area map.....	5
Figure 2.1 : Phases of El Niño (Canonical El Niño and El Niño Modoki) (Source: National Oceanic and Atmospheric Administration, Pacific Marine Environmental Laboratory) ..	10
Figure 2.2 : The west-east Indian Ocean Dipole, (red colour indicates above usually ocean temperatures and blue colour show below normal sea surface temperatures. (Source: Japan Agency for Marine Earth Science and Technology (JAMSTEC, 2015)	11
Figure 2.3 : An illustration showing the SIOD (Source: Reason 2001).....	12
Figure 2.4 : Schematic diagram showing the physical processes of the climate system in Global climate model (Source: NOAA, 2007).....	16
Figure 2.5: A diagram showing RCM inside a GCM with coarse and finer resolutions GCM and RCM respectively. Source: (World Meteorological Organization https://www.wmo.int/pages/themes/climate/climate_models.php).	17
Figure 2.6: An over view of convective clouds (Source: Saltfleet by weather)	18 c
Figure 2.7: Illustration showing clouds and their level in the atmosphere (Source: Saltfleet by weather)	20
Figure 2.8: Microphysics clouds in convective clouds (Source: Randall et al., 2003)....	21
Figure 2.9: An over view of microphysics parametrization (Source: Morrison, 2010)....	23
Figure 2.10: Configuration of SP CAM (Source: Randall et al, 2013).....	24
Figure 3.1: Location of SAWS weather stations around South Africa with at least 90% data availability from 1987 to 2016.....	28
Figure 4.1: Seasonal mean precipitation (mm/day) and Root Mean Squared Error (RMSE) over southern African region for the period 1987 -2016. a) observed December-January-February (DJF) from GPCP. (b) as with (a) but for June -July-August. (c) DJF mean from CAM. (d) as with (c) but for JJA (e) DJF SPCAM (f) as (e) but for JJA.	39
Figure 4.2: Seasonal mean SAWSs rainfall (mm/day) patterns DJF and JJA for the period of 1987 to 2016 over south Africa	40
Figure 4.3 : Seasonal mean precipitation (mm/day) Root Mean Squared Error (RMSE) over southern Africa region for the period 1987-2016. (a) Observed March-April-May (MAM) from GPCP. (b) as (a) but for September -October-November (SON). (c) MAM mean from CAM. (d) as with (c) but for SON. (e) MAM SPCAM (f) as with (e) but for SON.	41
Figure 4.4: Seasonal mean SAWS rainfall (mm/day) patterns for MAM and SON for the period of 1987 to 2016 over South Africa	42
Figure 4.5: The boxes are chosen as representative of the homogeneous regions of South Africa for the analysis of area averaged rainfall as simulated by CAM, SPCAM and observation. (LP-Limpopo; MP-Mpumalanga; KZN -KwaZulu Natal; ECP -Eastern Cape;	

NCP-Northern Cape; WCP-Western Cape; NW- North West; GP- Gauteng; FS -Free State).....	44
Figure 4.6 : Inter-annual variability of rainfall (mm/day) Root Mean Squared Error (RMSE) for different regions over South Africa as simulated by CAM and SPCAM against GPCP observation taken from NCEP reanalysis II for the period 1987 to 2016.	45
Figure 4.7 : Inter-annual variability of rainfall (mm/day) for different regions over South Africa as simulated by CAM and SPCAM against GPCP observation for the period 1987 to 2016.	46
Figure 4.8: Seasonal mean temperature (°C) Root Mean Squared Error (RMSE) over southern Africa region for the period 1987 -2016. a) observed December-January-February (DJF) from NCEP reanalysis II. (b) as (a) but for June -July-August (JJA). (c) DJF mean from CAM. (d) as with (c) but for JJA. (e) DJF SPCAM (f) as with (e) but for JJA.	49
Figure 4.9: Seasonal mean SAWS Maximum temperature (Tmax °C) pattern for DJF and JJA season for the period of 1987 to 2016 over South Africa.	50
.....	51
Figure 4.10 : Seasonal mean SAWS Minimum temperature (Tmin °C) pattern for DJF and JJA seasons for the period of 1987 to 2016 over South Africa.....	51
Figure 4.11: Seasonal mean temperature (°C) Root Mean Squared Error (RMSE) over southern Africa region for the period 1987 -2016. a) observed March-April-May (MAM) air temperature from NCEP reanalysis II. (b) as (a) but for September -October-November (SON). (c) DJF mean from CAM. (d) as with (c) but for SON. (e) DJF SPCAM (f) as with (e) but for SON.....	52
Figure 4.12: Seasonal mean SAWS Maximum temperature (Tmax °C) pattern for MAM and SON season for the period of 1987 to 2016 over South Africa South African	53
Figure 4.13 :Inter annual Variability of temperature (°C) for KwaZulu Natal, North Eastern Interior (Limpopo) and South Western Cape as simulated by CAM, SPCAM against air temperature observation taken from NCEP reanalysis II over South Africa for the period 1987 to 2016.	55
Figure 4.14: Inter-annual Variability of temperature (°C) Eastern Cape, Northern Cape and Free State as simulated by CAM, SPCAM against over South Africa for the period 1987 to 2016	56
Figure 4.15: Seasonal mean sea level pressure (MSLP/ hPa) and Root Mean Squared Error (RMSE) over southern Africa region for the period 1987 -2016. a) observed December-January-February (DJF) from NCEP reanalysis II. (b) as (a) but for June -July-August (JJA). (c) DJF mean from CAM. (d)as with (c) but for JJA (e) DJF SPCAM (f) as with (e) but for JJA.	58
Figure 4.16: Seasonal mean sea level pressure (MSLP / hPa) Root Mean Squared Error (RMSE) and over southern Africa region for the period 1987 -2016. a) Observed March-April-May (MAM) from NCEP reanalysis II. (b) as with (a) but for September -October-November (SON). (c) MAM mean from CAM. (d)as with (c) but for SON. (e) MAM SPCAM (f) as with (e) but for SON.	59

Figure 4.17: Seasonal planetary boundary layer height (PBLH /M) Root Mean Squared Error (RMSE) over southern Africa region for the period 1987 -2016. a) observed December-January-February (DJF) from NCEP reanalysis II. (b) as with (a) but for June -July-August (JJA). (c) DJF mean from CAM. (d) as with (c) but for JJA. (e) DJF SPCAM (f) as with (e) but for JJA. 61

Figure 4.18: Seasonal planetary boundary layer height (PBLH / M) Root Mean Squared Error (RMSE) over southern Africa region for the period 1987 -2016. a) observed March-April-May (MAM) from NCEP reanalysis II. (b) as with (a) but for September -October-November (SON). (c) MAM mean from CAM (d) as with c but for SON (e) MAM SPCAM (f) as (e) but for SON..... 62

Figure 4.19: 850hPa Geopotential height and wind (m/s) over southern Africa region for the period 1987 -2016. a) observed December-January-February (DJF) from NCEP reanalysis II. (b) as with a) but for June -July-August (JJA). (c) DJF mean from CAM. (d)as with c) but for JJA. (e) DJF SPCAM (f) as with (e) but for JJA (a scale vector is shown) 64

Figure 4.20 : 500hPa Geopotential height and wind (m/s) over southern Africa region for the period 1987 -2016. (a) observed December-January-February (DJF) from NCEP reanalysis II.(b) as with (a) but for June -July-August (JJA). (c) DJF mean from CAM (d) as c) but for JJA. (e) DJF SPCAM (f) as with (e) but for JJA (a scale vector is shown). 65

Figure 4.21: 850hPa Geopotential height and wind (m/s) over southern Africa region for the period 1987 -2016. a) Observed March-April-May (MAM) from NCEP reanalysis II. (b) as with (a) but for September -October-November (SON). (c) MAM mean from CAM. (d) as with (c) but for SON. (e) MAM SPCAM (f) as with (e) but for SON (a scale vector is shown)..... 66

Figure 4.22: 500hPa Geopotential height and wind (m/s) over southern Africa region for the period 1987 -2016. (a) observed March-April-May (MAM) from NCEP reanalysis II.(b) as (a) but for September -October-November (SON). (c) DJF mean from SPCAM. (d) as with (c) but for JJA. (e) MAM CAM (f) as with (e) but for SON (a scale vector is shown) 67

Figure 4.23: 850 omega (Pa/s) and specific humidity (kg/g) over southern Africa region for the period 1987 -2016. a) Observed December-January-February (DJF) from GPCP. (b) as with (a) but for June -July-August (JJA). (c) DJF mean from CAM. (d) as with (c) but for JJA. (e) DJF SPCAM (f) as with (e) but for JJA..... 69

Figure 4.24: 500 Omega (Pa/s) and Specific humidity (kg/g) over southern Africa region for the period 1987 -2016. a) Observed December-January-February (DJF) from GPCP. (b) as with (a) but for June -July-August (JJA). (c) DJF mean from CAM. (d) as with (c) but for JJA. (e) DJF SPCAM (f) as with (e) but for JJA..... 70

Figure 4.25: 850 omega (Pa/s) and specific humidity (kg/g) over southern Africa region for the period 1987 -2016. (a) observed March-April-May (MAM) from NCEP reanalysis II. (b) as with (a) but for September -October-November (SON). (c) MAM mean from CAM. (d) as with (c) but for SON. (e) MAM SPCAM (f) as with (e) but for SON..... 71

Figure 4.26: 500 omega (Pa/s) and specific humidity (kg/g) over southern Africa region for the period 1987 -2016. (a) observed March-April-May (MAM) from NCEP reanalysis

ll. (b) as with (a) but for September -October-November (SON). (c) MAM mean from CAM. (d) as with (c) but for SON. (e) MAM SPCAM (f) as with (e) but for SON.....	72
Figure 4.27: 850 Relative humidity (%) over southern Africa region for the period 1987 - 2016. a) observed December-January-February (DJF) from NCEP reanalysis ll. (b) as with (a) but for June -July-August (JJA). (c) DJF mean from CAM. (d)as with (c) but for JJA. (e) DJF SPCAM (f) as with (e) but for JJA.....	74
Figure 4.28: 500 Relative humidity (%) over southern Africa region for the period 1987 - 2016. a) observed December-January-February (DJF) from NCEP reanalysis ll. (b) as with (a) but for June -July-August (JJA). (c) DJF mean from CAM. (d)as with (c) but for JJA. (e) DJF SPCAM (f) as with (e) but for JJA.....	75
Figure 4.29 : 850 Relative humidity (%) over southern Africa region for the period 1987 - 2016. (a) observed March-April-May (MAM) from NCEP reanalysis ll. (b) as with (a) but for September -October-November (SON). (c) MAM mean from CAM. (d)as with (c) but for SON (e) MAM SPCAM (f) as with (e) but for SON.	76
Figure 4.30: 500 Relative humidity (%) over southern Africa region for the period 1987 - 2016. (a) observed March-April-May (MAM) from NCEP reanalysis ll. (b) as with (a) but for September -October-November (SON). (c) MAM mean from CAM. (d) as with (c) but for SON (e) MAM SPCAM (f) as with (e) but for SON	77
Figure 5.1 : Global sea surface temperatures over the south Indian Ocean for Nino 3.4 anomalies for the period 1987 to 2016	80
Figure 5.2 : Global sea surface temperatures over the south Indian Ocean for El Niño Mode Index for the period 1987 to 2016.....	80
Figure 5.3 : Global sea surface temperatures over the south Indian Ocean for Dipole Modoki Index for the period 1987 to 2016.....	81
Figure 5.4 : Correlation of Nino 3.4 Index and Modoki index.....	81
Figure 5.5 : Global sea surface temperatures of a) canonical El Niño and b) El Niño Modoki.....	82
Figure 5.6 : DJF rainfall (mm/day) anomalies as simulated by CAM, SPCAM and observation for the period 1991/92 (first row); 1997/98 (second row) and 2015/16 (third row).....	84
Figure 5.7 : 500 hPa geopotential height and wind vectors (m/s) anomaly as simulated by CAM; SPCAM and observation for the period of 1991/92 (first row), 1997/98 (second row) and (third row) 2015/16 (a scale vector is shown)	85
Figure 5.8 : 500hPa omega (Pa/s) and Relative humidity (%) anomaly as simulated by CAM; SPCAM and observation for the period of 1991/92 (first row), 1997/98 (second row) and (third row) 2015/16	86
Figure 5.9 : Rainfall (mm/day) anomalies as simulated by CAM; SPCAM and observation for the period of 1999/00 (first row), 2010/11 (second row) and (third row) 2011/12 Over southern Africa.	88
Figure 5.10 : 500 hPa geopotential height and wind (m/s) anomaly as simulated by CAM; SPCAM and observation for the period of 1999/00 (first row), 2010/11 (second row) and (third row) 2011/12 over southern Africa (a scale vector is shown).....	89

Figure 5.11 : 500 hPa omega (Pa/s) and relative humidity (%) anomaly as simulated by CAM; SPCAM and observation for the period of 1999/00 (first row), 2010/11 (second row) and (third row) 2011/12 over southern Africa. 90

List of Tables

Table 2. 1 Cloud classification and characteristics	19
Table 2. 2 Super Parameterization achievement to climate simulation over the past 18 years	25
Table 3.3 List of observation, reanalysis and simulation datasets used in the study.....	32
Table 5.2: Austral summer PCA variance and cumulative percentage sea surface temperature showing canonical El Niño	83
Table 5.3: Austral summer PCA variance and cumulative percentage sea surface temperature showing canonical El Niño Modoki.....	83

List of Acronyms

AAO	Antartic Oscillation
AMIP	Atmospheric Model Inter-comparison Project
CAM	Community Atmosphere Model
CCN	Cloud Condensation Nuclei
CESM	Coupled Community Earth System Model
CGCMs	Coupled General Circulation Models
COLs	Cut-off Lows
CRM	Cloud Resolving Model
CSIR	Council for Scientific and Industrial Research
CSU	Colorado State University
DJF	December-January-February
DSD	Dynamical downscaling
ECMWF	European Centre for Medium Range Weather Forecast) ERA- Interim reanalysis
EMI	El Niño Modoki Index
ENSO	El Niño Southern Oscillation
GCM	Global Climate Models
GCRM	Global Cloud Resolving Model
GCMs	General Circulation models
GDP	Gross Domestic Product
GHG	Green House Gases
GIS	Geographic Information Systems
GPCP	Global Precipitation Climatology Project
GrADS	Analysis and Display System
HadiSST	Hadley Centre Global Sea Ice and Sea Surface Temperature

HGT	Geopotential height
IOD	Indian Ocean Dipole
IPCC	Intergovernmental Panel on Climate Change
ITCZ	Intertropical convergence zone
JAMSTEC	Japan Agency for Marine Earth Science and Technology
JJA	June-July-August
KNMI	Royal Netherlands Meteorological Institute
MAM	March-April-May
MJO	Madden Julian Oscillation
MMF	Multiscale Modeling Framework
MSLP	Mean Sea Level Pressure
NCEP/NCAR	National Centers for Environmental Prediction /National Centre for Atmospheric Research
NICAM	Non-Hydrostatic Icosahedral Atmospheric Model
OISST	Optical Interpolated Sea Surface Temperatures
OLR	Outgoing Long- wave Radiation
PBLH	Planetary Boundary Layer Height
PRECC	Precipitation rate
QBO	Quasi Biennial Oscillation
RH	Relative Humidity
RMSE	Root Mean Square Error
SA	South Africa
SAF	Southern Africa
SAWS	South African Weather Service

SHUM	Specific Humidity
SIOD	Subtropical Indian Ocean Dipole
SON	September-October-November
SP	Super parameterization
SPCAM	Super Parameterized Community Atmosphere Model
SSTs	Sea Surface Temperatures
TC	Tropical Cyclone
TTT	Tropical Temperate Trough
U	Zonal wind
UCT	University of Cape Town
UKMO	United Kingdom Met Office
UP	University of Pretoria
V	Meridonal wind

CHAPTER ONE

INTRODUCTION

1.1 Background to the study

Weather and climate influence human and environmental health, water resources management, energy demand and supply, disaster risk management and many other sectors. It is therefore important to accurately forecast weather and predict climate to save lives and property, as well as better prepare for climate extremes such as droughts. A critical tool used to forecast and study weather as well as climate on different timescales is a numerical model which can be run over dissimilar domains. Global Circulation Models (GCMs) are run over the whole globe while Limited Area Models (LAM) are run over a selected area of interest. LAMS can run with higher resolution because they run over a smaller domain compared to GCMs, however, they require time-dependent lateral boundary conditions from GCMs. When used for weather forecasting purposes, several GCMs are currently run with a grid spacing of below 20 km. When used for seasonal forecasting and climate change studies, the grid spacing used ranges from about 40 km to 250 km.

The treatment of clouds in models is an important aspect of modelling, as it is responsible for a lot of the uncertainty in simulations and depends on the grid spacing used. The process of cloud formation and distribution in the atmospheric circulation system is very important, yet very difficult to understand and predict (Randall, 2013). Clouds are made up of liquid droplets and ice particles which scale from microns to millimetres in size (Randall et al, 2003). They are linked to convection and turbulence, which are characterised by eddies that range from meters to kilometres and organized within synoptic-scale dynamical systems and mesoscale and interact with the global atmospheric circulation system (Randall, 2013). Water vapour is a greenhouse gas which is vital in finding the net radiative balance. Therefore, any change in cloud coverage can lead to a new climate state (Kiehl, 1994).

Cloud processes occur on a minor scale, in the sense that models struggle to simulate them explicitly, and therefore they are parameterized. Parameterization schemes are statistical theories that describe the interaction of small-scale processes with the large-scale state (Randall, 2013). According to Randall et al., (2003), parameterization is designed to show the effects of small-scale processes in terms of larger a scale state. Parameterization schemes are used to represent sub grid processes in models statistically using mean variables that the model can solve. Since

the development of parameterization in 1960s, GCMs have used parameterization to simulate a large area of cloud processes which occurs on scales near to or lesser than the horizontal grid spacing (Randall et al., 2003). So much advancement has been achieved in simulating cloud and boundary layer processes, however, a lot of problems remain (Meikey and Stone, 2005).

It has been found that parameterized GCMs are struggling to simulate how clouds and aerosol particles affect the climate system (Randall, 2013). The Inter-Governmental Panel on Climate Change (IPCC), (2007; 2013) indicated that the representation of clouds in GCMs is the main source of uncertainty in climate predictions and projections. GCMs are used to predict seasonal climate on an operational basis, however, their skill has been found to have restrictions. This is partly because a skillful seasonal forecast needs a dependable simulation of the land surface, as well as ocean-atmosphere interactions. Coupled Ocean and Atmosphere General Circulation Models (CGCMs) can better simulate the Inter-annual variability of SST variations in the tropical Pacific Ocean especially when used with improved vertical and horizontal model resolutions (Guillyard, 2009; Randall, 2013).

Scientists of the National Centre for Atmospheric Research's (NCAR) developed a "multiscale" GCM where the physical processes related to clouds were simulated by inserting a Cloud-Resolving Model (CRM) inside a GCM (Figure 1) (Grabowski and Smolarkiewicz 1999; Grabowski 2001, 2004). This procedure is called super parameterization and the GCM that uses the super parameterisation is called a Multiscale Modelling Framework (MMF) (Khairoutdinov and Randall, 2001). Super-parameterization was then proposed as part of the solution to the cloud parameterization problem which had reached a "deadlock", in the sense that the rate of improvement had become unacceptably slow (Randall et al., 2003). Simulations produced with super-parametrized models have been shown to be better and to produce enhanced organized tropical convection in idealized experiments, where other models that use conventional parametrization schemes have been unsuccessful (Grabowsk and Smolarkiewicz, 1999).

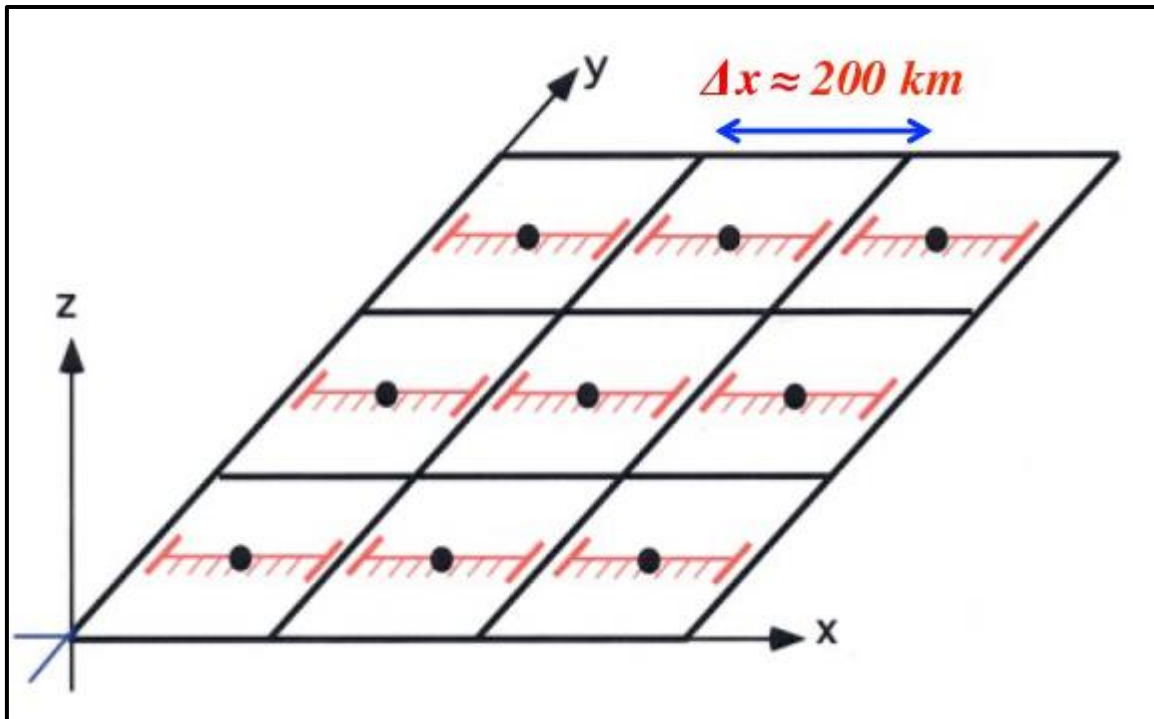


Figure 1.1 : Schematic diagram of super-parameterization. Red colour shows a cloud resolving model (CRM) which is a 2D (x-z) (CRMs, horizontal grid length ~1km) embedded in a large-scale model with the horizontal grid length ~200 km and aligned along the x-axis (Source: Randall et al, 2003)

1.2 Problem analysis and motivation

Agriculture is the largest contributor to the economy of Africa, and when this sector experiences problems significant reductions of the Gross Domestic Product (GDP) can be expected (Chikoore, 2005; Mwafuhurwa, 1999). This sector is sensitive to the weather and climate variability. The four years of El Niño episode (1991-1994) caused famine and death to thousands in southern Africa (SAF). During the periods of 1997-1998, 2002-2003, 2015-2016, the region experienced severe droughts due to El Niño events, which resulted in loss of livestock and brought about food scarcity in several parts of the SAF (Davis, 2011). In 2000 and 2001, Mozambique and the northern parts of South Africa were affected by floods which caused the deaths of more than hundreds of individuals while 200 000 were left without homes (Davis, 2011; Chikoore, 2005; Bopape, 2013). These catastrophic events are partially attributed to the inability to properly predict climatic events, hence limited preparedness to deal with the effects of drought and high rainfall conditions. It is therefore important that the models predict weather and climate with skill and confidence to inform decision making to save lives and properties.

South African scientists have been producing operational seasonal forecasts since the early 1990's (Landman, 2014). Initial work started with statistical models, where sea surface

temperatures (SSTs) were used as the predictor, and rainfall over South Africa was the variable being predicted (Landman, 2014). Predictions were also made and are still currently being made with GCMs (Lawal, 2015). Initially, only a two-tiered system was followed where SSTs were predicted first and used as surface boundary conditions in the model (Landman, 2014; Beraki, 2016). In the recent past, coupled ocean-atmosphere models were also introduced due to the availability of bigger computing systems (Landman, 2014; Beraki et al., 2015). Currently, the Council for Scientific and Industrial Research (CSIR), University of Cape Town (UCT) and the South African Weather Service (SAWS) are all using GCMs with different levels of sophistication to produce operational seasonal forecasts (Landman, 2014). It may be noted that statistical and dynamical downscaling (Kgatuke et al., 2008; Landman et al., 2009) are still being used in the country, however dynamical downscaling is not used on an operational basis.

Despite the use of sophisticated models in the region to predict the seasonal climate, challenges are still experienced with skill as well as confidence. The representation of clouds, convection, and precipitation in GCMs is still an issue (Lawal, 2015). These uncertainties arise from incomplete knowledge and the dynamic nature of the climate systems which restrict capacity to fully project and understand future climatic changes. Randall et al., (2003) proposed super parameterisation as part of the solution to improve simulations that conventional schemes fail at. In spite of the social and economic importance of predicting seasonal forecast, studies on the capability of super parameterization to simulate and predict seasonal forecast over South Africa are rare, if at all they exist. Reliability of seasonal climate forecasts (SCFs) will help in sectors such as agricultural management, water resources, health and environmental management. SCFs will also help in adaptation and coping measure to deal extreme weather events caused by variation in SSTs (drought and flood event). Therefore, this study focuses on the climate of South Africa as simulated by the Super Parameterised Community Atmosphere Model (SPCAM) compared to the Community Atmosphere Model (CAM) that uses the conventional convection parametrization scheme.

1.3 Research questions

- To what extent does the SP-CAM produce the climate of South Africa with skill?
- Are there statistically significant differences between results generated from SPCAM and the CAM over South Africa?
- Is the South African climate's response to ENSO well captured by SP-CAM?

1.4 Aim and Specific objectives

The aim of the study is to investigate the climate of South Africa as simulated by the Super Parameterised Community Atmosphere Model (SP CAM) for the period 1987-2016.

Specific research objectives

- To examine the capability of SP-CAM in producing climate over South Africa,
- To compare the simulated climate over South Africa using the CAM using a conventional cumulus scheme and SP CAM and
- To evaluate the simulated response of the South African climate to different phases of El Niño Southern Oscillation (ENSO) using SP-CAM.

1.5 Description of the study area

South Africa is positioned on the southern tip of the African continent bordered by Namibia, Botswana, Zimbabwe and Mozambique. The country is made up of 9 provinces and encompasses the independent mountain kingdoms of Lesotho and Swaziland. It is located between the Indian Ocean and South Atlantic Ocean with high pressure zones on the east and western part respectively. The region is prone to extreme weather and climate events such as droughts, heat waves and floods.

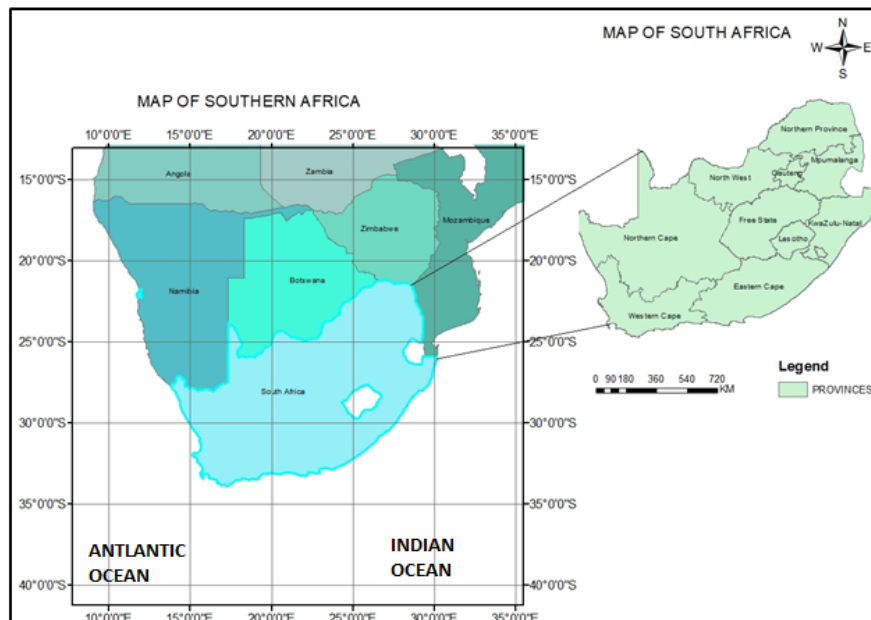


Figure 1.2: Study area map

1.6 Dissertation structure

The study consists of six chapters. Chapter 1 provides the aim and objectives, research questions, problem analysis and motivation and the location and description of the study area map.

Chapter 2 provides the literature review on the topic, focusing specifically on previous studies done in relation to the study. It further provides historical knowledge and current findings on this research topic to avoid replication of knowledge.

Chapter 3 presents the methods of analyses and the datasets that were used in the study to achieve the specific research objective.

Chapter 4 in this chapter results of the standard community atmosphere model (CAM) and super parameterized community atmosphere model (SPCAM) are contrasted. The focus was based on rainfall and temperature climatology, also analysing the inter-annual variability of rainfall and temperature for homogeneous regions around South Africa for the period of 1987 to 2016. In addition, present and discuss a climatology of circulation variables from low and middle levels as simulated by CAM and SPCAM against observation datasets from NCEP reanalysis II.

Chapters 5 investigate the most intense El Niño and La Niña years as simulated by CAM, SPCAM and observation for the period of 1987 to 2016.

Chapter 6 summary and conclusion of key findings.

CHAPTER TWO:

LITERATURE REVIEW

2.1 Introduction

The aim of this chapter is to review different works related to the study. It also helps to find the methods commonly used in similar studies and to avoid duplication of studies that have been conducted. Therefore, this chapter intends to review existing studies on super parameterization globally and modelling studies that have been conducted over South Africa for seasonal timescales. It focuses on approaches of cloud processes in Global Circulation Models (GCMs), seasonal forecasting challenges and opportunities, ocean atmosphere interaction, capabilities and limitations of GCMs.

2.2 Seasonal rainfall in southern Africa

Southern Africa (SAF) climate is governed by altitude, ocean currents such as cold Benguela current of the South Atlantic Ocean and the warm Mozambique and Agulhas currents of the Indian Ocean; position of high-pressure systems and the shift of the Inter-Tropical Convergence Zone (Mackellar et al, 2014). SAF region experiences predominantly summer rainfall between the month of November to March (Davis, 2011). Ocean currents and the track of trades winds govern the amount of rainfall being received over the eastern and western part of SAF. The eastern part of the region tends to receive high amounts of rainfall because of the Agulhas current which provides an additional source of moisture whilst the western part of the region experiences low amounts of rainfall due to the cold Benguela current, of the South Atlantic Ocean (Davis, 2011).

Summer rainfall of the region is characterized by the shift of the Inter Tropical Convergence Zone (ITCZ). The ITCZ symbolizes an area of strong convective activity that is associated with the equatorial through low-pressure. It is a zone of convergence where the northeasterly trade winds converge with the southeasterly trade winds and is the main rainfall bearing system over SAF region. During the month of March and September, the ITCZ is near the equator and moves south to the Southern Hemisphere bringing summer rainfall over the SAF region. During winter, the ITCZ migrates to the north in the Northern Hemisphere. Most of the region experiences summer rainfall except the arid South West, south coast and the moist tropics (Daron, 2014). The south cape coast experiences rainfall all year round while South West winter rainfall. The South African region receives summer rainfall when the ITCZ interact with other global and regional atmospheric patterns such as the El Niño Southern Oscillation (ENSO). There are several weather systems

that contribute to seasonal rainfall over SAF region such as tropical temperate trough, cut off low, tropical cyclones etc.

Tropical temperate through (TTT) known as clouds bands contribute considerably to summer rainfall over the South African region (Hart et al., 2013). TTT usually form when a tropical disturbance (trough) in the lower part of the atmosphere combined with a middle latitude in the upper part of the atmosphere (Pohl et al,2009) .TTT propagate eastward from southern Africa to the Mozambique channel and south Madagascar (Pohl et al ,2009) .Their location have a strong influence on intra-seasonal and inter-annual rainfall variability (Washington and Todd, 1999). TTT and cloud bands produce 40 - 60% of summer rainfall over South African region (Hart et al, 2013; Harrison, 1984). They are associated with northwest to southeast clouds bands extending from South Africa to the south East Indian Ocean (Harisson 1984). When cloud bands are positioned further east several parts of southern Africa tend to receive low rainfall (Usman and Reason, 2004). In southern Africa areas which are in the tropics and central Africa rainfall regimes depend on deep convection processes and water vapor convergence at different tropospheric levels (Cretat et al., 2012). Over southern Angola and Northern Namibia the Angola /Botswana low which normally develop in summer over the Kalahari tend to favor low-level of infiltration of moisture flux from the tropical southeastern Atlantic and could thus be another key mechanism for their initiation and development (Chikoore and Jury 2010; Hart et al., 2010).

COLs are known as cold cored systems that have been cut-off from westerly flow and displaced equatorward of the polar jet stream (Singleton and Reason, 2007a). COLs are synoptic scale weather systems that contribute to high amounts of rainfall in South African region and associated with wide spread rainfall (Molekwa, 2013; Zhao and Sun, 2007). The development of COLs is positively linked with a strong ridge of high pressure positioned in the southern part of South Africa. COLs are often allied with powerful rainfall and stratosphere-troposphere exchange in the South Atlantic Ocean (Singleton and Reason, 2007a). In South Africa COLs, are regarded as important synoptic scale weather systems that occur over the subtropics and which are usually associated with widespread of rainfall with one out of five events resulting in flood events, especially along the southern and eastern coastal belts to the adjacent interior of the country (Molekwa, 2013). Singleton and Reason (2007a) studied a climatology of cut-off flow for the period 1972 to 2000 and found that about 11 COLs occur per year, most of them being observed in autumn season (March-April- May)

Tropical cyclones (TCs) are low-pressure systems with a well-developed eye in the tropical Indian Ocean (Tyson and Preston-Whyte, 2000). TCs are more dominant in summer over the Indian

Ocean, with approximately 6 to 12 documented every year between the month of November and April over the south West Indian Ocean (Malherbe et al., 2012). An average of 10 to 12 of tropical depressions mature to TCs over the southwest Indian Ocean (Malan et al 2013). However, not all TC make a land fall over Mozambique channel but track south through the channel (Singleton and Reason, 2007b). Only about 5% of TCs developed in the south Indian Ocean make land fall over southern Africa mainland. TCs dump high amount of rainfall when they make a landfall over Mozambique for instance. TC Eline that made a landfall over Mozambique during 1999/2000 and killed thousands of people whilst 200 000 were left with no homes (Bopape, 2013).

2.3c Global remote influences

2.3.1 El Niño Southern Oscillation

El Niño Southern Oscillation (ENSO) drives inter-annual climate variability across the globe, including SAF region (Driver, 2014). ENSO is the disturbance of the ocean atmosphere system in the equatorial eastern Pacific Ocean and has a large influence on global weather systems which then makes it a strong predictor of rainfall over SA (Phakula, 2017; Brown, 2011). El Niño is associated with above average ocean temperatures in the eastern Pacific Ocean with cooler SSTs over the western pacific (warm ENSO) (Figure 2.1a) while La Niña is associated with colder SSTs over the eastern equatorial pacific (Figure 2.1c). There is a link between rainfall over SAF and ENSO, such that during El Niño season the region tend to receive below normal rainfall while during La Niña season the region experience high amount of rainfall (Figure 2.2). During El Niño event some regions experience drought while other regions experience floods (Browne, 2011). Not all ENSO events result in dry conditions over SAF region. For example, the 1997/98 El Niño did not result in the anticipated drought over most parts of South Africa (Richard et al, 2001). El Niño can interrupt seasonal spatial patterns of rainfall and temperature around the globe by carrying large changes in seasonal rainfall causing drought and flood in different regions respectively (Moatshe, 2008). ENSO events are important for understanding seasonal climate variability over a lead time of a few months to a year.

There are distinct phases of ENSO, which include canonical El Niño and El Niño Modoki (Johnson, 2013). Canonical El Niño occurs in the eastern equatorial pacific whilst El Niño Modoki occurs in the central pacific, flanked by cooler sea surface temperatures on both side of the equatorial basin creating a zonal tripolar pattern (Figure 2.1 b) (Ashok et al., 2007). La Niña Modoki is associated with cooler SSTs in the central pacific flanked by warm waters in the western and eastern equatorial basin respectively (Figure 2.1 d). Modoki is a Japanese word which means “similar but different “(Ashok et al., 2007). El Niño Modoki impact on SAF rainfall is

not as much as the one of canonical El Niño such that canonical El Niño is associated with significantly below normal rainfall over SAF compared to El Niño Modoki (Ashok et al., 2007).

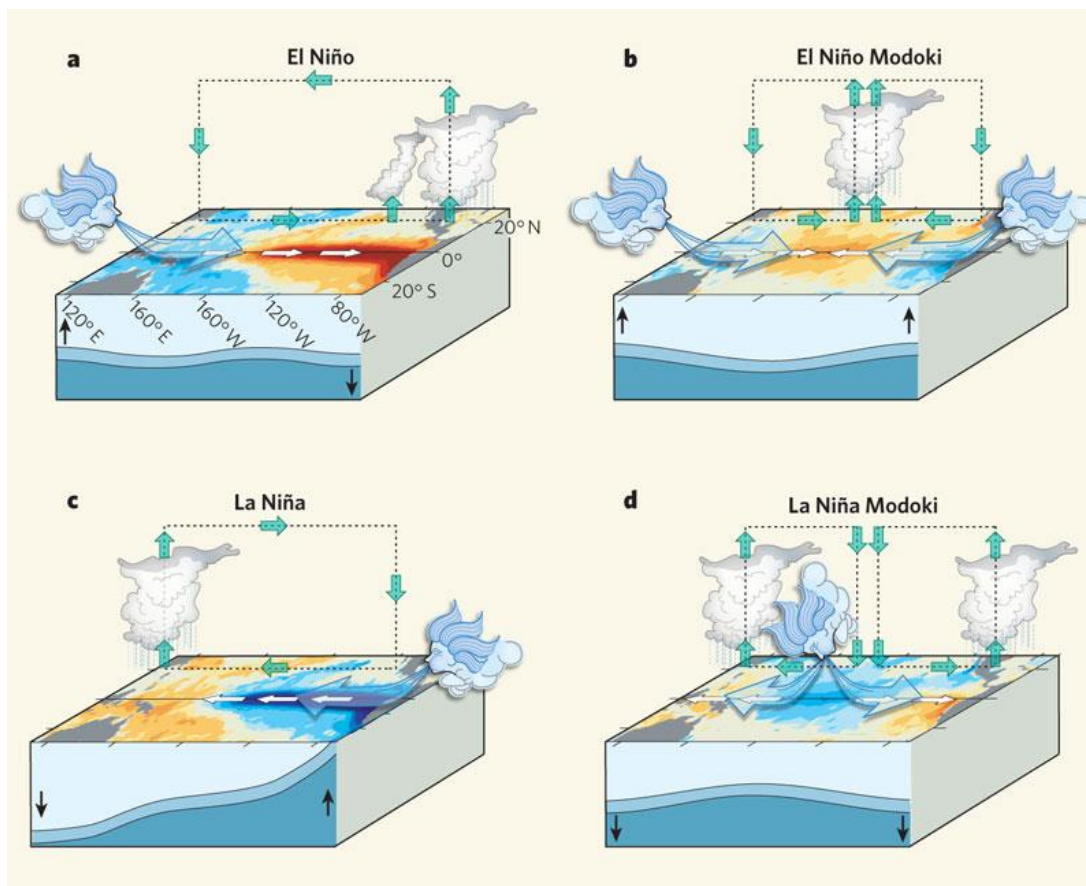


Figure 2.1 : Phases of El Niño (Canonical El Niño and El Niño Modoki) (Source: National Oceanic and Atmospheric Administration, Pacific Marine Environmental Laboratory)

2.3.2 Indian Ocean Dipole

The Indian Ocean Dipole (IOD) is a coupled ocean-atmosphere phenomenon such as ENSO in the Indian Ocean (Lawal, 2015; Chikoore 2016). It is associated with above usually SSTs in the western equatorial Indian Ocean and below normal SSTs in the south eastern equatorial Indian Ocean (Figure 2.3). IOD events usually occur in June and peak in October. The Positive phase of IOD is associated with increased summer rainfall over East Africa and droughts over southern Africa (Hasingo and Reason, 2008).

However, in summer monsoon (June to September), south easterly trade winds, crosses the equator and impacts the thermocline depth. From east to west, the wind pushes the warm water on the mixed layer zone, thus, cold water comes up to the surface of the ocean. Therefore, the thermocline rises in the east part of Indian Ocean that is the positive IOD.

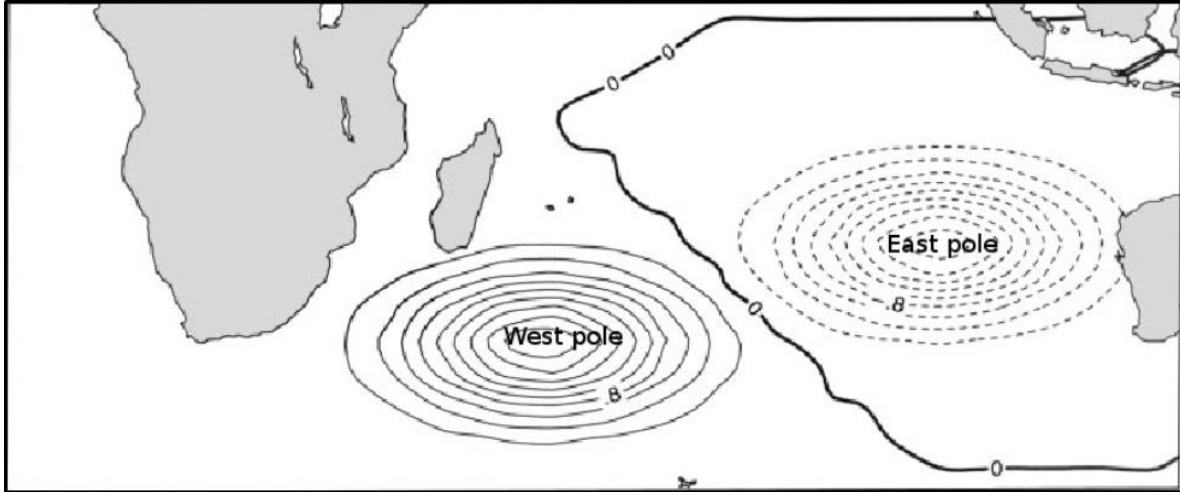


Figure 2.3 : An illustration showing the SIOD

2.3.4 Other modes of variability

a) Quasi-Biennial Oscillation

Quasi-Biennial Oscillation (QBO) is a fluctuation of equatorial wind that occurs in the lower stratosphere every two and half years (Hernandez, 2008). It is also known as a cycle of equatorial winds between easterlies and westerlies (Lindesay, 1998). The sequence of the westerly and easterly regimes starts above 30 km and propagates downward at a rate of 1 km per month (Hernandez, 2008). However, the westerly regime descends more often and quickly when compared to the easterly regime (Baldwin et al., 2001). QBO amplitude is constant between 30 to 23 km with quick weakening commencement under 23 km. QBO affects rainfall variability over SAF and the east phase of QBO has been related to below normal rainfall over the region (Chikoore, 2016). ENSO influence on rainfall variability also appeared to be governed by QBO (Richard et al, 2000).

b) Antarctic Oscillation

The Antarctic Oscillation (AAO) also known Southern Annual Mode (SAM) is a belt of westerly winds encircling Antarctica migrating south or north as its mode of variability (Australian Bureau of Meteorology). AAO is known as the cause of the winter rainfall in the Western Cape (Xulu, 2017). There's a link between the positive phase of AAO and central Africa rainfall, which is stronger in La Niña season (Pohl et al., 2010). The negative phase of AAO is positively linked with winter rainfall over the south Western Cape, more considerably the wet winters and vice versa (Reason and Rouault, 2005).

2.4 Seasonal forecasting

A seasonal forecast is a probabilistic statement on the future nature of the atmosphere over a period, usually three months (Lawal et al., 2015). The state of ENSO is the major predictor of seasonal climate over southern Africa (Phakula, 2017). A seasonal forecast is different from climate change projection and weather forecast. Weather forecasts provide information of weather such as frontal passages and rainfall prediction expected over a short period of time such as two days, but beyond about two weeks ahead it is not possible to predict these day-to-day changes in detail (Bartman, 2002). Climate change projections are the probabilistic nature of future climate over a very long time that are usually averaged for a 30-year period. Seasonal prediction is known to offer the future seasonal climate information as departures from the climatic mean. In seasonal climate forecasting rainfall and temperature variables are significant (Lawal 2015). Lawal (2015) states that seasonal prediction is articulated in terms of probabilities because of the uncertainties in predicting seasonal climate. Seasonal forecasting is based on slowly evolving surface conditions (e.g. sea surface temperatures) that can be predicted with skill, which in turn leaves memory in the atmosphere making the atmosphere partly predictable (Landman 2014).

South African scientists have been producing seasonal climate forecasts since the early 1990s. Landman et al (2001) used a COLA T30 GCM to simulate seasonal rainfall over southern Africa and found the model to have a forecast skill in simulating summer rainfall. Landman et al. (2012) tested the capability of coupled and uncoupled prediction systems (one versus two tiered systems) for seasonal rainfall forecasting and found both systems to have a forecast skill in predicting summer rainfall over South Africa. The coupled system was found to simulate summer rainfall more explicitly best compared to the uncoupled model. Landman and Beraki (2010) compared single forecast model against multi-models forecast and found the former to outperform the later in simulating mid-summer rainfall over southern Africa. Landman and Beraki (2012) evaluated the probabilistic rainfall forecast skill over southern Africa during summer season for the period 1980-2002 using several multi-model ensembles. They found the forecast to be more realistic during El Niño and La Niña seasons compared to neutral years. A combination of statistical models and Atmospheric General Circulation Models are vital for temperature and rainfall forecasting since different models have different strengths and weaknesses (Moatshe, 2008).

Well-timed and accurate predictions of seasonal climate will help lessen the calamity caused by climate extreme events (Lawal, 2015). The reliable and timely predictions of seasonal climate forecast are useful for planning and risk management in various socio-economic subdivisions, for

instance health, agriculture, environmental management, engineering, etc. (Moatshe, 2008). In the insurance sector seasonal climate forecasts are considered the most important since they can assist with operational tasks to prepare major pay-outs. However, it is important that seasonal forecasts are reliable because a wrong prediction leads to wrong decisions and reduces the confidence of the public in using forecast information for planning (Lawal, 2015). Again, social benefits that are associated with climate information include the improvement of the environment and travelling (Moatshe, 2008). For instance, if people want to travel from one place to another, they should know the seasonal climate forecast. For a region that is prone to malaria for example, it is important to know when wet conditions are expected (Moatshe, 2008). In the construction sector seasonal climate forecast is used by contractors such that when a contractor gets an opportunity to build a school, he /she must know what to expect in the next season /how the season will be like. If the season is wet it means that the project will be delayed because concrete might take time to dry (Moatshe, 2008).

2.5 Challenges of Seasonal forecasting

The prediction of seasonal climate from GCMs has restrictions, because a skillful simulation entail;

- i. A dependable simulation of land surface, ocean and atmospheric interactions (Pennell and Reichler, 2010);
- ii. Knowledge of the initial state of the ocean, the land surface and the atmosphere (Pielke et al., 2006) and
- iii. Knowledge of future changes in boundary conditions, such as the seasonal distribution of solar radiation and variations in chemical composition of the atmosphere (Buckle, 1996; Liniger et al., 2007).

While a reliable forecast can help reduce losses from disaster (such as floods, drought, and heat waves), an unreliable forecast can mislead and increase damage from disasters.

2.6 Climate Models

Climate models are tools for simulating climate at global, continental and regional scales (Lawal, 2015). These models use numerical approaches to simulate the interaction of the vital drivers of climate, including the atmosphere, ice and land surface. They are utilized for climate projection and dynamics of the climate system. Climate models are developed by researchers at climate research centres (e.g. UK Met Office (UKMO)). Application of these models involves supercomputers and the models can be applied effortlessly globally to produce climate

information. A regional climate model (RCM) runs over a selected domain of interest while a Global Climate Model (GCM) runs over the whole globe (Lawal, 2015). Over South Africa a number of models are run on the super-computer of the Centre for High Performance Computing which is funded by the Department of Science and Technology and hosted by the Council for Scientific and Industrial Research (CSIR).

2.6.1 Global Circulation Models

The Global climate models / General Circulation Model (GCMs) are tools for simulating climate at a global scale (IPCC, 2007 and 2013; Lawal, 2015). They simulate changes in climate because of slow changes in some physical parameters or boundary conditions such SSTs and solar radiation. These models use mathematical equations to represent several physical processes in global climate system and give information about the future climate. GCMs signify the key mechanisms of the climate system in three dimensional grids over the Earth due to high complexity compared to statistical models (New et al., 2000). GCMs give information on the assessment of large-scale aspects of climate variability, with a usually coarse spatial resolution which is about 40km or more. GCM is made up of vertical and horizontal grid boxes that show areas at the Earth surface. Low resolutions contribute to the limitations of GCMs as they prevent them from capturing microphysical processes that are vital in the simulation of climate variability and change (Mitchell and Jones, 2005; Randall, 2013). For example, clouds are poorly represented in GCMs because they occur on a small spatial scale (microphysics) (Lawal, 2015). Parameterizations are used to represent these small-scale features (Cretat et al., 2012).

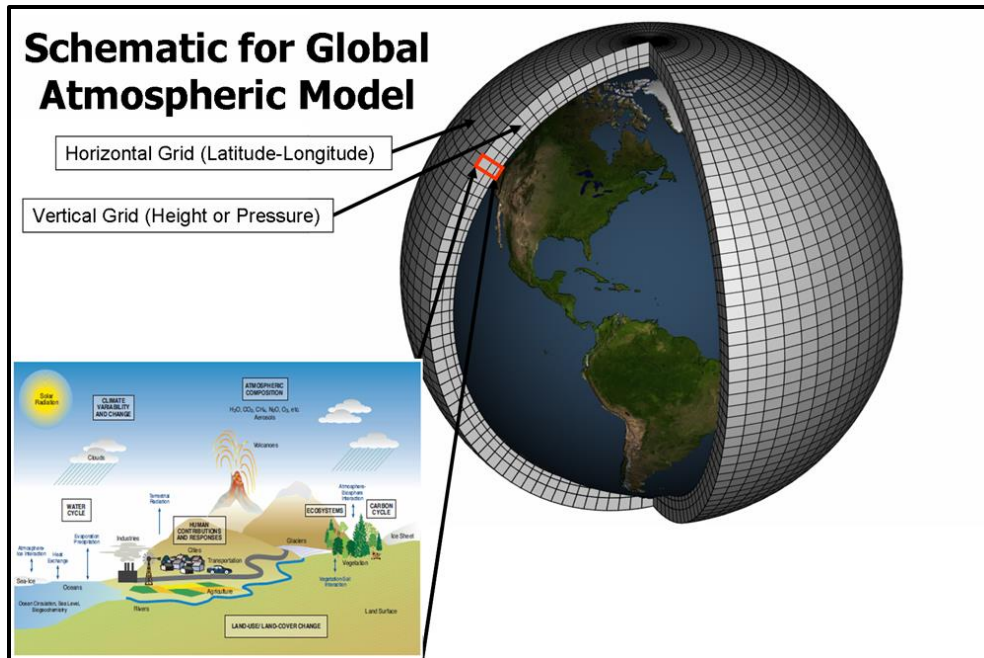


Figure 2.4 : Schematic diagram showing the physical processes of the climate system in Global climate model (Source: NOAA, 2007)

2.6.2 Dynamical downscaling

Dynamical downscaling (DSD) achieve a higher resolution by imbedding RCM of high resolution inside a GCM (Schmidti et al, 2007). RCM better simulates the impact of complex topography and vegetation on the climate system than GCM (Phakula, 2017). RCM are expressed in terms of physical principles and have the ability to capture fine spatial – scale non -linear effect which maximize their capability to downscale future climate (Phakula, 2017). GCM data is more crucial in RCM since it is used to give initial lateral boundary conditions, SSTs and initial land surface conditions to the nested RCM (Xu and Yang 2012). However, it is difficult to balance the performance of RCMs in adding the small -scale features while simultaneously retaining large scale features (Wang and Katamarth 2013). RCMs have biases that are associated with uncertainties in their parameterization boundary conditions and dynamics (Jakob et al., 2011). DSD is computational demanding and of high cost. RCM have been used as dynamical downscaling tools to study regional climate change and seasonal climate variability (Sylla et al 2009).

RCMs are tools for simulating climate at regional levels with a smaller domain that what is required for global models. In comparison with GCMs, RCMs provide more realistic climate information with finer details because they have higher spatial resolution than GCMs (IPCC, 2007 and 2013). RCMs are nested within a GCM or reanalyses to give more detailed simulations for a particular location (Cocke et al., 2007; Kgatuke et al., 2008). In this way, information such as aerosol forcing

of a particular region from a coupled GCM are used as initial conditions, surface boundary conditions, and time-dependent lateral meteorological conditions to drive the RCM. RCMs are usually run over a limited area because they operate at much higher resolution (usually less than 50km); which requires less computational resources than those required to run a GCM with the same resolution (Cocke et al., 2007).

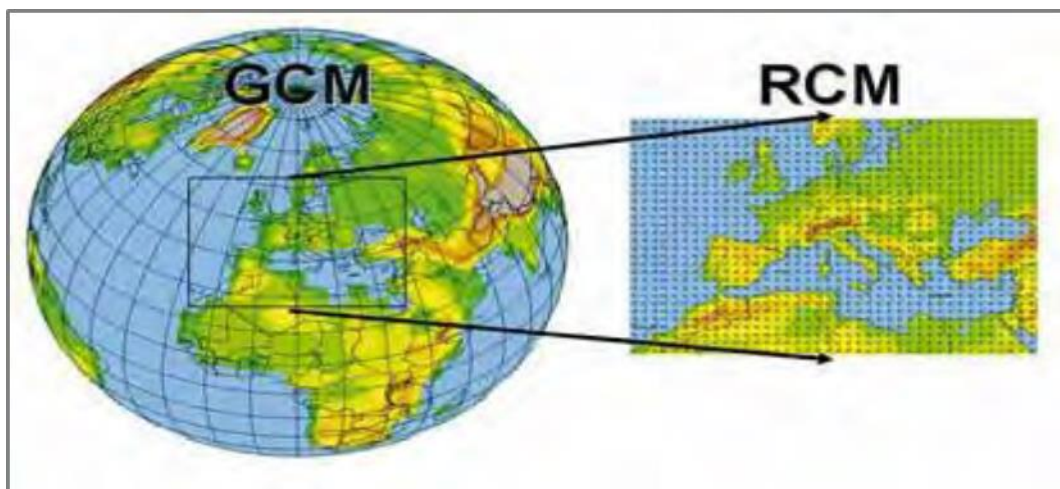


Figure 2.5: A diagram showing RCM inside a GCM with coarse and finer resolutions GCM and RCM respectively. Source: (World Meteorological Organization https://www.wmo.int/pages/themes/climate/climate_models.php).

2.6.3 Statistical Downscaling

In the statistical downscaling approach, a numerical relationship is created between GCM simulated large-scale circulation variables and the required regional climate variables such as rainfall and temperature (Phakula, 2017). It is not difficult to use and is also less expensive computationally compared to dynamical approaches (Phakula, 2017). The statistical downscaling approach relies on the assumption that the relationship between present large-scale circulation and local climate remains valid under different forcing conditions of possible future climates.

The relationship between predictors and predictands has to be strong in order to better explain the local climate variability; the predictor variable should be well simulated by GCMs, and the relationship between predictors and predictands should not change in time and remain the same in future climate (Busuioc et al., 2001). This approach is subdivided into three categories which involves weather classification, regression models and weather generators (Phakula, 2017).

2.7 Convective clouds

Convective clouds are very significant in the atmospheric system because they transport a high amount of energy and moisture from the surface of the earth to the upper troposphere. Convective clouds are widely known to produce heavy precipitation which initiates global -scale circulation (Randall et al., 2003). The simulation of convective clouds in GCMs is a challenging issue for conducting global climate simulation. Convective clouds are widely recognized by their spatial scale of a few kilometres to a few tens of kilometres. Convection needs to be parameterized in GCMs which have a horizontal resolution of 200 to 300 kilometres (Zhang and Song, 2016).



Figure 2.6: An over view of convective clouds (Source: Saltfleet by weather)

Clouds are the most vital controllers of weather and climate of the earth atmosphere. They are made up of water droplets or ice particles moving in the sky and they are the visible signs of atmospheric processes at work (TiedTke, 1993). The role of clouds is poorly understood since they interact with atmospheric processes such as turbulence, large -scale circulation and radiation in different ways (TiedTke, 1993). Because of this impaired cloud parameterization in climate and forecast models, the results from climate models are rather uncertain and influence the quality of operational weather forecast.

There are several types of clouds, which are an important part of the earth weather. Some clouds are convective whilst others are stratiform. This may also be distinguished by their level at which

they occur which may be low, middle or upper levels (Table 2.1). They contribute largely to the atmospheric system in many forms.

- Clouds control the earth's energy balance by regulating the flow of solar radiation.
- They are a vital component of the hydrological cycle because they help for precipitation to occur.
- They help us to know the type of atmospheric processes are occurring.
- They play a major role by redistributing additional heat from the equator toward the poles.

Table 2. 1 Cloud classification and characteristics

Types of clouds	Level	Characteristic
Cumulus	Low level	Cumulus clouds grow vertical and they are cellular in nature, with flat bottoms and rounded tops. Cumulus clouds forms cumulonimbus clouds when there is adequate atmospheric moisture, and strong updrafts which causes thunderstorm and heavy rainfall.
Stratus	Low level	Stratus clouds are associated with period of light precipitation, drizzles and sometimes no precipitation. Also, develop horizontal with a grey layer of cloud cover.
Strato cumulus	Low level	These are low level clouds in the atmosphere that appear in front or ahead of a frontals system.
Alto cumulus	Mid-level	Alto cumulus clouds organize themselves in streets of clouds, with cloud axis showing rising moist air and clear zones between rows signifying locally descending, drier air. Not forgetting that they show cimulo like cirrocumulus.
Altostratus	Mid-level	Altostratus clouds are mid-levels clouds with flat and uniform texture. They are related to the forthcoming of a warm front and thicken into stratus and nimbostratus clouds resulting in snow or rain.
Cirrocumulus	High level	Cirrocumulus are layered clouds with slight cumuliform lumpiness. They usually arrange in rows of clouds in the sky representing limited areas of ascent and descent.

Cirrus	High level	Cirrus are wispy clouds made up of an ice crystal. And associated with a warm front and upper-level jet streak. Also, thicken into cirrostratus to altostratus. Which then thicken into altostratus as well as Nimbostratus.
--------	------------	--

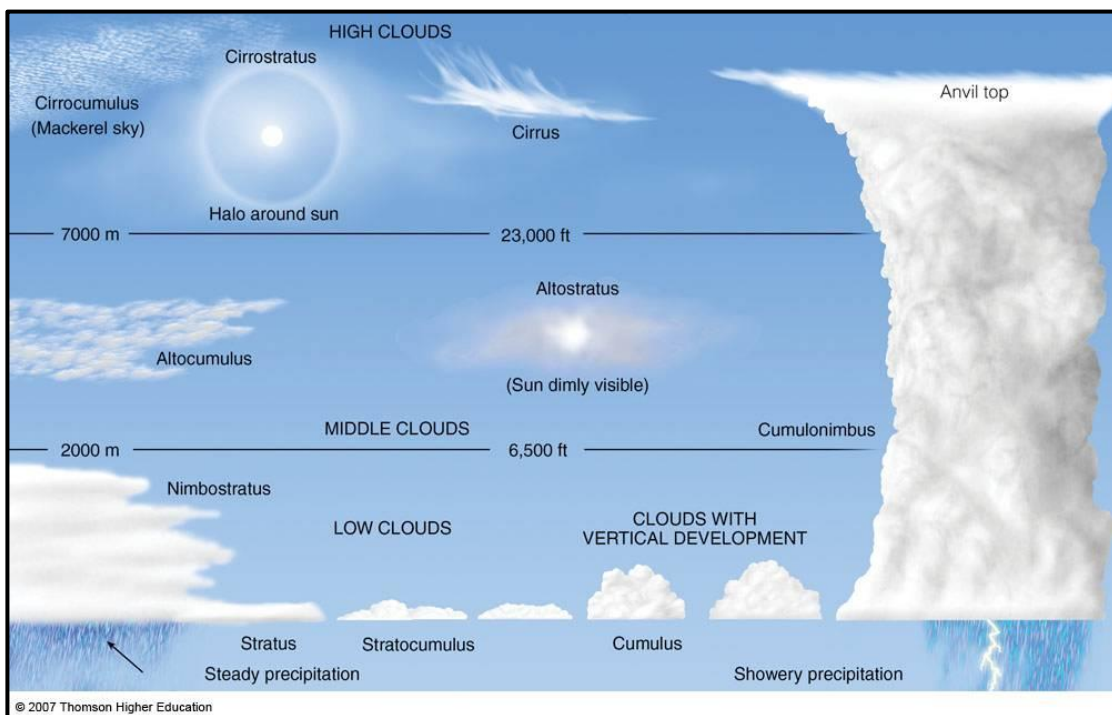


Figure 2.7: Illustration showing clouds and their level in the atmosphere (Source: Saltfleet by weather)

2.8 Cloud microphysics

The microphysical processes of clouds are at the heart of aerosol, cloud and climate interaction. During microphysical processes, aerosols that serves as cloud condensation nuclei (CCN) affect the climate by disturbing precipitation efficiency and cloud radiative processes (Solomon et al. 2007). Microphysics clouds in cooperate evaporation, cloud formation, collection of cloud particles by falling precipitation formation via coalescence, and complex induced interactions

among multiple cloud layers (Randall, 2013). They are also vital in convective clouds, because latent heat and condensate influence the cloud dynamics (Zhang and Song, 2016). The interactions between dynamical and microphysical processes complicate the impacts of aerosols on cloud and precipitation not withstanding climate.

Cloud microphysical processes are vital in the climate system since they govern the amount of detrainment of hydrometeor and water vapour from updrafts (Zhang and Song, 2016). The detrained water substance in turn affects upper –tropospheric water vapour distribution, the anvil cloud formation, and thus the atmospheric radiation budget (Zhang and Song, 2016). Convective parameterization schemes in GCMs struggle to capture microphysical processes explicitly (Randall et al, 2003).



Figure 2.8: Microphysics clouds in convective clouds (Source: Randall et al., 2003)

2.9 Methods of cloud processes in global circulation model

2.9.1 Convective parameterization

Parameterization in weather / climate models is a method of representing physical processes that are too small (cloud microphysics, aerosol) to be explicitly captured in GCM. (Lawal, 2015; Randall et al., 2013). These subgrid processes which are parametrized can be compared with the large-scale flow of the atmosphere which is explicitly resolved within the models. Parameterizations are associated with several parameters such as raindrops, convective clouds, cloud microphysics and simplification of the atmospheric radiative transfer based on atmospheric radiative transfer codes. The first conventional convection parameterization scheme was developed in 1960 to represent the collective effect of convective scheme and stratiform clouds

existing in big grid columns (Manabe et al, 2003). Cloud parametrization is based on highly idealized cloud models for entraining plume cumulus cloud and well mixed strata cumulus layers covered by discontinuous inversion (Randall et al, 2003; Lilly 1965). Convective parameterization is used with GCMs with a grid spacing of 50 km or larger (Randall, 2013).

Cumulus convection parameterization (CP) is an important parameter for rainfall forecasting. It was developed in 1960 and introduced by Charny and Eliassen (1964) and Ooyama (1964) in tropical modelling and Manabe et al (1965) in General circulation model. Since then many cumulus parameterization schemes have been developed for complete numerical weather prediction (NWP) and climate models to take into account the sub grid -scale characteristics of latent heat release and mass transport associated with convective clouds and to accurately predict rainfall (Hu ,1997). CP is widely known by its limitation in GCMs due to poor horizontal resolution which prevent them from capturing mesoscale convective systems explicitly (Kain and Fritsch 1993). Countless CP schemes have been developed to account for the collective effects of ensembles of discrete convective bubbles or plumes. Since most of CP schemes assume that deep convection only occupies a very small part of the grid.

2.9.2 Cloud Resolving Models

Cloud Resolving Models (CRMs) are high resolution models with a 4 km grid spacing or higher and have the capability to capture cloud microphysical processes and cloud system explicitly and run over a large enough domain to cover multitude of cloud cycles. CRMs are commonly used to model shallow-to deep convection as well as the transition between the two equally (Randall, 2003). The first global cloud resolving model (GCRM) that was developed is called the Non-Hydrostatic Icosahedral Atmospheric Model (NICAM), and it was tested on the Earth Simulator with a 3.5km grid spacing in Japan (Tomita et al., 2005). CRMs can simulate the in-depth spatial input needed for parameterization. CRMs output can be utilized to inform the development parameterizations. For instance, microphysics and radiation parameterization schemes use input of cloud fractional cloudiness (Randal, 2013). Parameterization of microphysics needs information on cloud scale vertical velocity analysed with entraining plume model (Donner et al, 2011). CRMs use the first principle approach to modelling the dynamics of cloud processes with the exception of cloud microphysics which is still highly parameterized. It has been demonstrated by several studies that CRM results outperformed results of other models (Khairoutdonov et al, 2004). CRM is also used to study the atmosphere where observation are deficient, and the findings be used to improve convective parameterization schemes (Grabowski et al., 2006).

GCMs struggle to simulate convective updrafts and mass fluxes and are not capable to treat precipitation ice species explicitly. GCMs prevent mesoscale and microphysical processes to feed back to the large scale (Grabowski et al., 2000). CRMs have a better chance at improving microphysics processes simulations, which are suitable to tropical deep convective clouds studies and their detrainment to anvils. CRM can serve as a tool to improve GCM errors when used as super parameterization in GCM (e.g., Khairoutdinov and Randall 2001; Benedict and Randall 2009).

Microphysical processes play a crucial role in the formation and breakout of cloud and precipitation particles (Bopape, 2013). Condensation is a microphysics process that converts water vapour to cloud water, whilst increasing the atmospheric temperature through the release of latent heat (Bopape, 2013). Several CRM employ bulk of microphysics parameterization (BMP) which uses a specified functional form for the particles size distribution and predict the particle mixing ratio (Graboski, 2008).

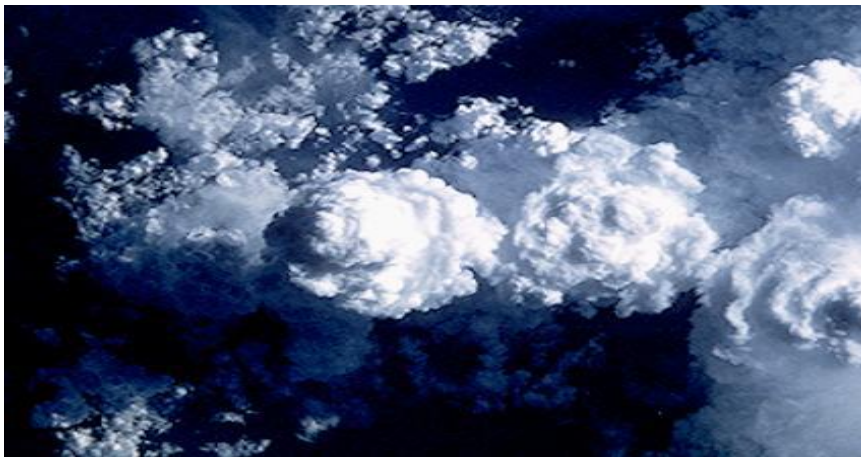


Figure 2.9: An over view of microphysics parametrization (Source: Morrison, 2010)

2.9.3 Super parameterization

Super parameterization (SP) may be defined as “a method to global atmospheric modelling that lies midway among convective parameterization and GCRMs” Randall (2003). It was developed by Grabowski and Smolarkiewicz (1999) and was called “cloud resolving convection parameterization. It was proposed by Randall et al., (2003) for use as the solution to the cloud parameterization deadlock. The SP grid convection was represented by introducing CRMs in each grid column of a GCM (Figure 2.1), thus, accruing a second resolved scale that eliminates the

necessity to make the idealized estimation used in the convection parameterizations (Randall, 2013). Super-parameterization achieves a compromise between treating clouds as an ensemble, and determining individual clouds (Randall et al., 2003). In most of the previous studies, the grid spacing used for the CRM is 4 km, and it is run inside each GCM column as shown in Figure 2.1 (Kooperman et al., 2014). The CRM uses equations to define cloud motions instead of the simpler formulations used in GCMs. SP can be used to improve the skill of climate more competently to simulate climate cheaper than Global Cloud Resolving Model (GCRM). SP has been found to improve the diurnal cycle of precipitation and reduce the rainfall overestimation over a complex topography. For more details about the improvement of super parameterization in GCM see Table 2.2.

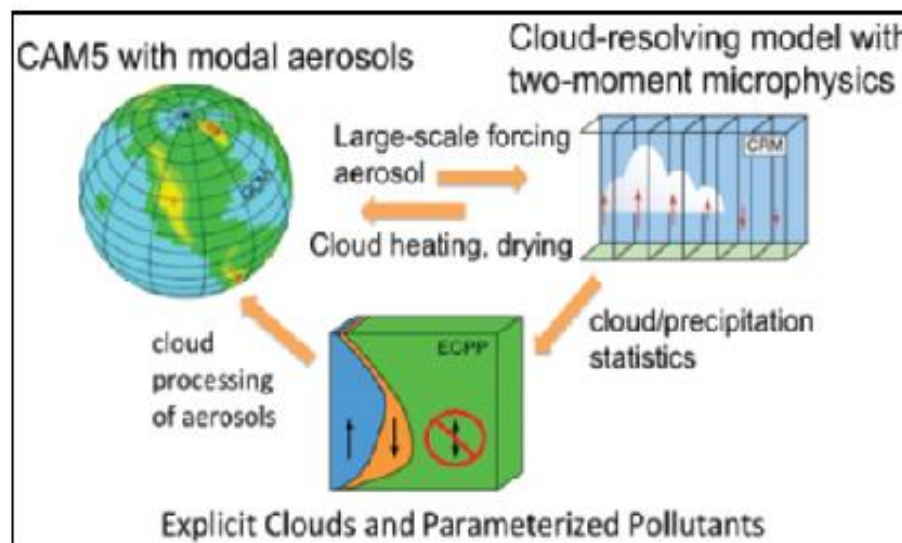


Figure 2.10: Configuration of SP CAM (Source: Randall et al, 2013)

Table 2. 2 Super Parameterization achievement to climate simulation over the past 18 years

SIMULATIONS	MODELS	RESULTS	REFERENCES
Role of moisture in the MJO	CAM, SPCAM and observation	The CAM was not able to generate a moistened atmosphere which failed to produce MJO. However, the SPCAM generated an overly moist column and produced a vigorous MJO.	Thayer-Calder, (2008)
Simulated the inputs of anthropogenic aerosols and greenhouse gases emission on clouds convection ad precipitation.	CAM and SPCAM	The SPCAM improved the variability and intensity of simulated cloud convection and representation of aerosol-cloud interaction compared to the convectonal Global Climate Model (GCMs).	Kooperman et al., (2014)
Simulated the MJO using multiple GCMs	SP-CAM, NCAR, NCEP, and GFDL models	SPCAM result showed an improvement in the simulation of MJO compared to parameterized induced GCMs.	Kim et al., (2009).
Simulated the Indian summer monsoon and monsoon intraseasonal oscillations in SP-CAM simulations.	SPCAM	The results showed enhancement over traditional GCMs, but vital problems contended to derive from unrealistic convective heating profiles simulated by the embedded CRMs.	Goswami et al. (2011)
Simulated global distribution of precipitation	SPCAM	They found that SP-CAM simulations had the best skill at representing MJO when compared to the multiple Global climate models that featured traditional representation of small-scale processes	Khairoutdinov et al., (2005)
Simulated the structure of the MJO in the super parameterized CAM.	SPCAM	Result show that the spacetime structures of the MJO were well represented in the SPCAM with progression of the free tropospheric moistening and heating that agreed with observations.	Benedict and Randall, (2009)
Simulation of variability of statistical measures to evaluate model performance at representing the MJO.	SPCAM, NCAR, NCEP, GFDL models	SPCAM was found to outperform the other GCM such as NCEP, NCAR and GDFL model in simulating MJO	Kim et al., (2009)
Simulated regional extreme precipitation	SP CAM, CAM	SPCAM was able to simulate the distribution of extreme and light precipitation events than the CAM over the continental United States.	Li et al., (2012)

2.10 Summary

This chapter reviewed literature related to the study. It examined advantages and disadvantages of seasonal rainfall forecasting over South Africa. In addition, climate models which have been used to simulate seasonal rainfall over the subcontinent were discussed. Some are GCMs whilst others are RCM focusing on their capabilities and limitations. Different parameterization schemes that are used inside GCM to simulate cloud processes are also identified in this chapter. Methods of modelling cloud processes such as those used in CRMs, GCMs using conventional parametrisation schemes as well as those using super parameterization which uses CRMs that are embedded in GCM in order to improve the simulation of clouds are presented in this chapter. Studies that have been done globally using super parameterized community atmosphere model (SPCAM) are also reviewed. It is found that climate models tend to overestimate rainfall over South Africa, making the whole country wet. Whilst GCM and RCM bring about a lot of uncertainties in simulating mesoscale and microphysics in the atmosphere. Meanwhile super parameterization studies have been found to better simulate seasonal rainfall more explicitly in other regions.

CHAPTER THREE

RESEARCH METHODOLOGY

3.1 Introduction

This chapter describes the datasets and methods used to study the climate of South Africa as simulated by an atmospheric model that uses super-parametrization compared to one that uses a conventional scheme. It provides a description of different datasets and methods of analyses that were used, including precipitation, temperature, zonal and meridional wind and Sea Surface temperatures (SSTs). The models used in this study is the Community Atmosphere Model (CAM), and the Super Parameterized Community Atmosphere Model (SPCAM). The reanalysis datasets taken from National Center for Environmental Prediction (NCEP/NCAR) are also used.

3.2 Observed data

3.2.1 Rainfall

Several rainfall datasets are used in this study. Two rainfall datasets were used in the study which served as observation for verification. The study used monthly rainfall data which was obtained from the Global Precipitation Climatology Project (GPCP) Version 2.2. GPCP combines gauge data with microwave sensed data from polar-orbiting meteorological satellites and infrared estimates from geostationary satellites (Huffman et al, 2009). The GPCP rainfall datasets are available from 1979 to present and are gridded at $2.5^{\circ} \times 2.5^{\circ}$ resolution on a monthly time scale. Many researchers in the field of climatology have used GPCP (e.g. Mulenge, 1999). This study also used daily rainfall data from the South African Weather Service (SAWS) which were used to calculate monthly and seasonal (3 months) averages, Forty (40) weather stations were available for the study but only 30 stations distributed around South Africa were selected based on data availability (no gaps) and a long record of 1987 to 2016.

3.2.2 Temperature

Maximum temperature is defined as the highest temperature of the day, while minimum temperature is defined as the lowest temperature recorded diurnally. The study used quality controlled daily minimum and maximum temperature from SAWS climate data base. The climate databank of the SAWS collects, maintains and runs a quality control process of South Africa's meteorological and climate data (Phakula, 2017). The stations temperature data are used to calculate monthly and 3-month seasonal averages. Monthly mean air temperature was further obtained from NCEP reanalysis II. NCEP reanalysis II is a modernized version of the NCEP reanalysis I and consists of updated parameterization schemes and physical processes. NCEP

reanalysis 2 model consists of more accurate data, with fixed errors of the past model datasets resulting from physical processes (Kanamitsu *et al.* 2002). The model consists of datasets of global grids with varying resolutions (Kanamitsu *et al.*, 2002).

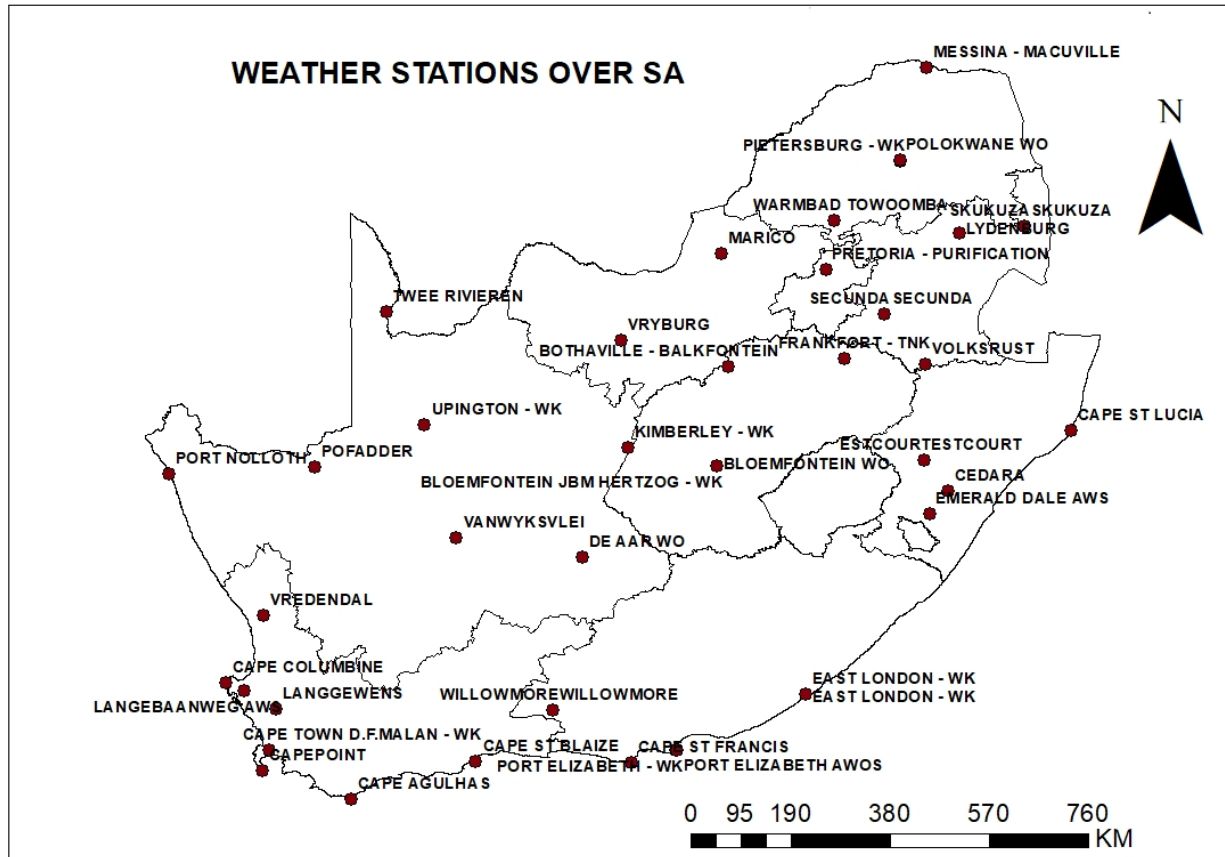


Figure 3.1: Location of SAWS weather stations around South Africa with at least 90% data availability from 1987 to 2016.

3.2.3 Sea surface temperatures

Sea surface temperature (SSTs) is the temperature of water close to the ocean's surface and is more considered in the study of ocean - atmosphere and dictates the connections of heat, gases and momentum amongst the ocean and the atmosphere (Tennant, 1999). Monthly optimally interpolated sea surface temperatures (OISST) datasets were obtained from NCEP reanalysis II. OISSTs was analyzed to show the evolution of the different phases of ENSO such as canonical El Niño and El Niño Modoki (Reynolds *et al.*, 2002) as one of the objective in the study to evaluate the simulated response of the South African climate to different phases of El Niño Southern Oscillation (ENSO) using SP-CAM.

3.3 Reanalysis and derived variables

Reanalysis circulation parameters such as vertical velocity, geopotential height, zonal and meridional wind, mean sea level pressure are investigated at the surface and at 500hPa (Table 3.1). In this study circulation parameters from NCEP reanalysis II were analyzed to validate CAM and SPCAM datasets in reproducing the climate of south Africa.

3.3.1 Vertical velocity

Vertical velocity (Omega) is a useful parameter to determine the rise or fall of air. Data is obtained from the NCEP/NCAR reanalysis II and visualized via Grid Analysis and Display System (GrADs).

Vertical velocity (ω) may be defined as,

$$\text{Equation} \quad \omega = \frac{Dp}{Dt}.$$

Where Dp is the change in pressure and Dt is the change in time. Since pressure decreases monotonically with height in the earth's atmosphere, ω is negative for uplift and positive for subsidence. In the study, vertical velocity is used for CAM and SPCAM validation to identify typical weather system associated with heavy rainfall and drought event over the South African region.

3.3.2 Mean Sea Level Pressure

Mean Sea Level Pressure (MSLP) average atmospheric pressure at mean sea levels. MSLP shows patterns of high pressure and low-pressure systems. In the study MSLP datasets were obtained from NCEP reanalysis II from the period of 1987 to 2016 and visualized via GrADs. MSLP datasets are then compared with CAM and SPCAM datasets obtained from Colorado State University (CSU) for the same period.

3.3.3 Wind

In this study wind vectors are analyzed at different important levels (e.g. 850 hPa and 500 hPa) for model (CAM and SPCAM) validation in reproducing the mean climate of southern Africa. The study also maps wind vectors during wet and dry seasons.

Zonal wind (u) is a significant atmospheric flow consisting of west to east components (latitudinal). Whereas, meridional wind (v) is a large-scale atmospheric flow consisting of a south to north components (longitudinal) (Xulu, 2017). Wind circulation patterns have been used by many researchers (e.g., Mwafhuliwa, 1999; Chikoore 2016).

3.3.4 Geopotential height

Geopotential height represents the height of a pressure surface in the atmosphere. Geopotential height can show highs and lows in the upper air and may help identify weather systems that have triggered high amounts of rainfall or drought in a region. Areas of high geopotential height are characterized by a warm column of air whilst areas of low geopotential height are associated with cold column of air between the middle levels and the surface (Mbokodo, 2017). In this study mean geopotential height is analyzed for model validation (CAM and SPCAM) at 850hPa and 500hPa in reproducing the mean climate of south Africa as well as ENSO events during wet and dry season. Geopotential height data was obtained from NCEP/NCAR reanalysis II. The NCEP /NCAR reanalysis II geopotential height has as resolution of $2.5^\circ \times 2.5^\circ$ global grids and the data start from January 1948 till present. Geopotential height can also be expressed through the following equation:

$$h = z_2 - z_1 = \frac{R_d \bar{T}_v}{g} \ln \left(\frac{p_1}{p_2} \right)$$

Where, z_1 and z_2 are geometric heights at pressure levels p_1 and p_2 , respectively. R_d is the gas constant for dry air, \bar{T}_v is the mean virtual temperature of the layer and g is gravity.

3.3.5 Relative humidity

Relative Humidity (RH) is a measure of the amount of water vapor in the atmosphere. It is the ratio of the mass of water vapor in the air relative to what the air can hold at the same temperature and is usually expressed as percentage. McIntosh and Thon (1978) defined RH as the quotient between saturation vapour pressure and vapour pressure at a corresponding temperature. The datasets are obtained at $2.5^\circ \times 2.5^\circ$ resolution and are available online from <https://www.esrl.noaa.gov/psd/data/since/1948/>. In this study the RH dataset was used to validate CAM and SPCAM in reproducing the climate of south Africa.

3.3.5 Planetary boundary layer

Planetary boundary layer (PBL) is the lowest layer of the troposphere. The PBL influences the hydrological cycle, ocean and cloud processes. Weather and climate models struggle to simulate PBL processes since most of the processes occur at sub grid scales when compared to typical climate and weather prediction horizontal grid scales. PBL data from the period of 1987 to 2016 for the reanalysis was obtained from the European Centre for Medium Range Weather Forecast (ECMWF) ERA-interim reanalysis. The ECMWF enhanced their reanalysis datasets ERA-40 by

using an improved atmospheric model and assimilation technique to create ERA-Interim (Driver, 2014). They have managed to correct errors of the previous dataset (Driver, 2014). The ECMWF PBL data used in the study have a spatial resolution of $0.5^\circ \times 0.5^\circ$ for the period of 1979 to the present and is available in both monthly and daily timescale. Furthermore, it was used to validate the performance of CAM convective scheme and super parameterized convection scheme in simulating the climate of south Africa.

3.4 Description of models

In this study simulations made with CAM and SPCAM for the period of 1987 to 2016 were obtained from Colorado State University (CSU). The 30-year climate simulation was analysed, and the analyses were made for the austral summer and winter seasons defined as December - February (DJF) and June - August (JJA) respectively but simulations were made for the whole year.

CAM is the atmospheric component of the fully Coupled Community Earth System Model (CCESM), consisting of an interactive ocean, sea ice, and land surface models (Lawal, 2015; Kooperman et al., 2016). CAM uses a convective cumulus parameterization to represent cloud scale processes (Collins et al., 2006). It is run as a separate atmospheric GCM and forced by monthly mean SSTs and sea ice boundary conditions from observations or CCESM output with an interactive land surface. The first simulations were performed with a conventional convection scheme (e.g. Lawal, 2015; Randall 2013). SP CAM is a modified CAM with more mathematics per simulated day than CAM and devours time but not as much as Global Cloud Resolving Model (GCRM) (Kooperman et al., 2016). The SP-CAM uses a two-dimensional (2D) cloud-resolving model (CRMs) instead of conventional parameterizations of the CAM for boundary layer and cloud processes in each atmospheric grid column (Randall et al., 2003; Stan et al., 2010). The CRM is inserted in each grid column of the CAM in order to simulate cloud processes explicitly. SPCAM also replaces the convective and boundary layer parameterization used (Randall et al., 2003). SP-CAM has been found to be more truthful in producing variability than CAM, although the mean state was found to be less realistic in the northern hemispheric summer. SPCAM has been used by several studies (e.g. Randall et al., 2003; Stan et al, 2010; McCrary, 2012). The CAM and SPCAM model have been detailed by Kooperman et al., 2016). The CAM and SPCAM horizontal resolution used in the study is $2.5^\circ \times 1.875^\circ$.

Table 3.3 List of observation, reanalysis and simulation datasets used in the study

	Variables	Levels	Source and reference
Observation	Rainfall Air temperature	Surface Near surface	20 th Century reanalysis data provided by the physical Science Division of the Earth System Laboratory -NOAA/OAR/ESRL PSD, Boulder, Colorado, USA (Compo et al., 2011; http://www.esrl.noaa.gov/psd)
	Tmin and Tmax Rainfall	Surface Surface	South African Weather Services (SAWS)
	Nino 3.4	Surface	KNMI Climate Explore
	HAdi SST	Surface	
Reanalysis	Geopotential height Relative humidity Omega Zonal and meridonal wind Planetary boundary layer Specific humidity Mean sea level pressure	850hPa-500hPa 850hPa-500hPa 850hPa-50 0hPa 850hPa-500hPa surface 850hPa-500hPa Surface	20 th Century reanalysis data provided by the physical Science Division of the Earth System Laboratory -NOAA/OAR/ESRL PSD, Boulder, Colorado, USA (Compo et al., 2011; http://www.esrl.noaa.gov/psd)
CAM and SPCAM	Relative humidity Geopotential height Vertical velocity Specific humidity Planetary boundary layer Mean sea level pressure Precipitation rate temperature	850hPa-500hPa 850hPa-500hPa 850hPa-500hPa 850hPa-500hPa surface surface surface surface	Community atmosphere model (CAM) and super parameterized community atmosphere (SPCAM) data sets Colorado state university

3.5 ENSO Indices

Seasonal rainfall in the South Africa region is linked to phases of the El Niño Southern Oscillation (ENSO). The phase and strength of ENSO may be measured using Nino 3.4 index or El Niño Modoki index (Mwafhulirwa, 1999; Ashoek et al., 2007) and also the Southern Oscillation Index. The Nino 3.4 indices measure the difference in SSTs anomaly in the eastern equatorial and central equatorial Pacific Ocean. El Niño Modoki index is used to quantify the anomalous warming over central pacific and has a unique tripolar nature of SSTA and is defined as follows:

$$\text{Equation: } \text{EMI}=(\text{SSTA})_A-0.5*(\text{SSTA})_B-0.5*(\text{SSTA})_C \quad (1)$$

The brackets in the equation denotes the area- averaged SSTA per region, A (165°E–140°W, 10°S–10°N), B (110°W–70°W, 15°S–5°N), and C (125 °E–145°E, 10°S–20°N), respectively. El Niño Modoki index data were obtained from Japan Agency for Marine-Earth Science and Technology (JAMSTEC) whilst Nino 3.4 Index data were obtained from Royal Netherlands Meteorological Institute (KNMI).

3.6 . Methods

This section focuses on the various methods of analysis used to further understand super parameterization. Many are standard methods which have been used by scholars. These are Root mean square error, Composite analysis, correlation analysis principal component analysis.

3.6.1 Root Mean Square Error

The Root Mean Square Error (RMSE) is commonly used to measure the relationship between values performed by model and actual observed values and is usually utilized in model evaluation studies (Chai and Draxler, 2014). RMSE has been used for various purposes such as measuring model performance in air quality, meteorology, and climate research studies (Chai and Draixier, 2014). In this study the accuracy of the model output from CAM and SPCAM was testing using RMSE and it can be defined using the following Equation:

$$\text{RMSE} = \sqrt{\frac{\sum_{i=1}^n (P_i - O_i)^2}{n}}$$

RMSE has been used by many researcher's (e.g Kooperman et al, 2016; Herbst 2016).

3.6.2 Principal Component Analysis

Principal Components Analysis (PCA) or Empirical Orthogonal Function (EOF) is defined as a standard technique for visualizing high dimensional data. It minimizes the dimensionality/number of variables of datasets by maintaining as much variance as possible. This technique is applied to study spatial modes and patterns of variability together with how they change in time (space-time variance). In statistics, the description of the PCA analysis technique is categorized as a multivariate statistical technique. In this study PCA was used to show the dominant mode of SSTs variability between Canonical El Nino and El Nino Modoki.

EOF analysis is the same as performing a principal component analysis (PCA), except that the EOF method calculates both time series and spatial patterns (Driver, 2014).

3.6.3 Correlation analysis

Correlation analysis was used to measure the association between result performed by CAM and SPCAM in simulating rainfall and temperature over a 30 years period in South Africa. Correlation Analysis is also used to measure the relationship between inter-annual variability of rainfall and their relationship with global phenomena such as ENSO. According to Mwafhulirwa (1999), correlation measures the relationship between two variables and indicates how or to what extent variables are linked to each other. It does not distinguish between cause and effect, so it should be used widely to prevent incorrect analysis. The significance of low correlations is tested using p values.

3.6.4 Composite analysis

Composite analysis seeks to identify common characteristics between common events. Composite analysis is a method used in the geophysical sciences to study collective patterns and features. It minimizes the number of maps and make analysis to be easily interpreted (Mwafhulirwa, 1999). In this study composite analysis was used to compare results performed by CAM and SPCAM in analyzing different seasons and simulating rainfall and temperature forecast over SA for the period 1987 to 2016. This technique has been widely used in climate research (Jury, 1996; Mulenge, 1999; Chikoore, 2005).

3.7 Analysis software

3.71 KNMI Climate Explorer

Royal Netherlands Meteorological Institute (KNMI) Climate Explorer is a collaborative web-based climate analysis tool used to extract climate data and perform statistical analyses. Surface and upper air parameters on KNMI include those from NCEP (CFS-R), ECMWF (ERA40 and ERA Int.) and NASA (MERRA) (Chikoore, 2016). The Climate Explorer allows users to upload their own time series and investigate them; display, detrend or correlate them with a prescribed time series or climate indices (Chikoore, 2016). Statistical analyses performed include EOF and correlations with a field.

3.72 Grid Analysis and Display System version 2.0.2 oga.2

Grid Analysis and Display System (GrADS) is a software that is used to visualize and display earth science data. It was established by the Center for Ocean-Land-Atmosphere Studies (COLA) and can be used on binary, NetCDF and HDF-SDS. Some of the atmospheric variables displayed in this study has been generated through the use of the GrADS software. Monthly meteorological variables derived from CAM, SPCAM and NCEP reanalysis has been display using GrADS.

3.73 Geographic Information system

Geographic Information Systems (GIS) offers a range of statistical methods to interpolate rainfall and temperature based on data recorded at several irregularly spaced gages (Royle et al., 1981). Spatial Analyst offers three simple interpolation techniques for raster such as Inverse Distance Weighting (IDW), Spline, and Kriging. Kriging is similar to DWI in that it weights surrounding data points and have two methods such as ordinary and universal kriging (Royle et al., 1981). Ordinary kriging is widely used since it assumes that the constant mean is unknown whilst universal kriging assumes that there is an overriding trend in the data. However, in this analysis, ordinary kriging interpolation methods were employed to predict average seasonal rainfall and temperature (Tmin and Tmax) observation from SAWS for the period 1987-2016 from 28 weather station distributed around South Africa.

3.74 Summary

This chapter outlined different datasets and methods of analysis that were used to achieve the objectives of the study. CAM and SPCAM datasets used for simulation were obtained from Colorado State University. Whist dynamic and thermodynamic fields were obtained from NCEP reanalysis II. The study also used rainfall and temperature data which was obtained from the SAWS climate database and GPCP from NCEP reanalysis II for model validation. KNMI climate

explorer was used for data manipulation and visualization whilst RMSE was used to evaluate the performance of the models against observation. GrADS was used in the study to display most of the datasets that have been used.

CHAPTER FOUR

THE CLIMATE OF SOUTH AFRICA FROM A SUPER PARAMETERIZED COMMUNITY ATMOSPHERE MODEL (SPCAM)

4.1 Introduction

Summer rainfall over southern Africa is convective in nature and realistic simulation of precipitation is still a challenge for current generation models such as Global Climate Models (GCMs) and Regional Climate Models (RCMs) (Stan et al., 2010). They are usually run at a resolution where convection is not captured well by the models. Semi-empirical parameterization schemes have been used to represent the effect of cloud processes in these models (Khairoutdonov et al., 2004). Recently a procedure called super parameterization was introduced where a cloud resolving model (CRM) is embedded inside each grid column of GCM and replaces parameterization schemes (Khairoutdonov et al., 2004). In this chapter results of the standard community atmosphere model (CAM) and super parameterized community atmosphere model (SPCAM) are contrasted and compared with the reanalysis.

The CAM and SP-CAM 30 year's climate simulation were obtained from the Colorado State University (CSU).

4.2 Rainfall climatology

4.2.1 Seasonal rainfall

Figure 4.1 compares the seasonal mean of simulated precipitation by CAM, SPCAM against observed climatology of GPCP for austral summer (DJF) and winter (JJA) taken from NCEP reanalysis II. The observed rainfall for the two seasons obtained from the South African Weather Service (SAWS) observations is also shown in Figure 4.2. The observed mean precipitation indicates a high amount of rainfall over the eastern part of the region, in areas of KwaZulu Natal, Mpumalanga and the North Eastern Interior region (Figure 4.1a and 4.2a). This also includes some part of Lesotho and Swaziland whilst rainfall is observed during winter in the South Western Cape region. Summer rainfall over the subcontinent comes through tropical temperate through (TTT) while winter rainfall is produced mainly through the passage of cold fronts and cut-off-lows (Tyson and Preston-White 2000). Nevertheless, both CAM and SPCAM (Figure 4.1c and 4.1e) simulated rainfall over the South African region during DJF season, but SPCAM simulations shows a higher performance than the standard CAM for simulating summer rainfall over South Africa at seasonal timescales. CAM overestimate rainfall over the interior and central part of the

region (Figure 4.1c). The results are consistent with a study done by Stan et al (2010) who found that Super parameterized Community Climate System Model (SPCCSM) improved many shortcomings of the Community Climate System Model (CCSM) in the simulation of global distribution of mean precipitation due to a better representation of clouds in the atmospheric model. For the winter season (JJA) both configurations (Figure 4.1d and 4.1f) had a dry bias in simulating winter rainfall over the South Western Cape region in cases of low rainfall in the observations. Stan et al. (2010) also found that in the Northern Hemisphere during boreal summer, SPCAM had notable precipitation bias over the western Pacific Ocean and the Asian region. However, the study went further to use a 3-dimensional cloud resolving model (3D) SPCAM and realized that the 3D improves all shortcomings of the (2D) SPCAM. Hence, this could be the reason for SPCAM inability to realistically produce winter rainfall over the south Western Cape of South Africa due to model distortion of topographical features.

SPCAM depicts a greater performance than the standard CAM in simulating SON rainfall over the north eastern interior and central part of the south African region (Figure 4.3f). The simulation of SON rainfall in the SPCAM results is similar to the SAWS SON rainfall (Figure 4.4b). Whilst CAM had a skill in simulating MAM rainfall explained better by an RMSE of 0.66 but found to underestimate rainfall over the north eastern interior of South Africa (Figure 4.3 c). The CAM default convection scheme also indicates an overestimation of rainfall in some parts of Namibia, Mozambique, extending to the Mozambique channel during the summer season (Figure 4.1c). Meanwhile, the super parametrization convection scheme in the Model (SPCAM) indicates satisfactory values of rainfall during DJF than the standard CAM particularly in Namibia, Botswana, and Northeast of the Mozambique channel (Figure 4.3f). During SON season (Figure 4.3c) CAM was found to overestimates rainfall in the north eastern interior and the central part of south African region. This also include some part of Namibia and Botswana. Therefore, it can be concluded that SPCAM outperformed the standard CAM in simulating rainfall at seasonal timescale over southern Africa which is also shown by the RMSE values. Therefore, there is a need to account for extra expense in South Africa with the use of SPCAM to improve the climate information /seasonal climate forecast and agricultural management.

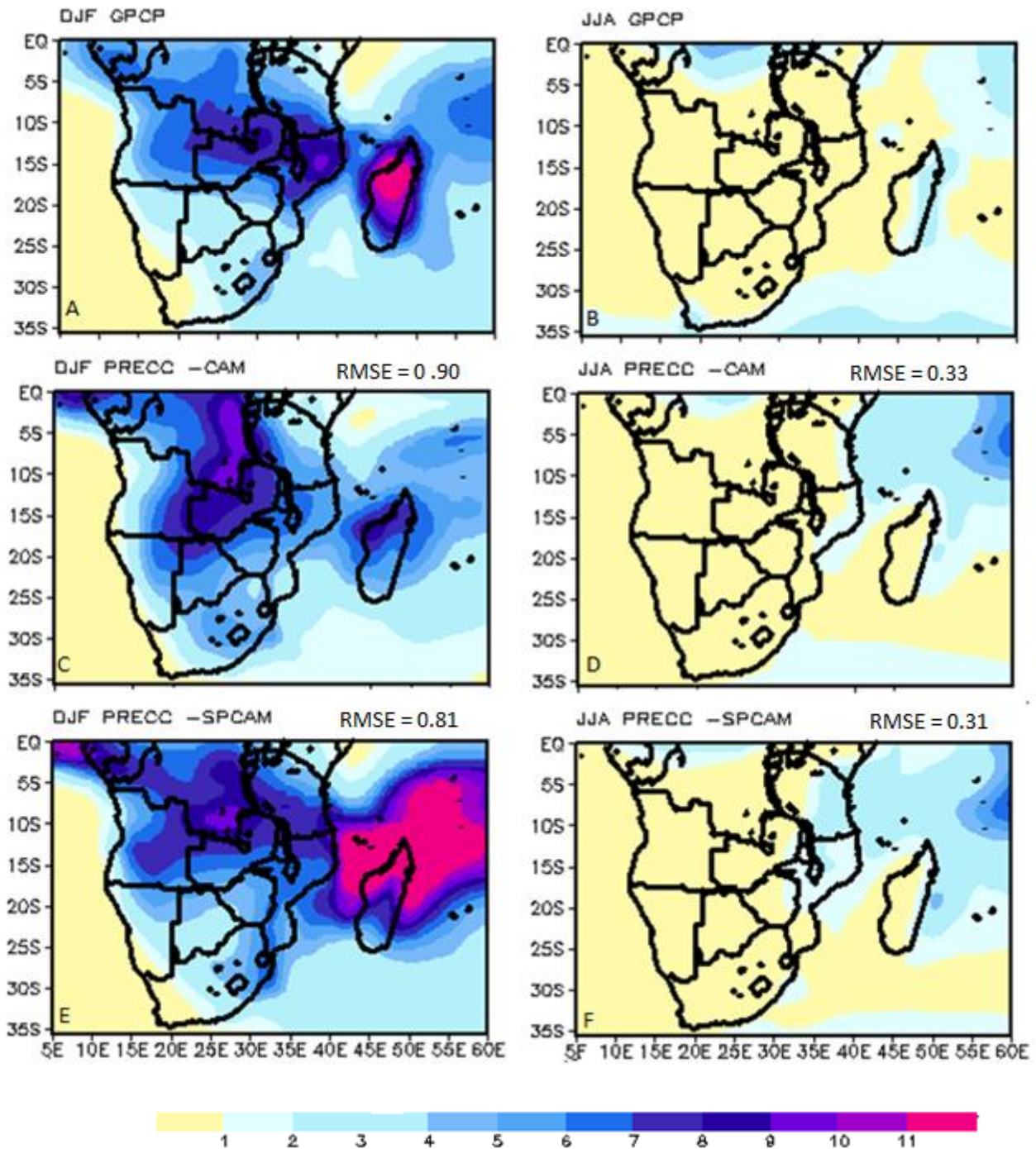


Figure 4.1: Seasonal mean precipitation (mm/day) and Root Mean Squared Error (RMSE) over southern African region for the period 1987 -2016. a) observed December-January-February (DJF) from GPCP. (b) as with (a) but for June -July-August. (c) DJF mean from CAM. (d) as with (c) but for JJA (e) DJF SPCAM (f) as (e) but for JJA.

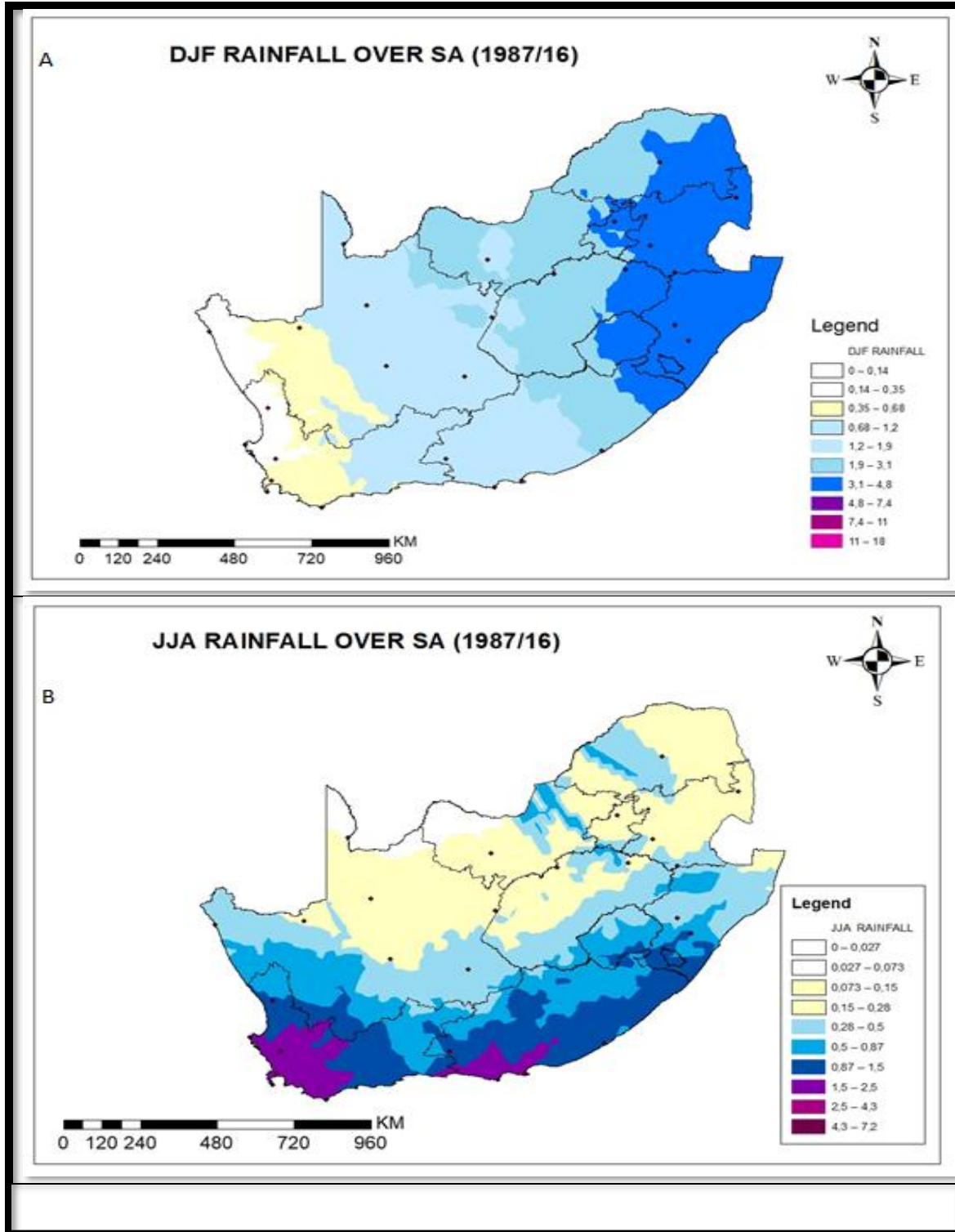


Figure 4.2: Seasonal mean SAWS rainfall (mm/day) patterns DJF and JJA for the period of 1987 to 2016 over south Africa

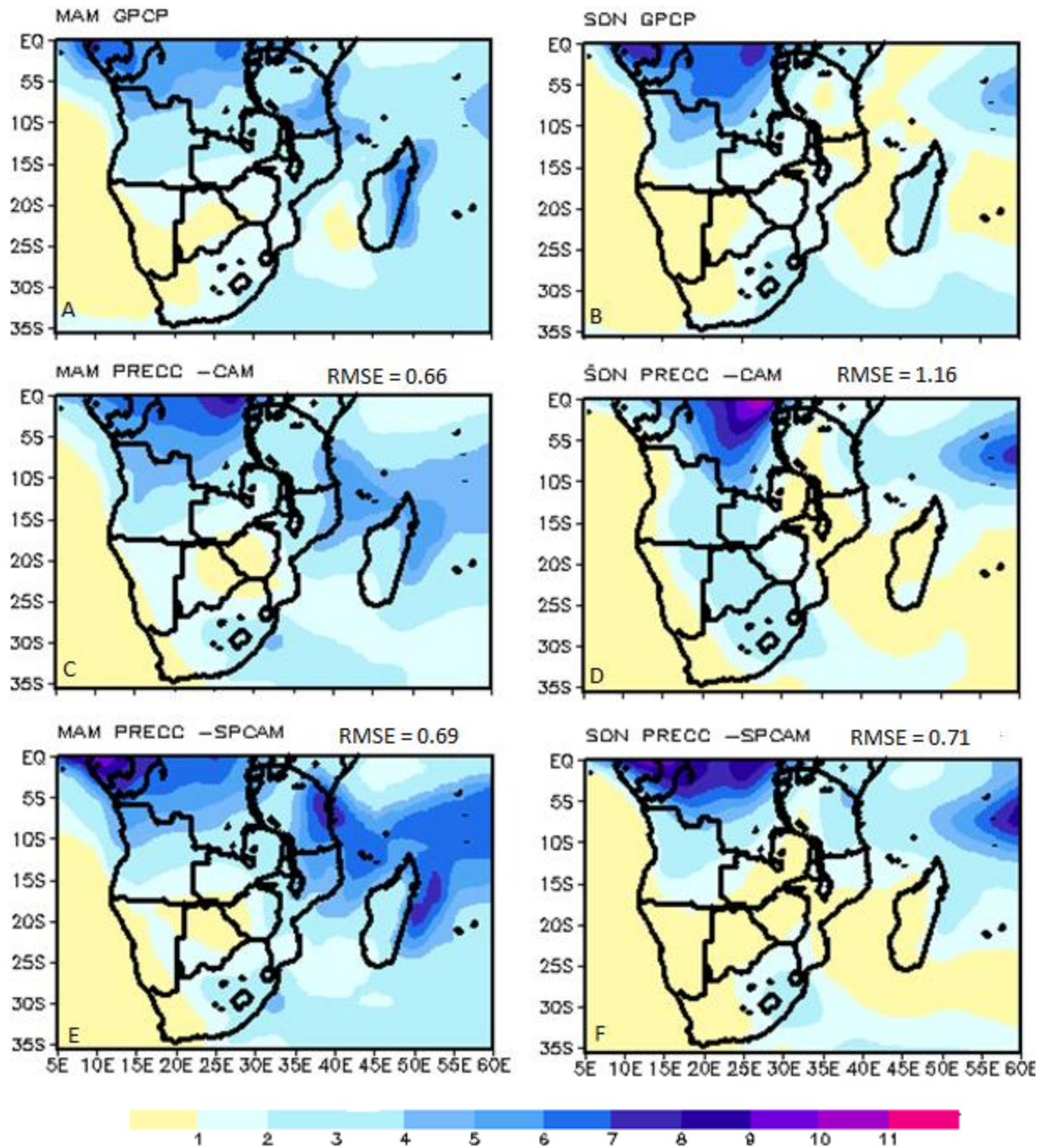


Figure 4.3: Seasonal mean precipitation (mm/day) and Root Mean Squared Error (RMSE) over southern Africa region for the period 1987-2016. (a) Observed March-April-May (MAM) from GPCP. (b) as (a) but for September -October-November (SON). (c) MAM mean from CAM. (d) as with (c) but for SON. (e) MAM SPCAM (f) as with (e) but for SON.

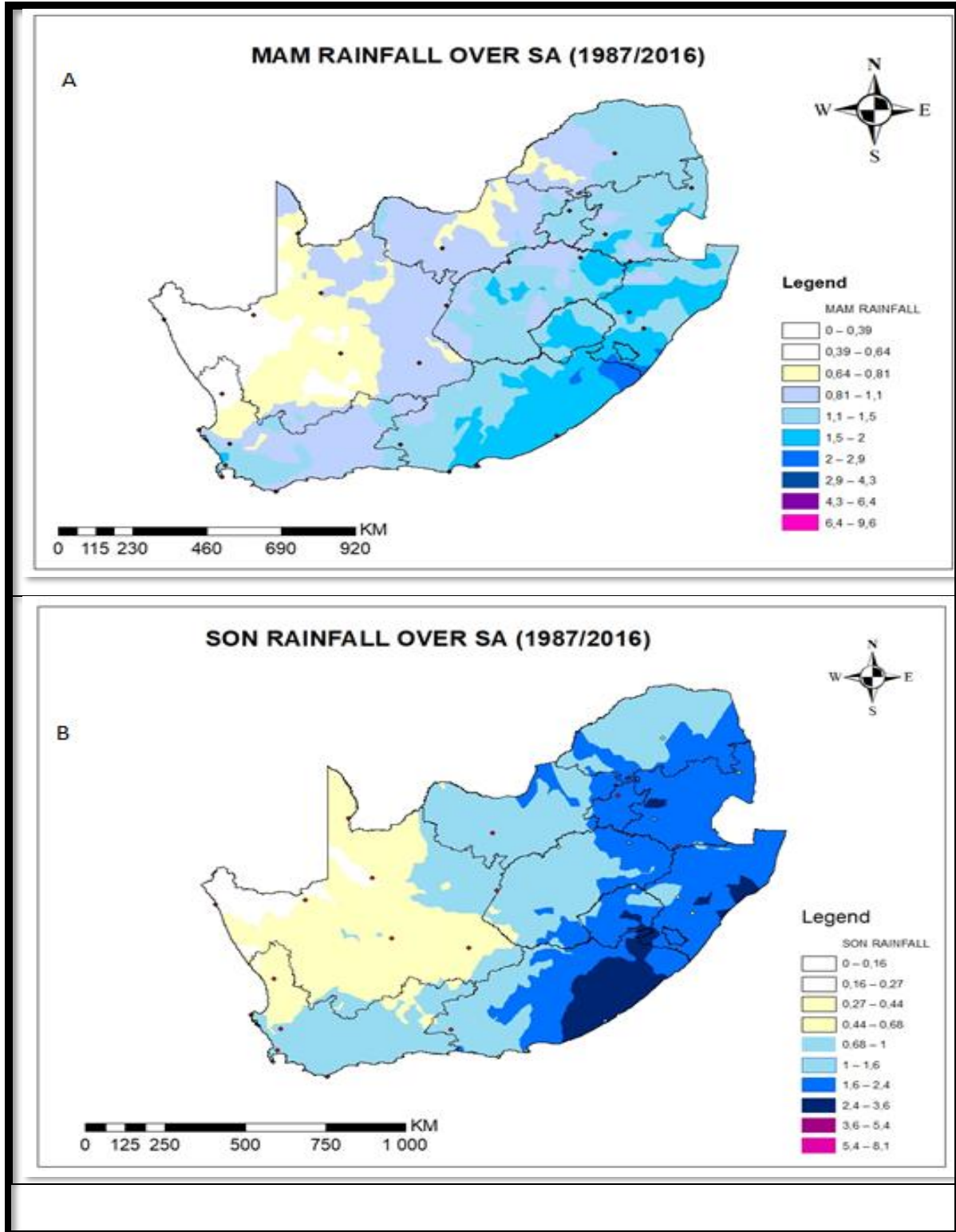


Figure 4.4: Seasonal mean SAWS rainfall (mm/day) patterns for MAM and SON for the period of 1987- 2016 over South Africa

4.2.2 Inter-annual variability

Rainfall over South Africa varies from year to year. Climate models tends to overestimate rainfall over South Africa especially where there is a complex topography basically making the whole country wet. Figure 4.6 and 4.7 compares inter-annual variability of rainfall for the homogeneous regions of South Africa (Richards and Roanault, 2003) simulated by CAM, SPCAM against GPCP rainfall taken from NCEP reanalysis II for the period 1987 to 2016. Figure 4.6a and 4.7a shows that SPCAM poorly resolved inter-annual variability of rainfall over the North Eastern Interior (Limpopo) and KwaZulu-Natal respectively. The inability of SPCAM to simulate inter-annual variability of rainfall for the above summer rainfall regions is more observed during the period of 1995/96 when the regions experienced high amount of rainfall due to La Nina season. CAM shows results which are more comparable with the reanalysis in simulating inter-annual variability of rainfall in the North Eastern Interior. In addition, SPCAM exhibited much greater skill than the CAM in simulating inter-annual variability rainfall over the Central interior, Western interior and Free State. Whilst CAM poorly resolved inter-annual variability of rainfall as it was found to overestimate rainfall when comparing the simulation against observation. In the south Western Cape both configurations underestimate rainfall simulation but SPCAM outperformed the standard CAM even in this case. It can be concluded that SPCAM has higher performance more than the CAM in simulating inter-annual rainfall variability over the summer and winter rainfall regions.

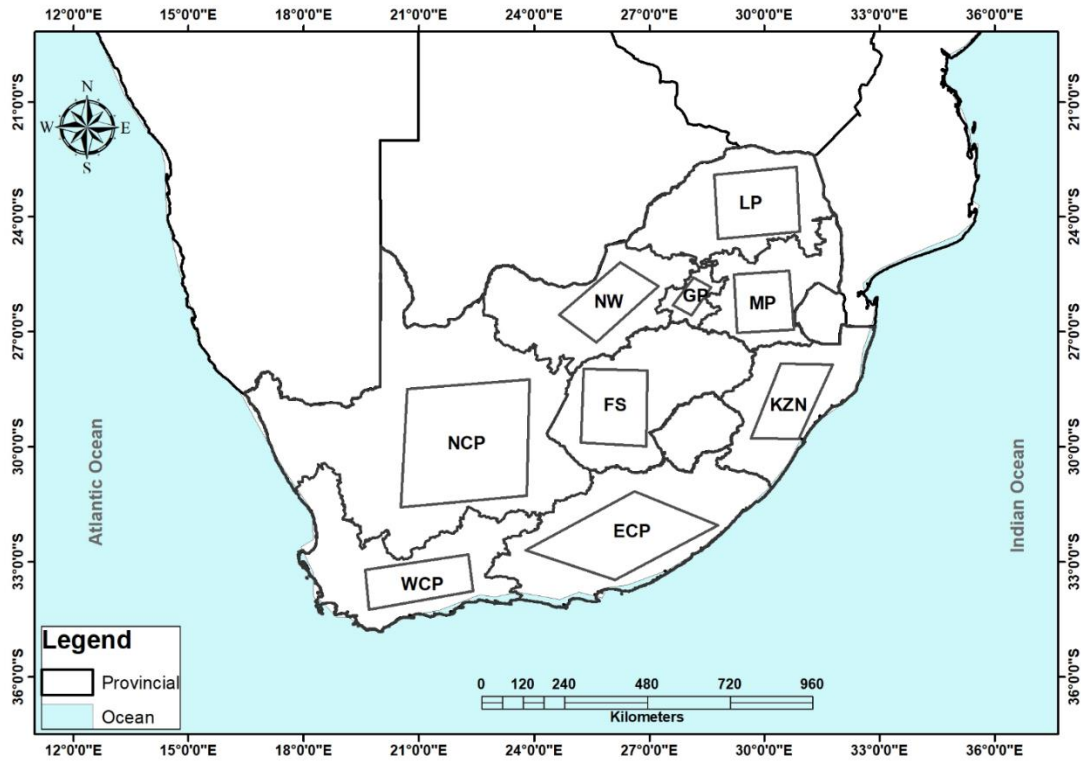


Figure 4.5: The polygons are chosen as representative of the homogeneous regions of South Africa for the analysis of area averaged rainfall as simulated by CAM, SPCAM and observation. (LP-Limpopo; MP-Mpumalanga; KZN -KwaZulu Natal; ECP -Eastern Cape; NCP-Northern Cape; WCP-Western Cape; NW- North West; GP- Gauteng; FS -Free State).

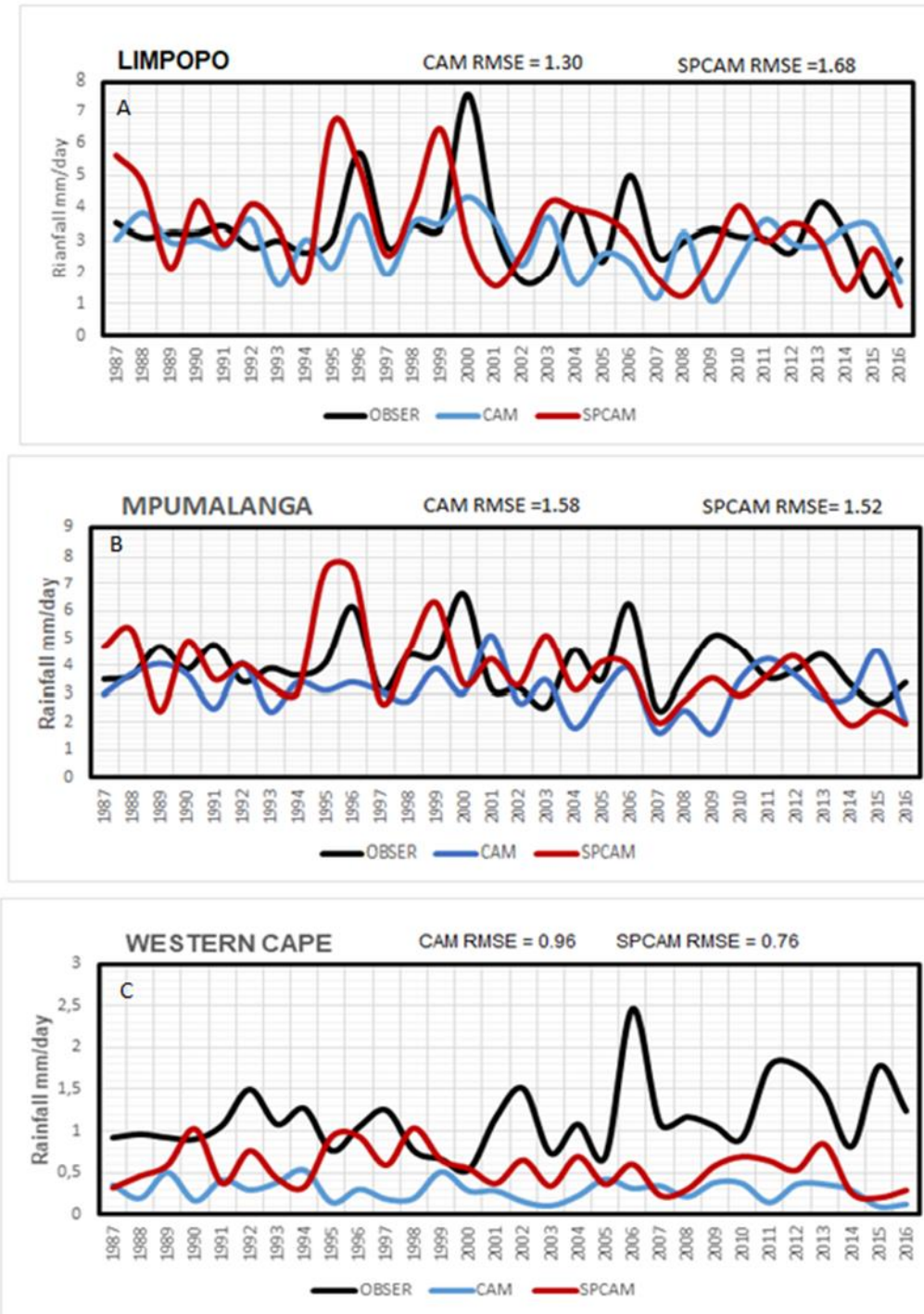


Figure 4.6: Inter-annual variability of rainfall (mm/day) and Root Mean Squared Error (RMSE) for different homogeneous regions over South Africa as simulated by CAM and SPCAM against GPCP observation taken from NCEP reanalysis II for the period 1987 to 2016.

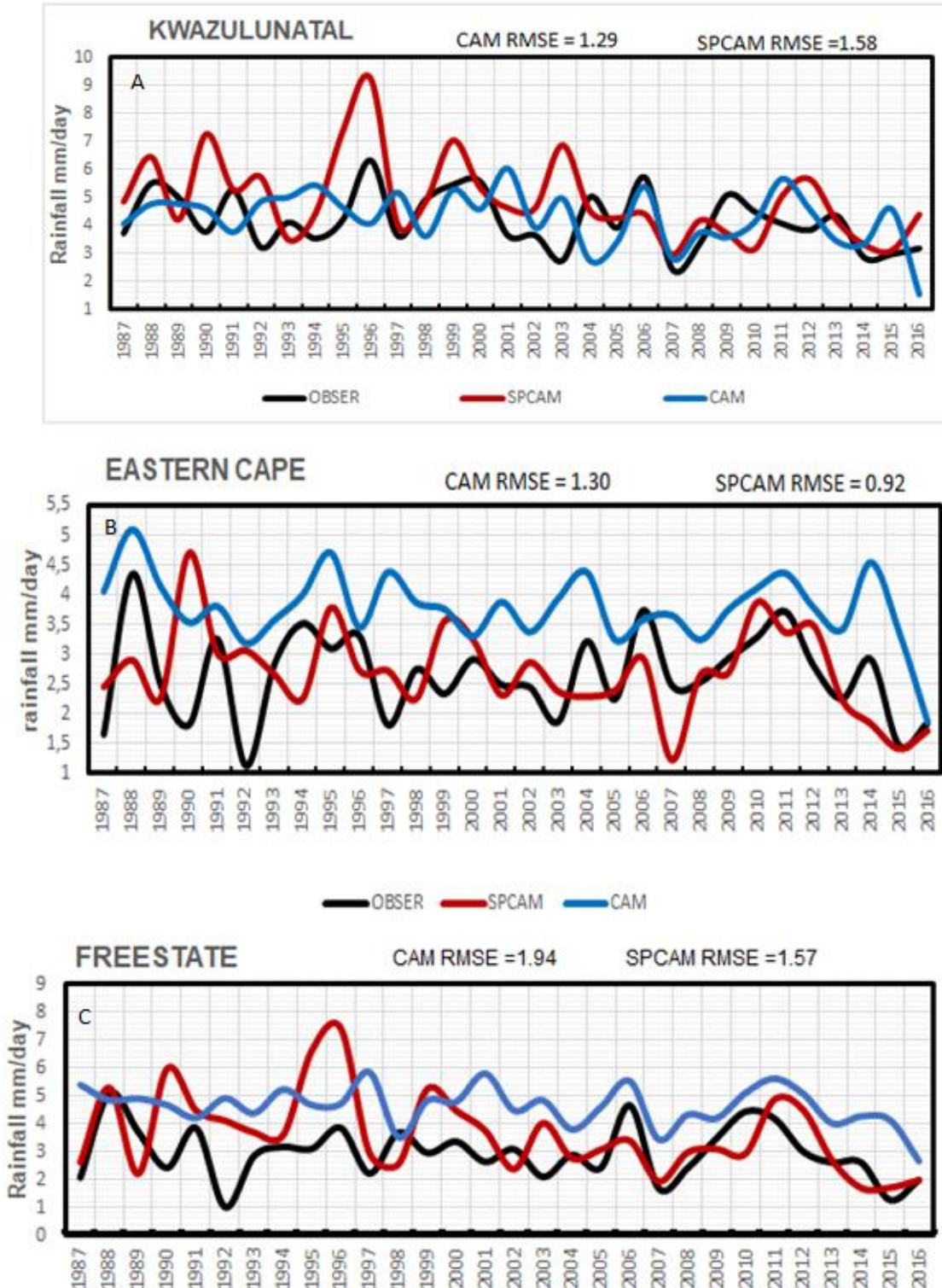


Figure 4.7: Inter-annual variability of rainfall (mm/day) and Root Mean Squared Error (RMSE) for different regions over South Africa as simulated by CAM and SPCAM against GPCP observation taken from NCEP reanalysis II for the period 1987 to 2016.

4.3 Temperature climatology

4.3.1 Seasonal temperature

Average near-surface temperatures in South Africa vary seasonally but the winters are not comparable to Northern Hemisphere winters which are colder. Figure 4.8 to 4.12 examines results performed by CAM and SPCAM with temperature observation from the reanalysis and SAWS. Areas of South Africa such as northwest experiences higher temperatures during austral summer months (Figure 4.8a and 4.9a), due to the fact that tropical air mass as well as cloud bearing impact on surface temperatures that influence short wave radiation from reaching the earth surface (Browne,2011, Tomczak and Godfrey,2003). Both CAM and SPCAM configurations (Figure 4.8c and e) simulated temperatures during austral summer (DJF) season over the subcontinent, but SPCAM show much greater skill than the CAM in simulating temperatures during DJF season particularly over the west. Moreover, CAM simulated cooler temperatures over the central part and Eastern Cape when compared to observations.

CAM also simulated temperatures of less than 24°C over Limpopo region and temperatures of less than 20°C over the eastern part of South Africa during DJF (Figure 4.8c). Meanwhile, SPCAM display temperatures of above 26°C in the Eastern Cape Province and some part of Namibia comparable to the reanalysis (Figure 4.8e). This strongly supports the review SPCAM simulations outperform the standard CAM during austral summer in simulating temperatures at seasonal timescale supported by the RMSE values. In JJA season CAM and SPCAM poorly resolved temperatures, both configurations had a cold bias particularly over the eastern part of the subcontinent (Figure 4.8d and 4.8f). In MAM season CAM had a cold bias in simulating temperatures over the south African region particularly over the eastern part whereas SPCAM shows results which are similar to the reanalysis (Figure 4.11c and e) respectively. During the SON season CAM was found to outperform the SPCAM in simulating temperatures (Figure 4.11d and e).

Much of South Africa is on a plateau which is at its highest on the eastern side where there is the Drakensberg mountain extending from Lesotho to Mpumalanga and the south of Limpopo where the peaks can go as high as 1500 m above sea level. Therefore, the distribution of minimum and maximum temperatures in summer may not be similar to that in winter as it is strongly regulated by the plateau. High values of maximum temperatures are observed over the west of the country in areas of North west whilst much of the country experience low values of minimum temperatures during winter (Figure 4.9a and b). Coldest temperatures in the region particularly in winter season tends to be determined by the terrain more than the weather systems. Figure 4.10b shows that it is very much cold in the central part of the region than it is in Limpopo. Figure 4.12b shows that much of the country experienced high temperatures during SON season than in MAM season.

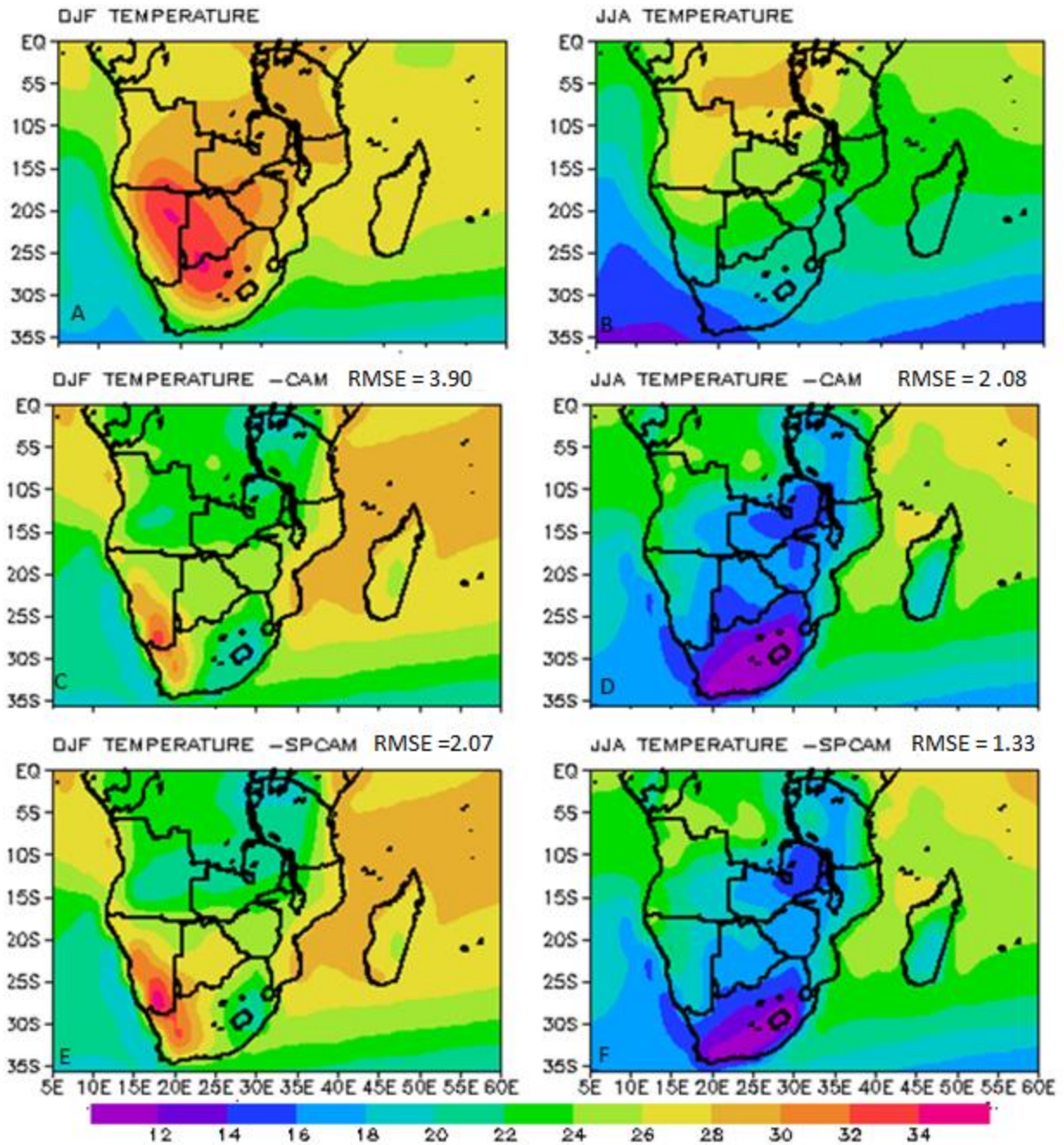


Figure 4.8: Seasonal mean temperature ($^{\circ}\text{C}$) and Root Mean Squared Error (RMSE) over southern Africa region for the period 1987 -2016. a) observed December-January-February (DJF) from NCEP reanalysis II. (b) as (a) but for June -July-August (JJA). (c) DJF mean from CAM. (d) as with (c) but for JJA. (e) DJF SPCAM (f) as with (e) but for JJA.

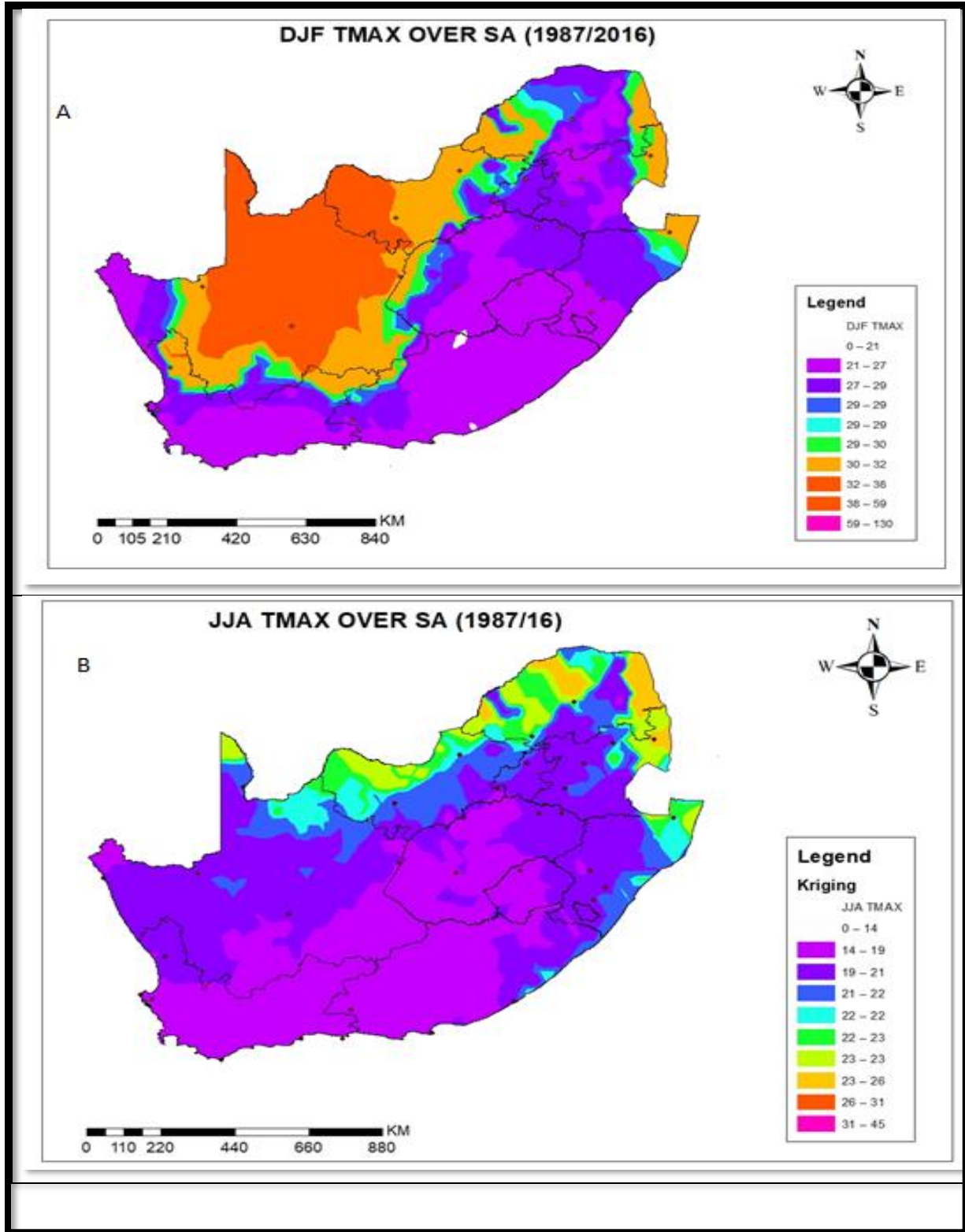


Figure 4.9: Seasonal mean SAWS Maximum temperature (Tmax C) pattern for DJF and JJA season for the period of 1987 to 2016 over South Africa.

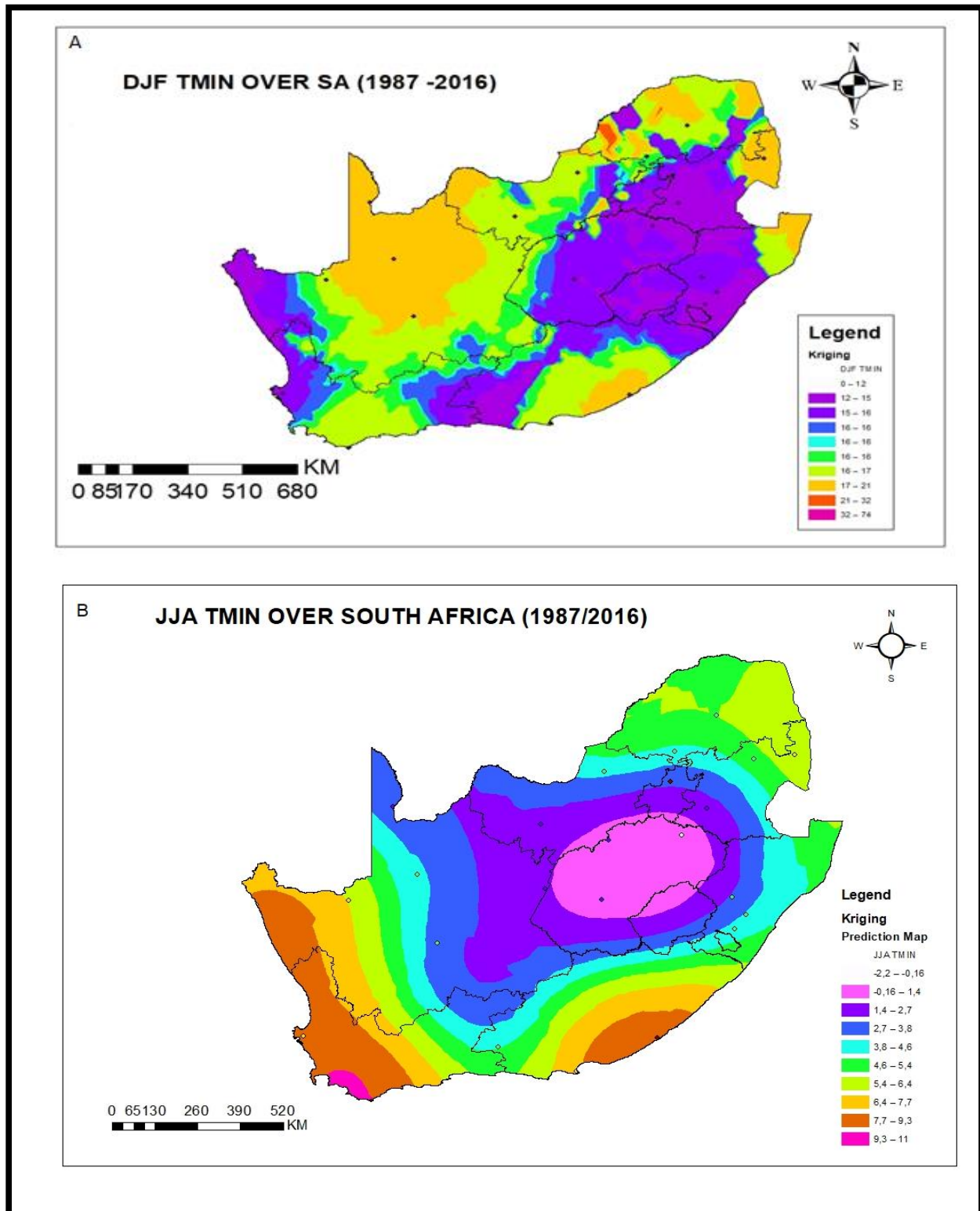


Figure 4.10: Seasonal mean SAWS Minimum temperature (Tmin C) pattern for DJF and JJA seasons for the period of 1987 to 2016 over South Africa

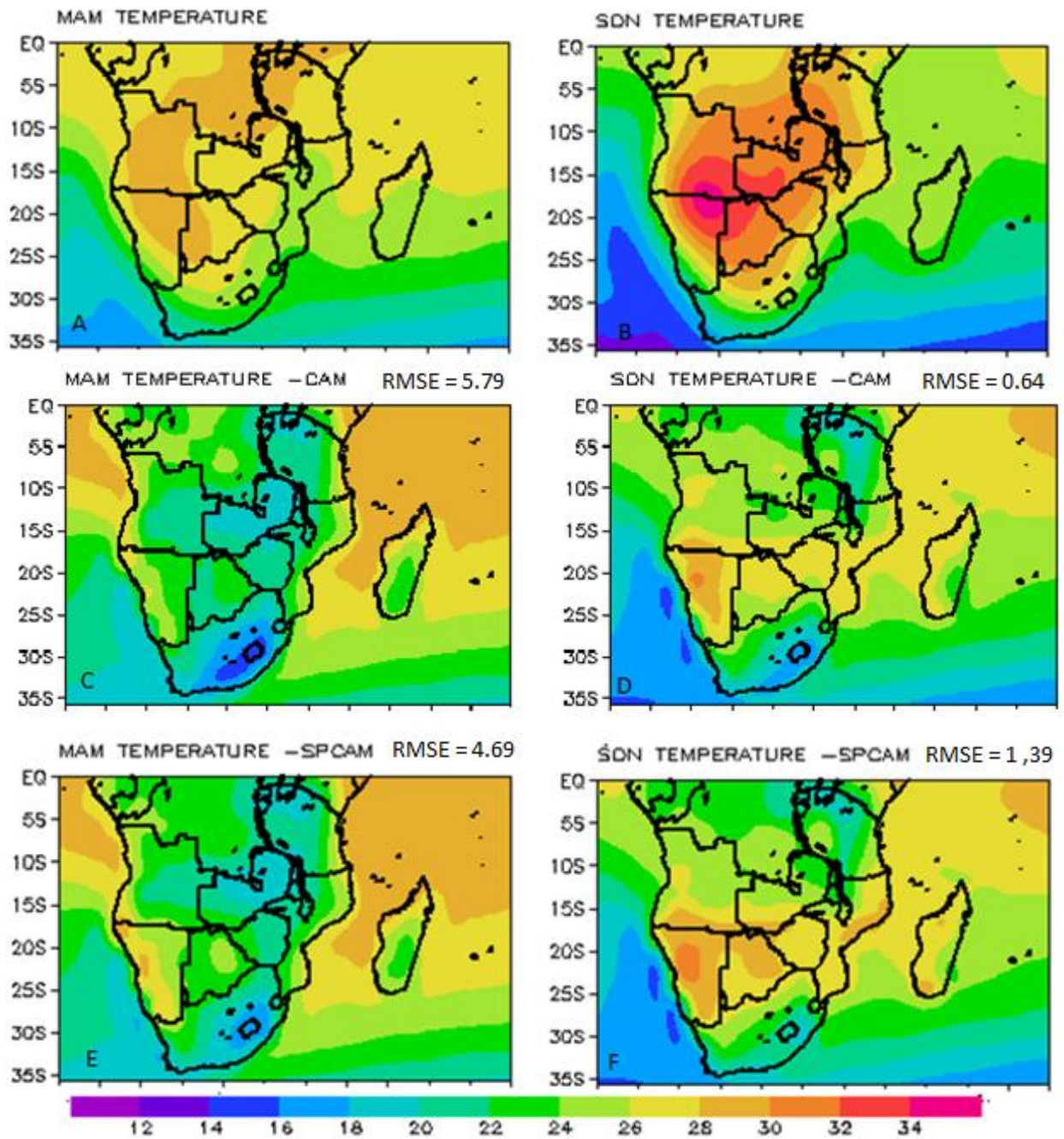


Figure 4.11: Seasonal mean temperature ($^{\circ}\text{C}$) and Root Mean Squared Error (RMSE) over southern Africa region for the period 1987 -2016. a) observed March-April-May (MAM) air temperature from NCEP reanalysis II. (b) as (a) but for September -October-November (SON). (c) DJF mean from CAM. (d) as with (c) but for SON. (e) DJF SPCAM (f) as with (e) but for SON.

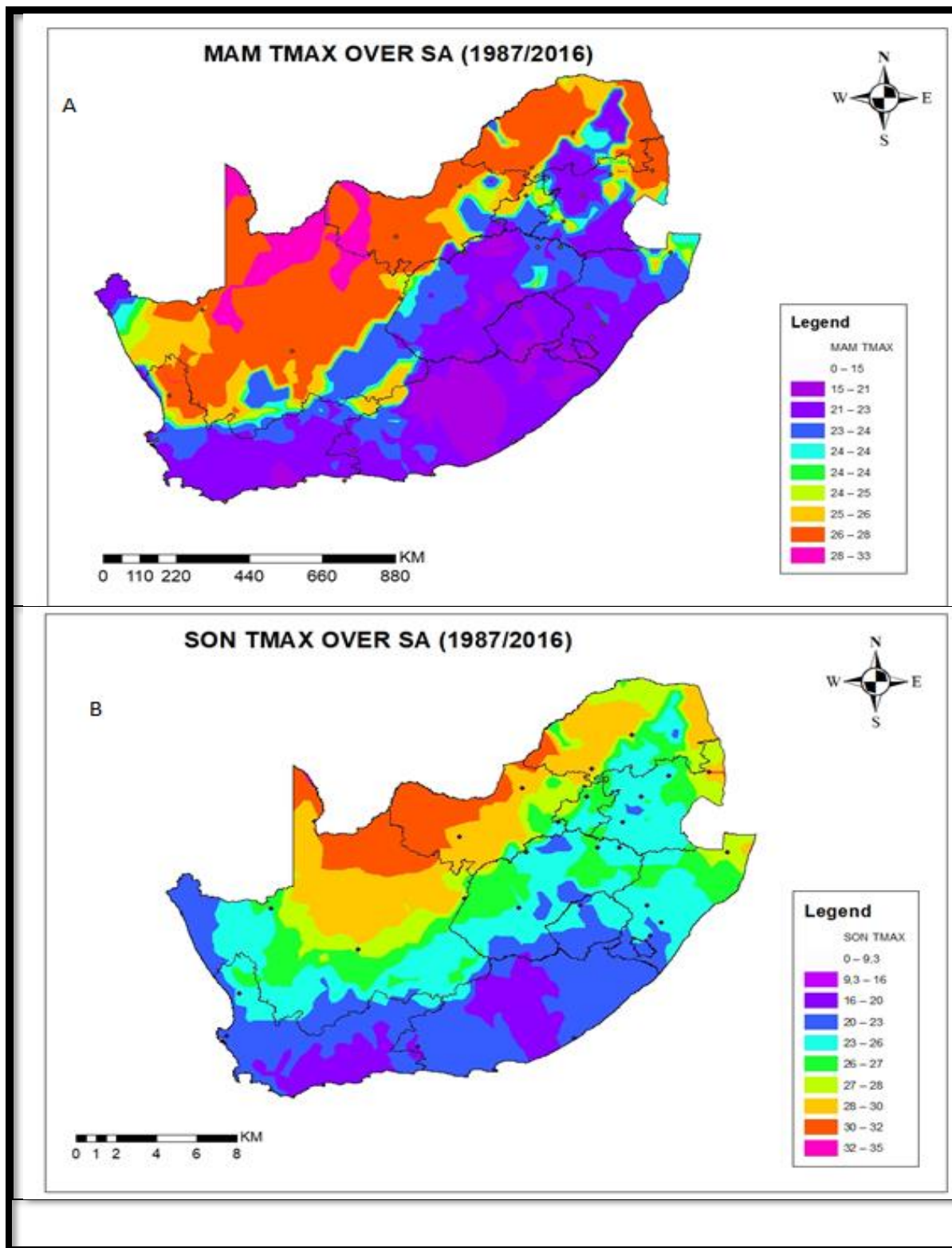


Figure 4.12: Seasonal mean SAWS Maximum temperature (Tmax C) pattern for MAM and SON season for the period of 1987 to 2016 over South Africa South African

4.3.2 Inter-annual variability

Figure 4.13 and 4.14 compare inter annual variability of temperature simulation by CAM, SPCAM against reanalysis for different regions around South Africa for the period of 1987 to 2016. Both CAM and SPCAM are found to underestimate temperatures over all the regions except the Western Cape, where CAM almost matches the observations while SP-CAM has a warm bias. In all the other parts of the country SPCAM is found to outperform CAM with its line almost always appearing in the middle of the observations and the CAM. Over Limpopo and KZN, the performance of both the CAM and SPCAM is comparable, with the two lines overlapping in a number of years. The CAM and SPCAM lines are slightly more removed from each other over the Free State. The largest cold biases for the both SPCAM and CAM are found over KZN and Limpopo, and to some extent the Free State. The cold bias over the Northern and Eastern Cape are improved by the SPCAM quite a bit. The observation for 2010 for Eastern Cape and 2011 SPCAM simulation for the Northern Cape appeared to be erroneous (Figure 14a and b).

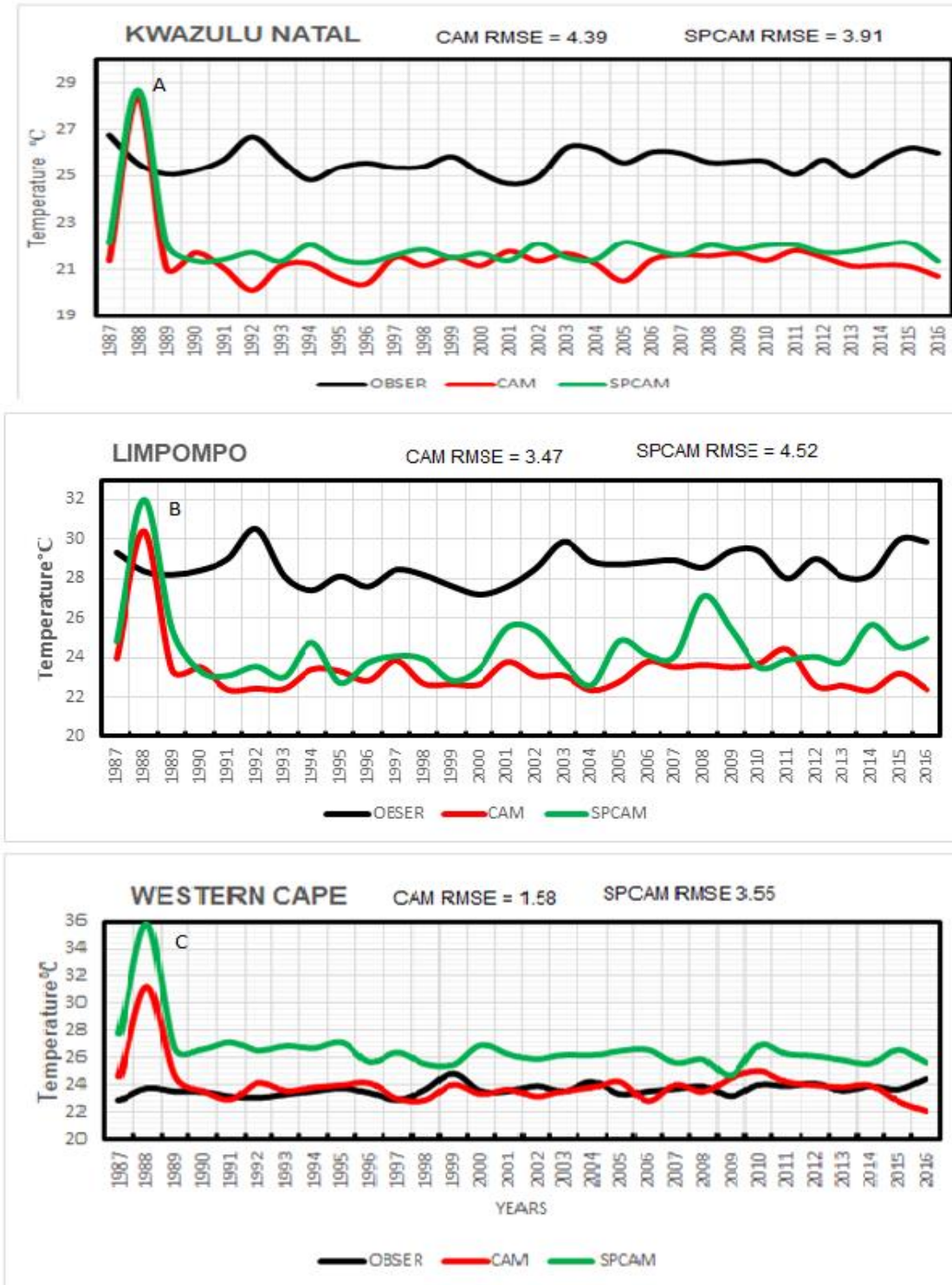


Figure 4.13: Inter-annual Variability of temperature (°C) and RMSE for KwaZulu Natal, North Eastern Interior (Limpopo) and South Western Cape as simulated by CAM, SPCAM against air temperature observation taken from NCEP reanalysis II over South Africa for the period 1987 to 2016.

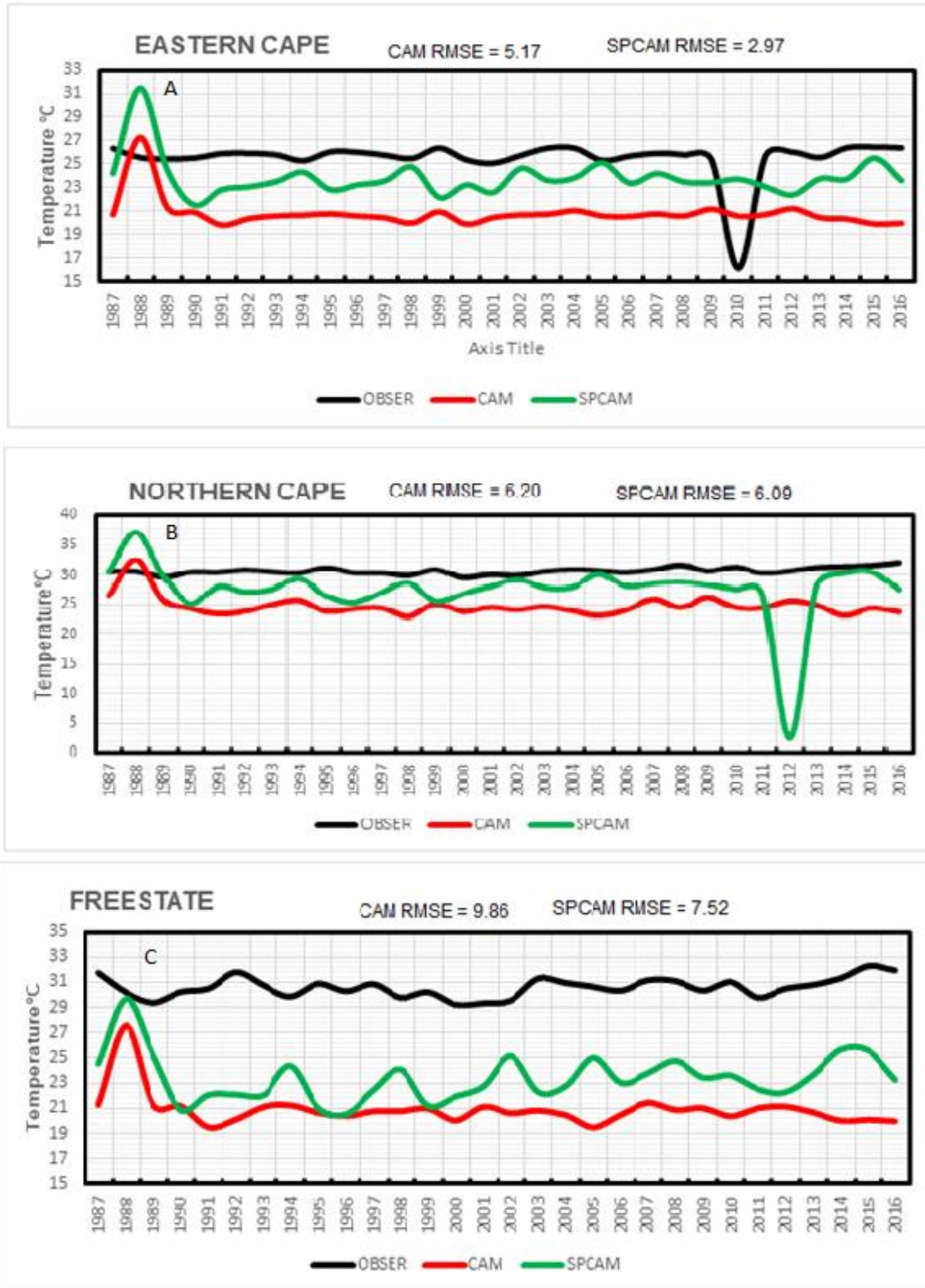


Figure 4 .14: Inter-annual Variability of temperature (°C) and RMSE for Eastern Cape, Northern Cape and Free State as simulated by CAM, SPCAM against observation over South Africa for the period 1987 to 2016

4.4 The mean circulation

4.4.1 Seasonal mean sea level pressure (MSLP)

Southern Africa climate is influenced by surface ocean currents and position of subtropical high-pressure systems (Mascarene High and St Helena High). Figure 4.15 compare results of MSLP for summer and winter seasons (DJF and JJA) as simulated by CAM, SPCAM against reanalysis. Both CAM and SPCAM configurations simulate the MSLP over the subcontinent realistically (Figure 4.15c and 4.15e) during DJF. However, CAM underestimate MSLP by about 10hPa or more over almost the entire sub-continent of southern Africa. This result corresponds with those found for precipitation where CAM was found to overestimate rainfall over the interior and eastern part of South Africa. The underestimation of the MSLP by CAM is also found for other seasons, namely MAM and SON whilst SPCAM simulation is more comparable to the reanalysis (Figure 4.16). The St Helena High and Mascarene High as well as heat low over Angola play a major role in the formation and distribution of precipitation around South African region (Reason et al, 2006). During DJF season, the high-pressure systems are located southward of the subcontinent with a trough of low pressure located over the central part and eastern part of the subcontinent (Tyson and Preston, 2000). They are characterized by moisture advection from the subtropical Indian Ocean anticyclone which results in more rainfall towards the eastern part of the region and less over the western part. In winter the Mascarene and St Helena High shifts northward and merge over the country which largely creates the dry conditions over much of the subcontinent (Tyson and Preston, 2000). MSLP modulates moisture convergence over the subcontinent (Chikoore, 2016).

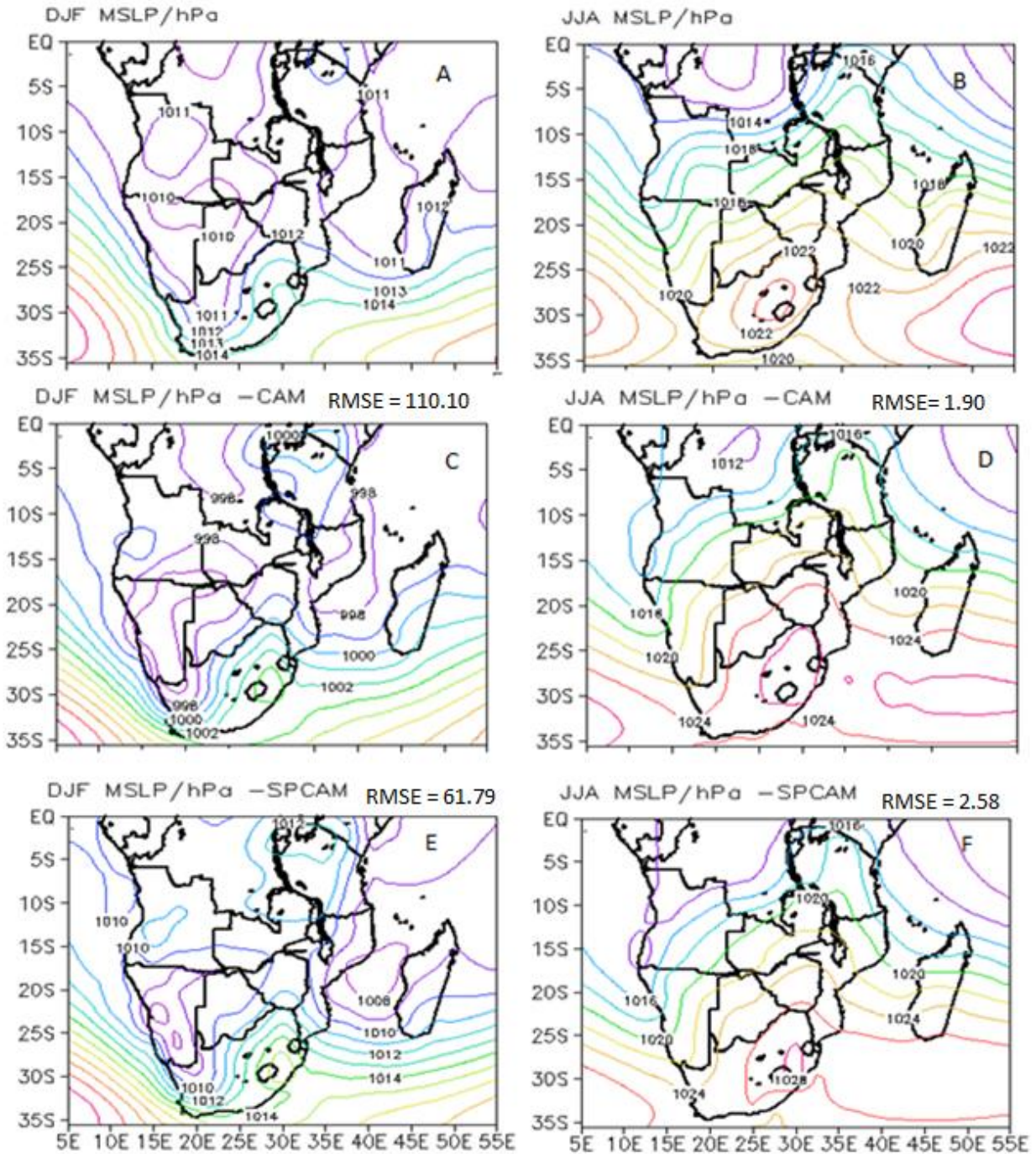


Figure 4.15: Seasonal mean sea level pressure (MSLP/ hPa) and Root Mean Squared Error (RMSE) over southern Africa region for the period 1987 -2016. a) observed December-January-February (DJF) from NCEP reanalysis II. (b) as (a) but for June -July-August (JJA). (c) DJF mean from CAM. (d)as with (c) but for JJA (e) DJF SPCAM (f) as with (e) but for JJA.

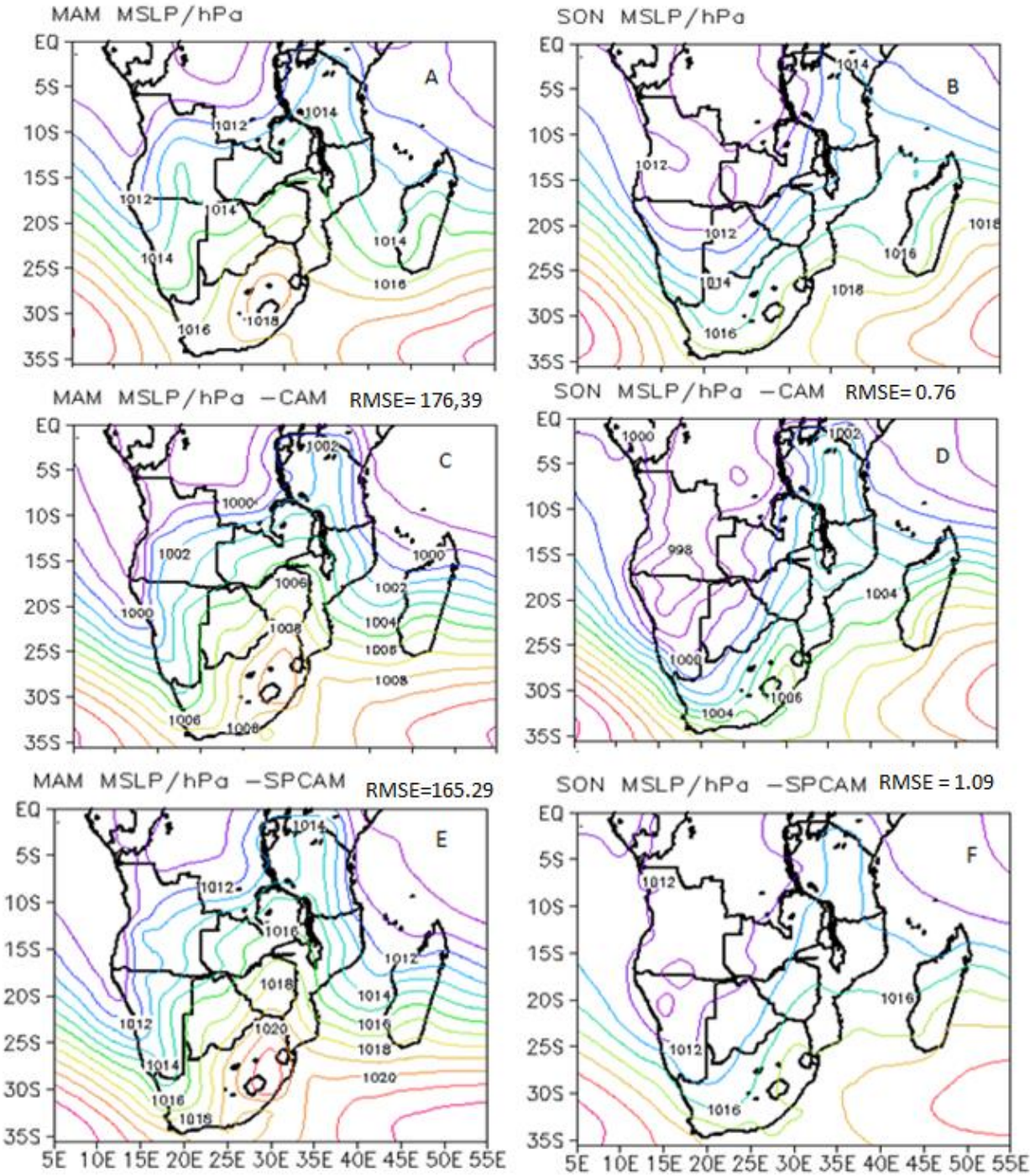


Figure 4.16: Seasonal mean sea level pressure (MSLP / hPa) and Root Mean Squared Error (RMSE) and over southern Africa region for the period 1987 -2016. a) Observed March-April-May (MAM) from NCEP reanalysis II. (b) as with (a) but for September -October-November (SON). (c) MAM mean from CAM. (d)as with (c) but for SON. (e) MAM SPCAM (f) as with (e) but for SON.

4.4.2 Seasonal planetary boundary layer height

The planetary boundary layer is the lowest layer of the troposphere where friction and exchanges of heat, moisture and momentum with the earth's surface occur. The top of this layer determines the planetary boundary layer height (PBLH), which fluctuates diurnally and seasonally. A convective boundary layer is generally associated with a higher PBLH, while stable conditions are associated with a lower one. The PBLH has a clear diurnal cycle with larger values during the day and smaller values at night when stable conditions are expected. Figure 4.17 and 4.18 shows the average PBLH of the day. Figure 4.17a shows that during summer season low PBLH is observed over the eastern part of the region in areas of KwaZulu Natal whilst high PBLH is observed over the western part in the North West, Namibia and Botswana which is consistent with high temperatures over there. It does not rain much over the western part of the subcontinent; therefore the atmosphere tends to be hot and deep. This is also an indication of stability since a warm column of air is more stable than the one which is cooling such that as a result the convection is inhibited. Figure 4.17c and 4.17e shows that CAM and SPCAM simulated PBLH during DJF season but SPCAM simulation exhibited a much greater skill than the standard CAM simulation. If the models (CAM and SPCAM) poorly resolved temperatures, there is a whole bunch of variables that will be affected of which in this case is the PBLH since it depends on the skill of the model to simulate temperatures. In this study CAM was found to poorly resolve MAM temperatures whilst SPCAM had low skill in simulating SON temperatures. Therefore, these results correspond with CAM and SPCAM's inability to realistically simulate MAM and SON PBLH respectively. SPCAM was found to overestimate PBLH over the interior of South African region during SON season (Figure 4.18 f) whilst CAM was found to underestimate the PBLH over the eastern part of the region during MAM season (Figure 4.18 c).

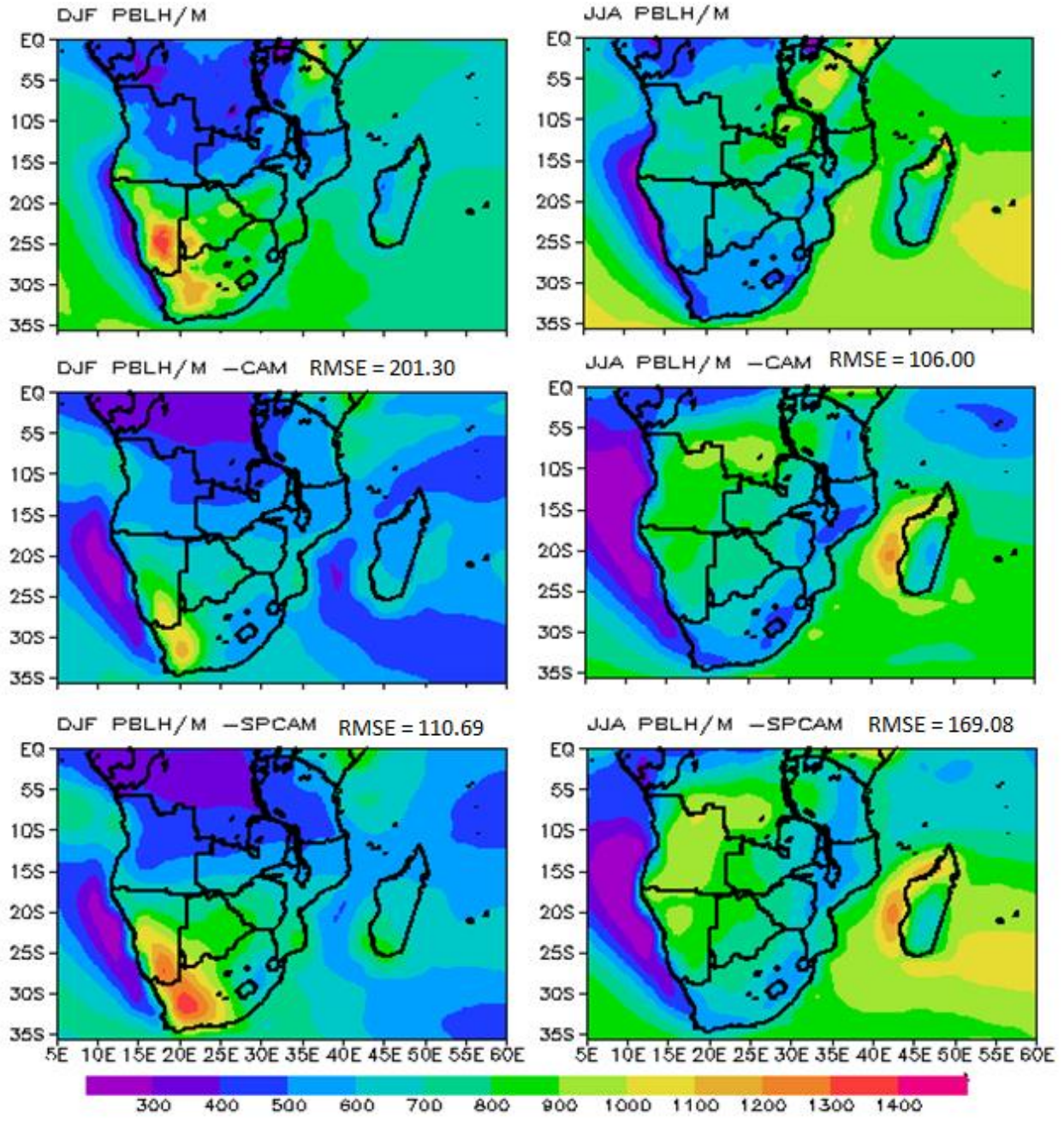


Figure 4.17: Seasonal planetary boundary layer height (PBLH /M) and Root Mean Squared Error (RMSE) over southern Africa region for the period (1987 -2016. a) observed December-January-February (DJF) from NCEP reanalysis II. (b) as with (a) but for June -July-August (JJA). (c) DJF mean from CAM. (d) as with (c) but for JJA. (e) DJF SPCAM (f) as with (e) but for JJA.

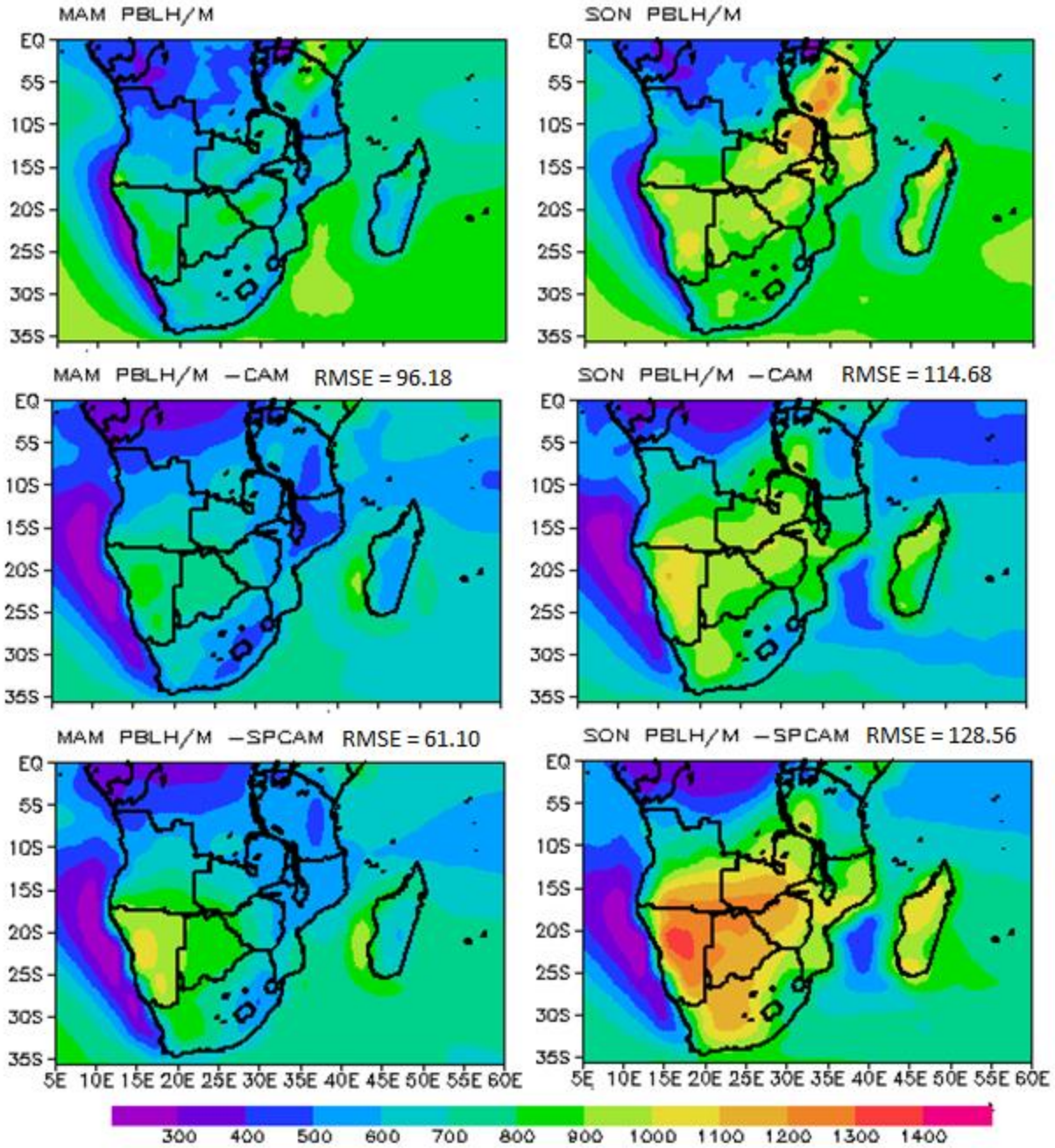


Figure 4.18: Seasonal planetary boundary layer height (PBLH / M) and Root Mean Squared Error (RMSE) over southern Africa region for the period 1987 -2016. a) observed March-April-May (MAM) from NCEP reanalysis II. (b) as with (a) but for September -October-November (SON). (c) MAM mean from CAM (d) as with c but for SON (e) MAM SPCAM (f) as (e) but for SON.

4.4.3 Geopotential height and wind vectors (850 hPa and 500 hPa)

Figure 4.19 and 4.20 shows the geopotential height with corresponding wind vectors at the surface and 500 hPa levels as simulated by CAM, SPCAM against observation. Figure 4.19a shows that at the low levels the subcontinent is dominated by low pressure systems. There is the Angola Low centered over Angola and northern Namibia, a trough over the Mozambique Channel and a low-pressure system over the North West Province during DJF season (Figure 4.19a). In addition, the St Helena high over the South Atlantic Ocean and the Mascarene high over the south West Indian Ocean are also observed. Whilst at the middle levels the Botswana high is observed over central Namibia and western Botswana during austral summer (Figure 4.20a) with westerly wind. Although both configurations (CAM and SPCAM) poorly resolved the high over western Botswana and central Namibia during DJF season, the SPCAM simulation indicates a greater skill more than the standard CAM in simulating geopotential height over the subcontinent (Figure 4.20c and f). The Botswana high is a mid-tropospheric anticyclone that modulates rainfall variability over southern Africa depending on its strength and position (Driver, 2014). A stronger than usual Botswana high is associated with dry weather conditions due to subsidence (Chikoore, 2016; Ratna et al., 2013). During JJA season CAM and SPCAM poorly resolved the geopotential height, (Figure 4.19d and f). As with other seasons namely MAM and SON, there is a much greater skill in simulating geopotential height over SPCAM than the standard CAM (Figure 4.21 and 22). The SPCAM was also found to outperform the standard CAM in simulating the winds filed, wind rotates in an anticlockwise direction along a high-pressure system (Figure 4.19a and 4.20f). In DJF season the subcontinent is under the influence of easterly wind whilst offshore over the west (Chikoore, 2016).

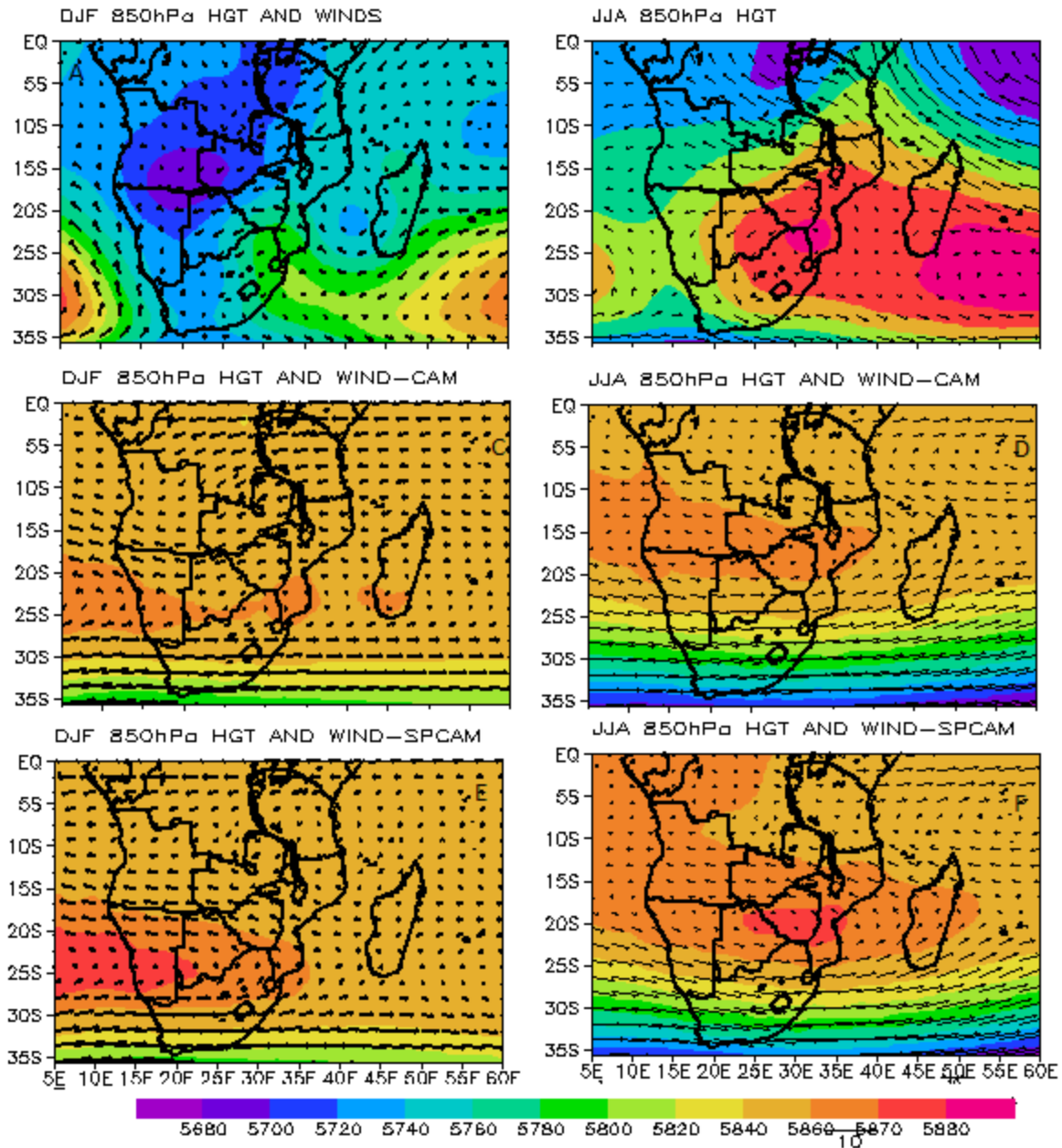


Figure 4.19: 850hPa Geopotential height and wind (m/s) over southern Africa region for the period 1987 -2016. a) observed December-January-February (DJF) from NCEP reanalysis II. (b) as with a) but for June -July-August (JJA). (c) DJF mean from CAM. (d)as with c) but for JJA. (e) DJF SPCAM (f) as with (e) but for JJA (a scale vector is shown)

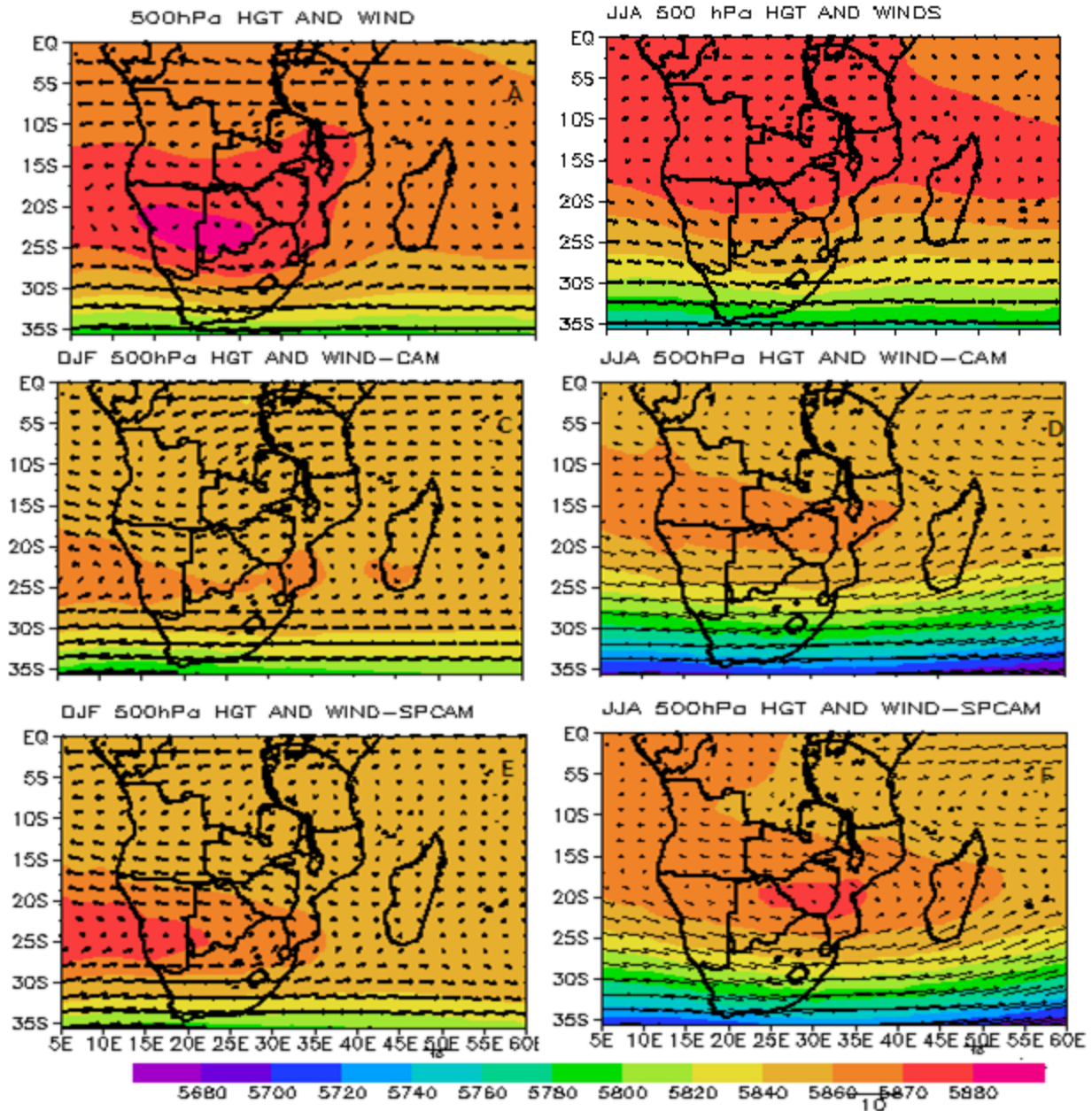


Figure 4.20: 500hPa geopotential height and wind (m/s) over southern Africa region for the period 1987 -2016. (a) observed December-January-February (DJF) from NCEP reanalysis II.(b) as with (a) but for June -July-August (JJA). (c) DJF mean from CAM (d) as c) but for JJA. (e) DJF SPCAM (f) as with (e) but for JJA (a scale vector is shown)

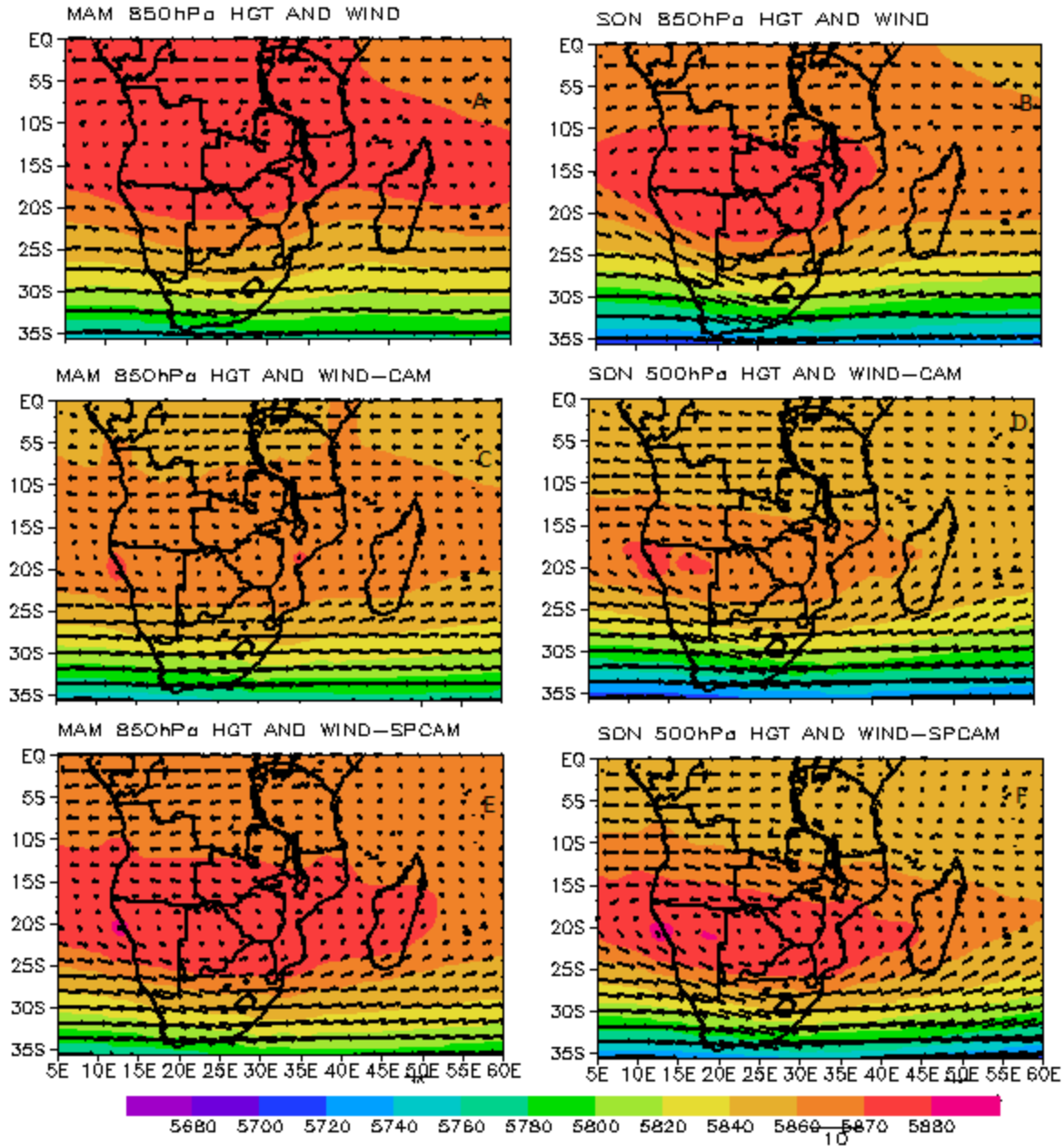


Figure 4.21: 850hPa geopotential height and wind (m/s) over southern Africa region for the period 1987 -2016. a) Observed March-April-May (MAM) from NCEP reanalysis II. (b) as with (a) but for September -October-November (SON). (c) MAM mean from CAM. (d) as with (c) but for SON. (e) MAM SPCAM (f) as with (e) but for SON (a scale vector is shown)

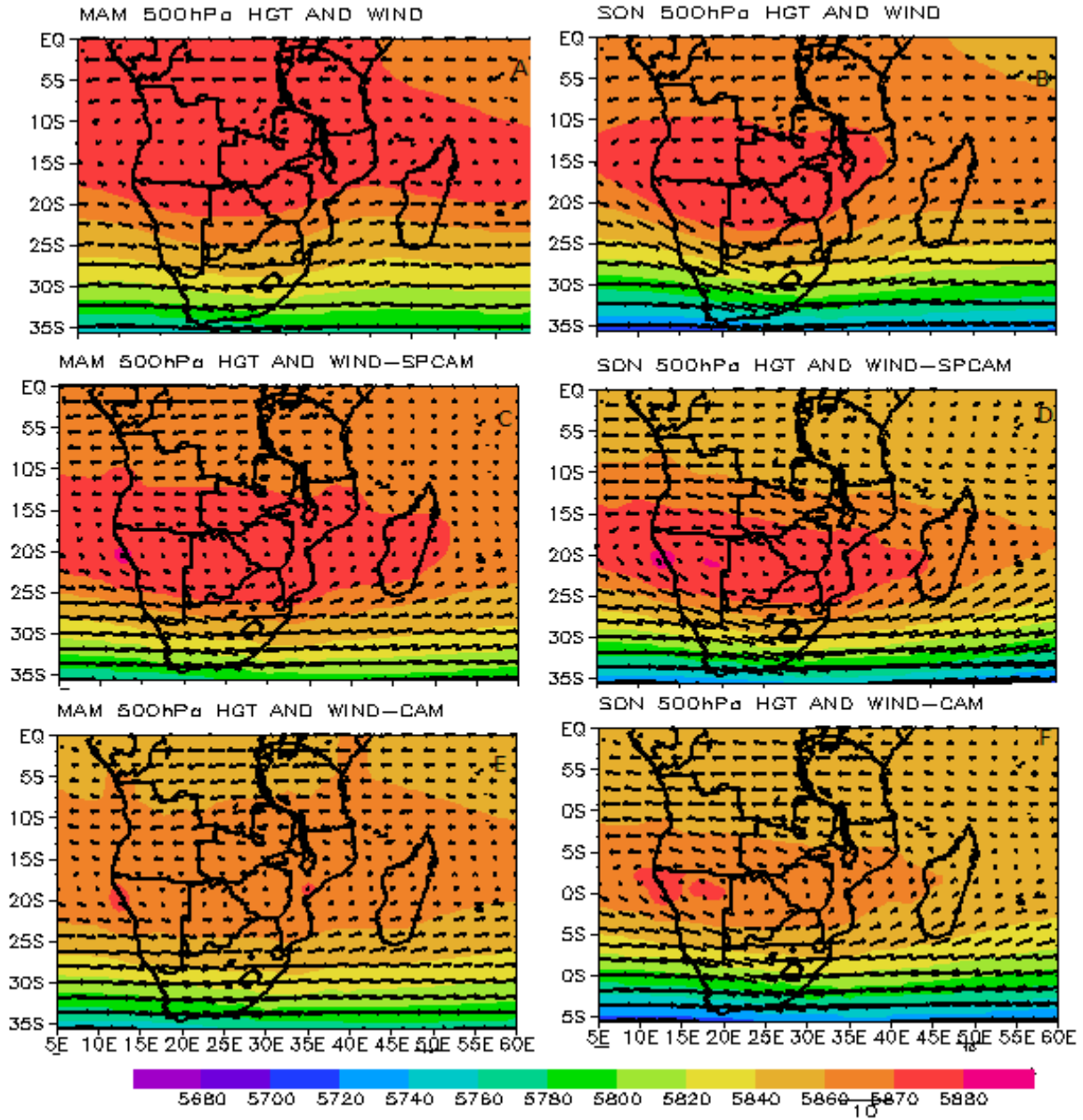


Figure 4.22: 500hPa geopotential height and wind (m/s) over southern Africa region for the period 1987 -2016. (a) observed March-April-May (MAM) from NCEP reanalysis II.(b) as (a) but for September -October-November (SON). (c) DJF mean from SPCAM. (d) as with (c) but for JJA. (e) MAM CAM (f) as with (e) but for SON (a scale vector is shown)

4.4.4 Omega and specific humidity (500hPa and 850hPa)

Figure 4.23 and 4.24 indicate that CAM and SPCAM had skill in simulating omega during austral summer season over the South African region, but the SPCAM parameterization exhibits much greater skill than the standard CAM. SPCAM simulated the observed pattern whilst CAM indicated more convergence over the central and eastern part of the region in areas of KwaZulu-Natal. This also includes some parts of Lesotho and Swaziland. This result corresponds with those found for precipitation where CAM was found to overestimate rainfall over the interior and eastern part of South Africa

In the JJA season a frontal belt is observed over the south Western Cape indicates the passage of cold fronts and cut-off flows that brings winter rainfall over the South African region (Figure 4.23b and 24b). Figure 4.23b indicates that there is subsidence in much of the subcontinent during JJA in the observation but being exaggerated by both configurations (CAM and SPCAM). The configurations show high values of positive omega (Figure 4.23d and f) since they are neglecting orographic lifting. In addition, both CAM and SPCAM poorly resolved the frontal belt over the South Western Cape, although they tried to simulate part of it over the North Western Cape. This result also corresponds with those found for precipitation where both configurations had a dry bias in simulating winter rainfall in cases of little rainfall in the observation.

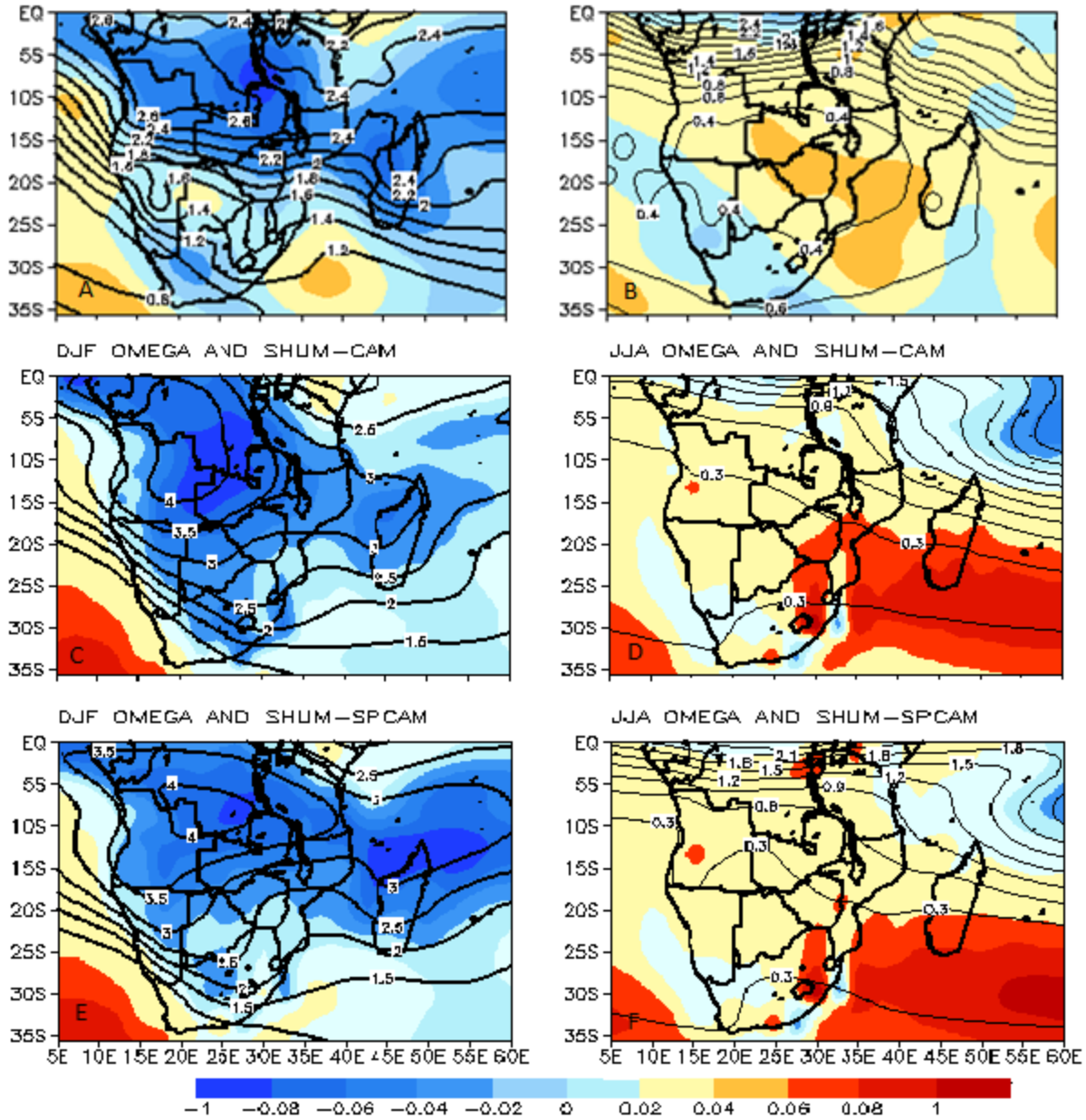


Figure 4.23: 850 omega (Pa/s) and specific humidity (kg/g) over southern Africa region for the period 1987 -2016. a) Observed December-January-February (DJF) from GPCP. (b) as with (a) but for June -July-August (JJA). (c) DJF mean from CAM. (d) as with (c) but for JJA. (e) DJF SPCAM (f) as with (e) but for JJA

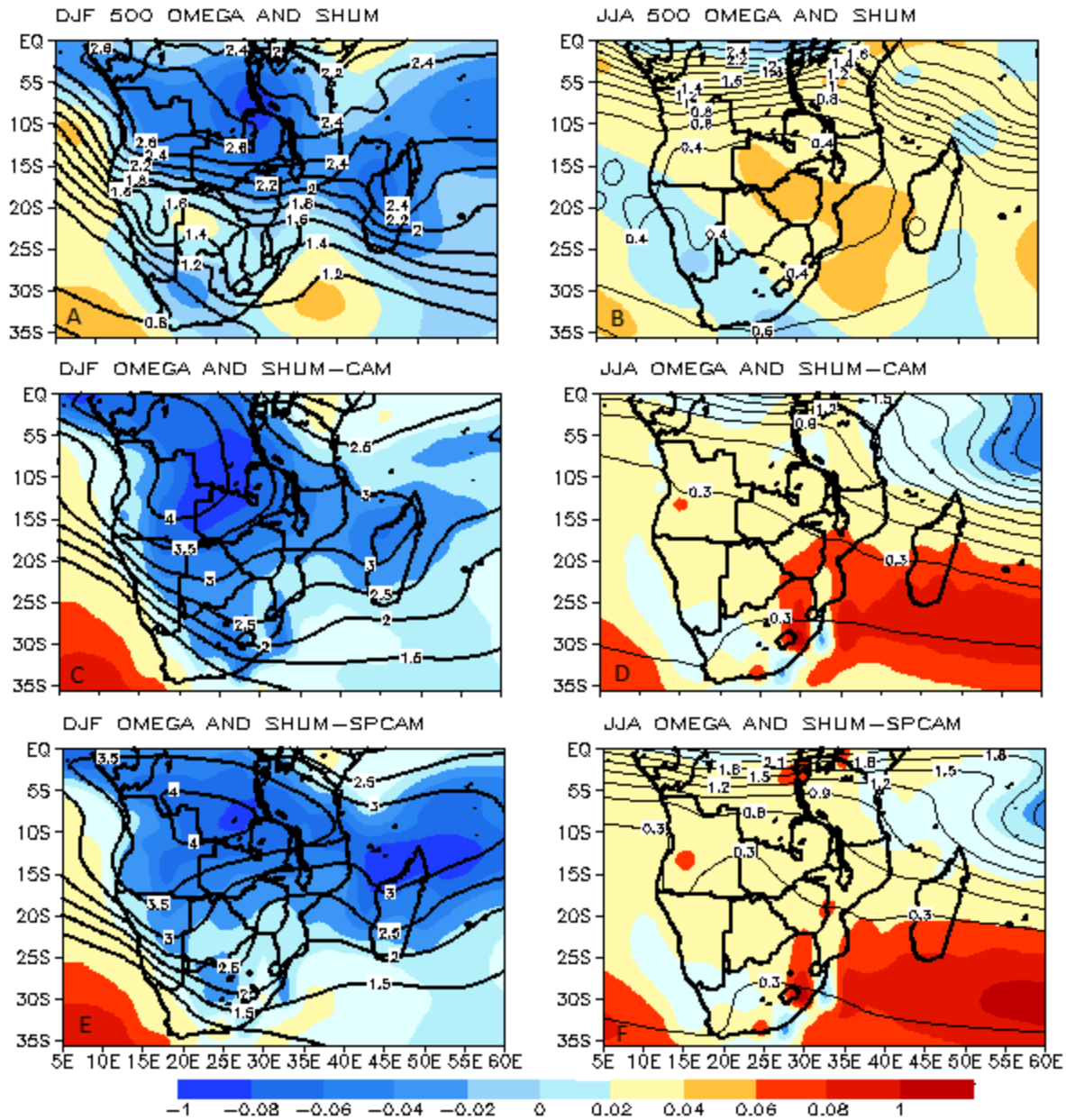


Figure 4.24: 500 Omega (Pa/s) and Specific humidity (kg/g) over southern Africa region for the period 1987 -2016. a) Observed December-January-February (DJF) from GPCP. (b) as with (a) but for June -July-August (JJA). (c) DJF mean from CAM. (d) as with (c) but for JJA. (e) DJF SPCAM (f) as with (e) but for JJA.

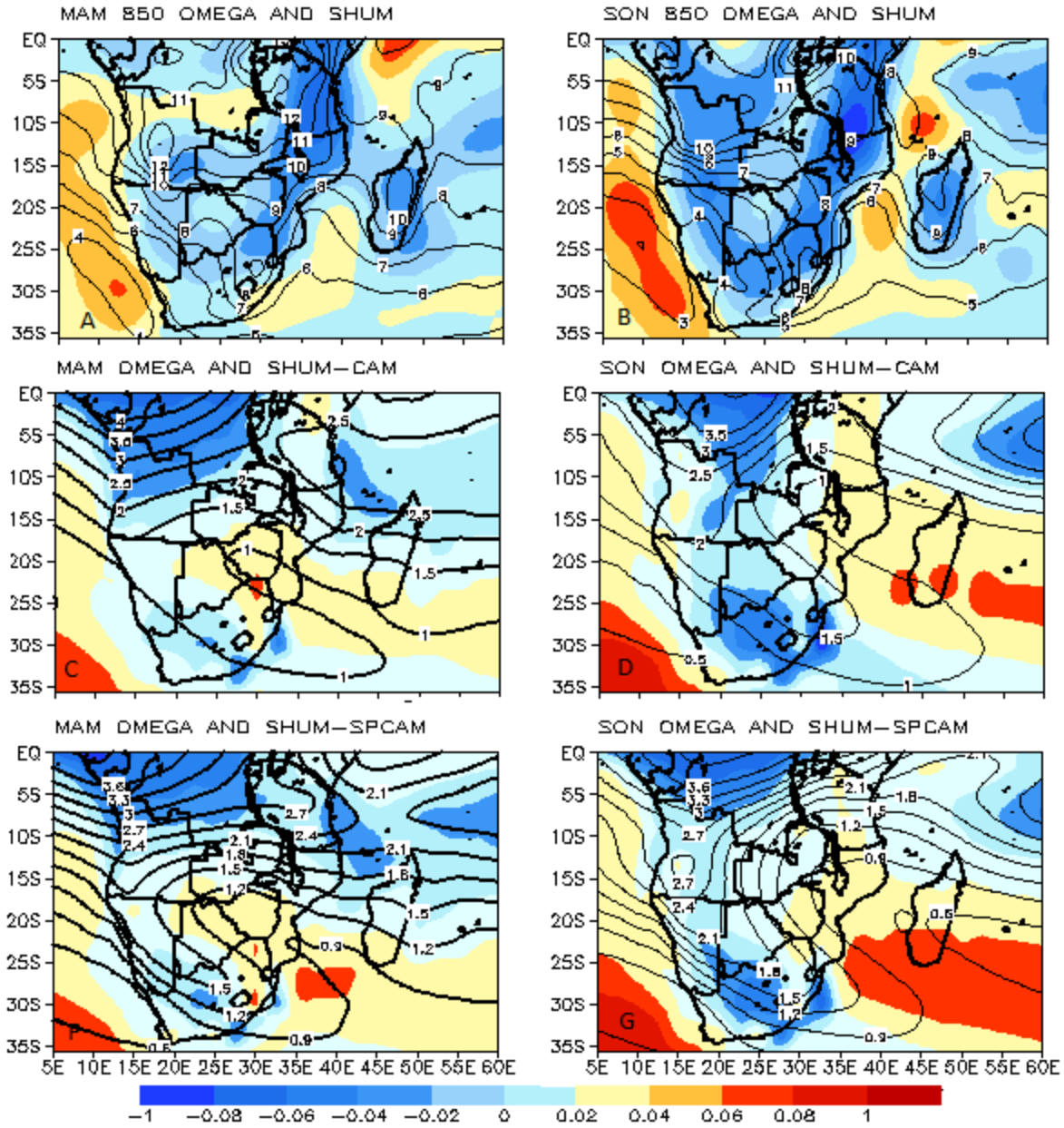


Figure 4.25: 850 omega (Pa/s) and specific humidity (kg/g) over southern Africa region for the period 1987 -2016. (a) observed March-April-May (MAM) from NCEP reanalysis II. (b) as with (a) but for September -October-November (SON). (c) MAM mean from CAM. (d) as with (c) but for SON. (e) MAM SPCAM (f) as with (e) but for SON.

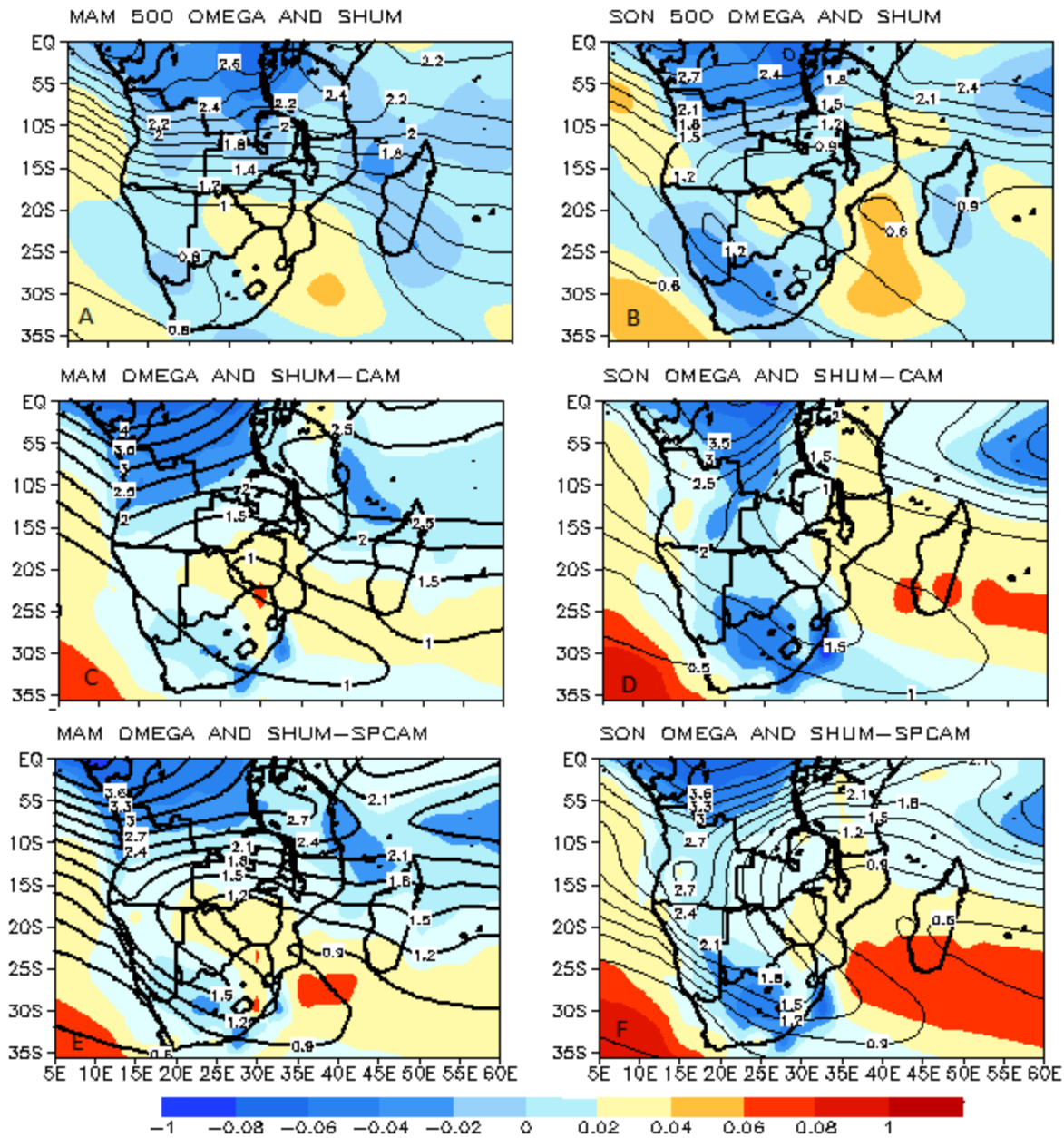


Figure 4.26: 500 omega (Pa/s) and specific humidity (kg/g) over southern Africa region for the period 1987 -2016. (a) observed March-April-May (MAM) from NCEP reanalysis II. (b) as with (a) but for September -October-November (SON). (c) MAM mean from CAM. (d) as with (c) but for SON. (e) MAM SPCAM (f) as with (e) but for SON

4.4.5 Relative humidity (850 hPa and 500 hPa)

Relative humidity is a function of temperature and is not independent. A warm atmosphere carries more moisture than a cold one. Figure 4.26 to 4.30 shows relative humidity simulations of CAM and SPCAM against reanalysis. Both CAM and SPCAM configurations were found to underestimate the percentages of relative humidity in the low levels (850 hPa) particularly over the south Western Cape for all seasons (DJF, JJA, MAM, and SON). In addition, during JJA both CAM and SPCAM dried up the atmosphere by underestimating relative humidity (Figure 4.27d and f). This poor resolution of relative humidity is a function of a poor simulation of temperatures in both CAM and SPCAM simulations, during JJA season they had a cold bias. In addition, this result also corresponds with those found for precipitation where CAM and SPCAM did not produce winter rainfall over the Western Cape region they had a dry bias due to model distortion of topographical features. During MAM and SON season, SPCAM was found to outperform the standard CAM in simulating relative humidity at 850 hPa levels (Figure 4.29c and e). In addition, SPCAM was also found to outperform the CAM in simulating relative humidity at the 500 hPa level during MAM season whilst CAM shows high skill in simulating relative humidity during SON season.

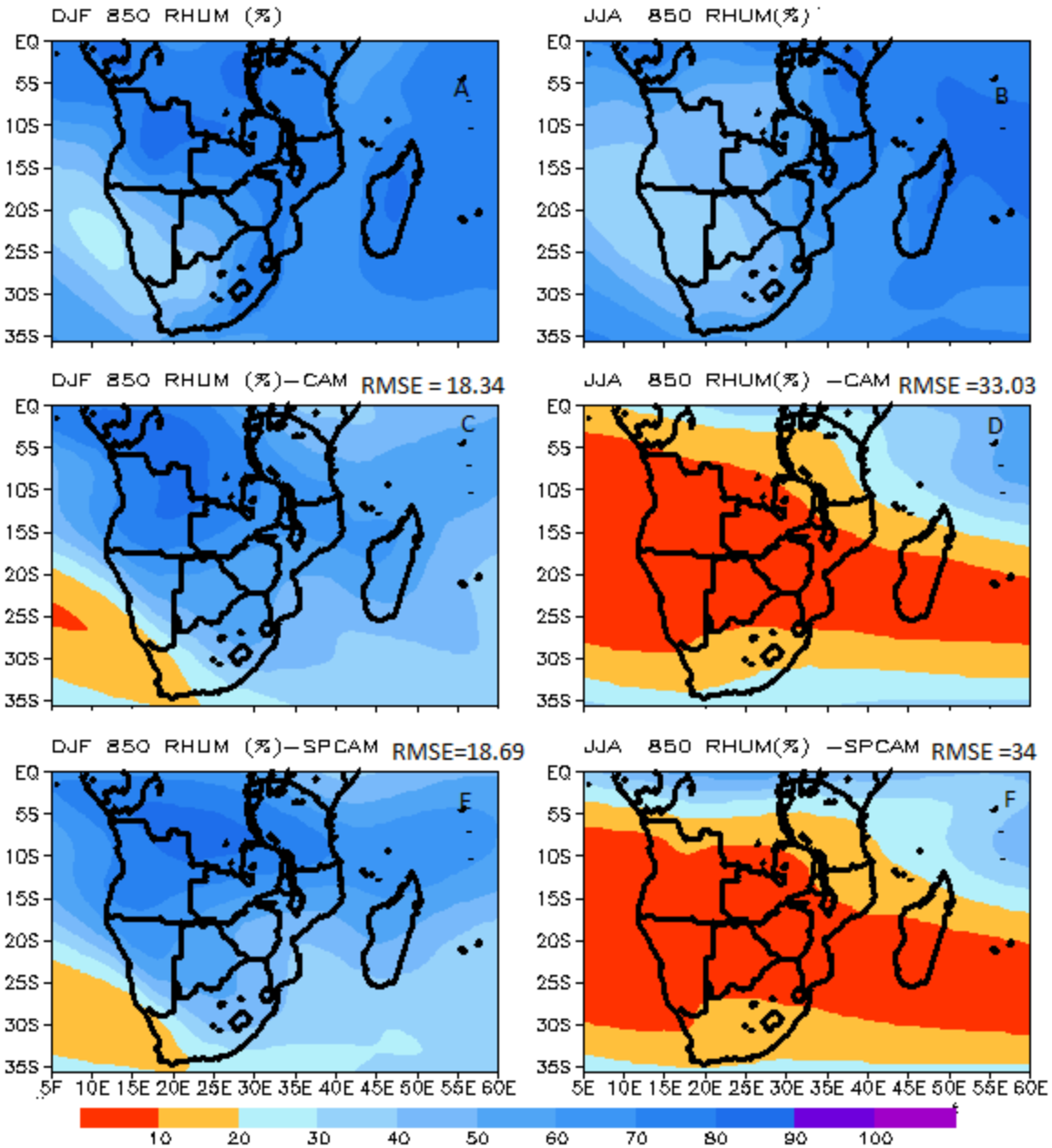


Figure 4.27: 850 Relative humidity (%) and RMSE over southern Africa region for the period 1987 -2016. a) observed December-January-February (DJF) from NCEP reanalysis II. (b) as with (a) but for June -July-August (JJA). (c) DJF mean from CAM. (d) as with (c) but for JJA. (e) DJF SPCAM (f) as with (e) but for JJA.

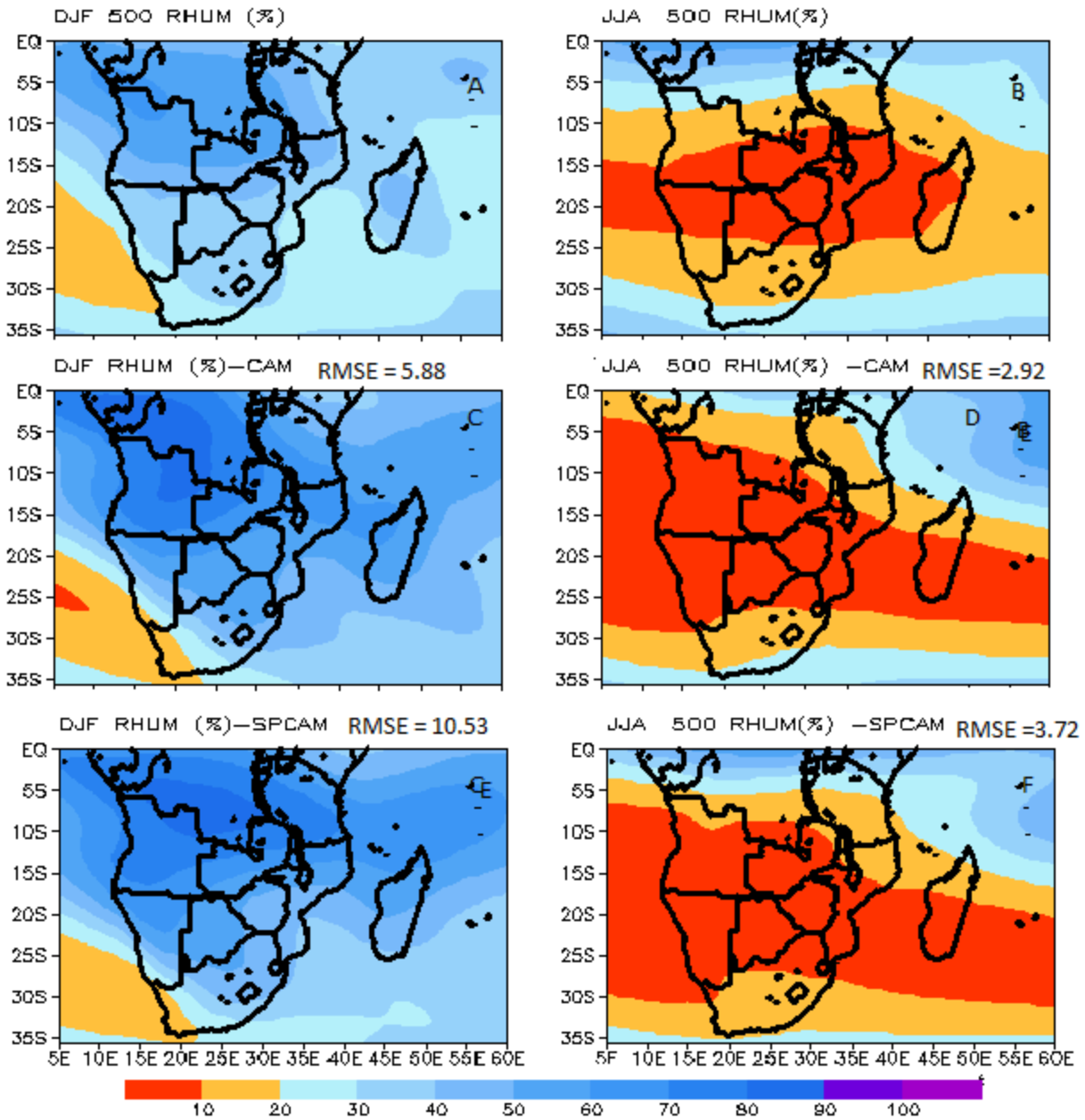


Figure 4.28: 500 Relative humidity (%) and RMSE over southern Africa region for the period 1987 -2016. a) observed December-January-February (DJF) from NCEP reanalysis II. (b) as with (a) but for June -July-August (JJA). (c) DJF mean from CAM. (d)as with (c) but for JJA. (e) DJF SPCAM (f) as with (e) but for JJA.

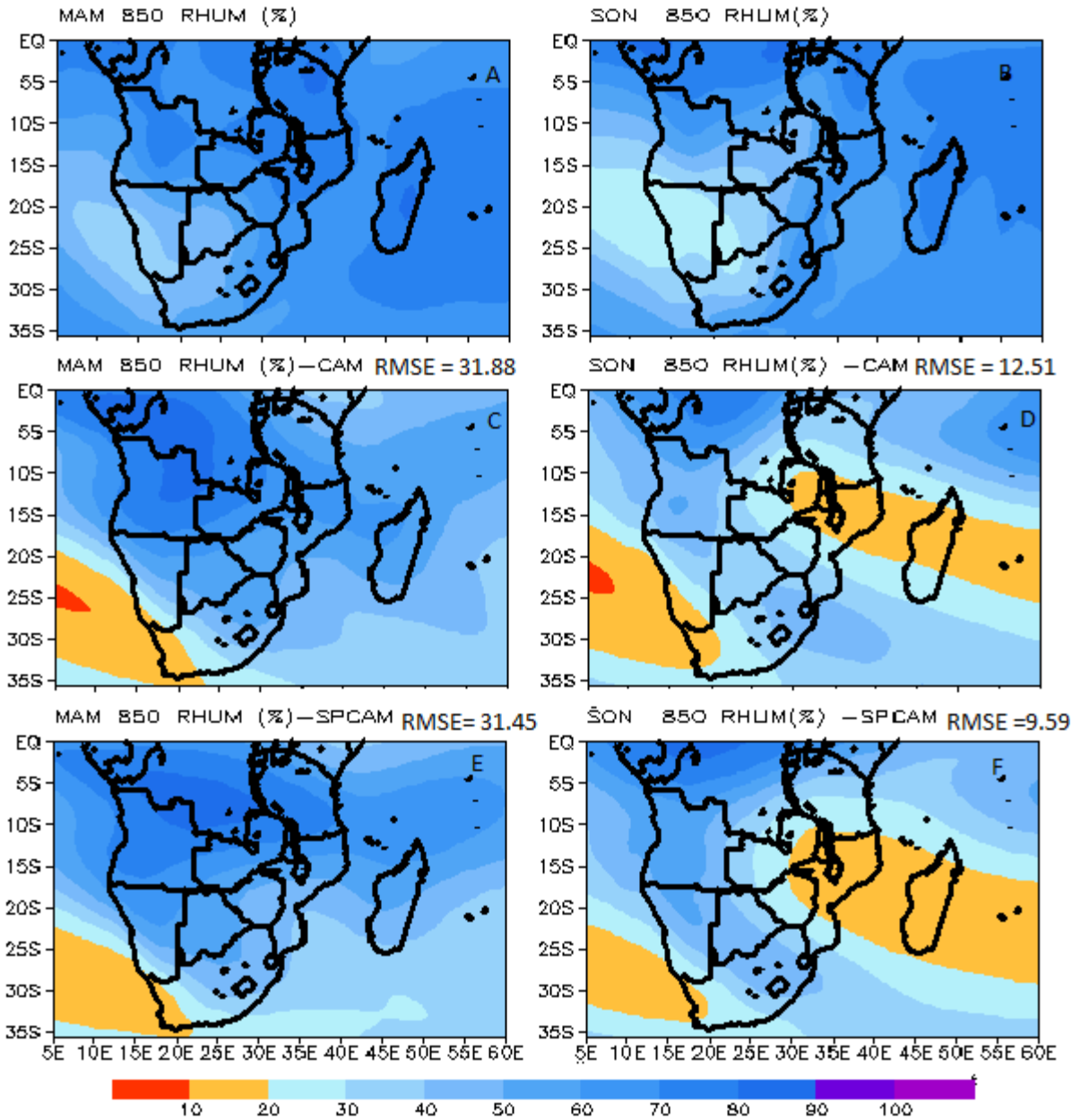


Figure 4.29: 850 Relative humidity (%) and RMSE over southern Africa region for the period 1987 -2016. (a) observed March-April-May (MAM) from NCEP reanalysis II. (b) as with (a) but for September -October-November (SON). (c) MAM mean from CAM. (d)as with (c) but for SON (e) MAM SPCAM (f) as with (e) but for SON.

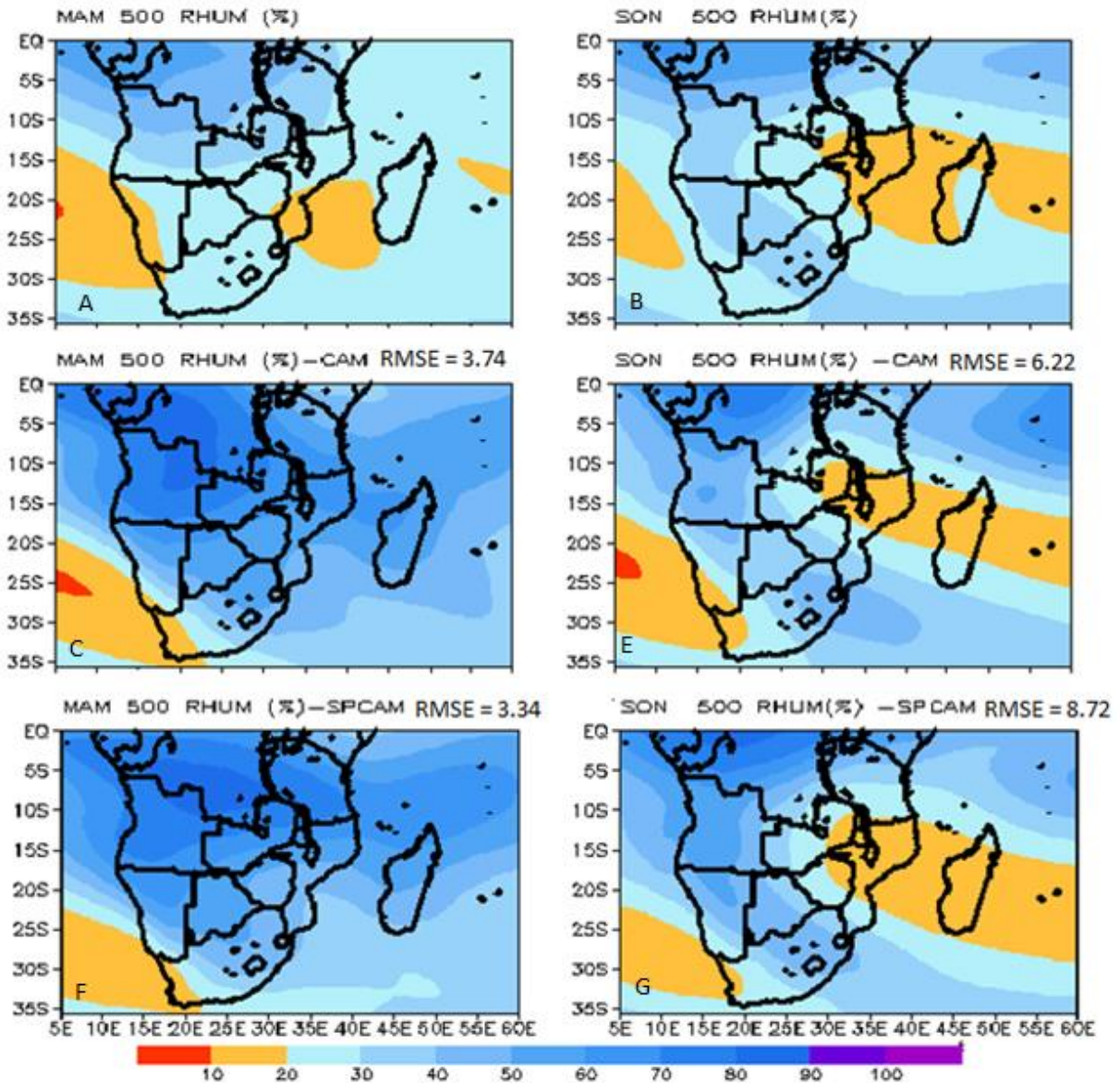


Figure 4.30: 500 Relative humidity (%) and RMSE over southern Africa region for the period 1987 -2016. (a) observed March-April-May (MAM) from NCEP reanalysis II. (b) as with (a) but for September -October-November (SON). (c) MAM mean from CAM. (d) as with (c) but for SON (e) MAM SPCAM (f) as with (e) but for SON

4.5 Summary

This chapter presented a climatology of key variables simulated by CAM, SPCAM against reanalysis in order to test the predictability of rainfall, temperature, and circulation variables at a seasonal time scale. During the summer season, CAM was found to overestimate rainfall over the interior of South African region whilst SPCAM is more close to the reanalysis. However, CAM and SPCAM configurations did not produce the winter rainfall over the Western Cape they both had a dry bias. SPCAM also exhibited a greater skill than the standard CAM in simulating rainfall for other seasons namely MAM and SON. The chapter also simulated interannual variability of rainfall and temperature and found more skill in the SPCAM results than the CAM. In addition, SPCAM was also found to have outperformed the standard CAM in simulating circulation variables from low levels and middle levels (850 hPa and 500 hPa). For instance, CAM was found to underestimate MSLP, geopotential height, PBL etc during summer season whilst SPCAM was close to the reanalysis. These results can be used to improve predictability and current modelling at seasonal timescales over the South African region.

CHAPTER FIVE

SIMULATED RESPONSE OF THE SOUTH AFRICAN CLIMATE TO DIFFERENT PHASES OF El Niño SOUTHERN OSCILLATION (ENSO) USING SUPER PARAMETERIZED COMMUNITY ATMOSPHERE MODEL (SPCAM)

5.1 Introduction

Southern Africa is a semi-arid region and is more likely to be affected by climate extremes such as droughts and flood events which tend to have a noticeable impact on water resource management, agricultural management and many other sectors. Despite the use of sophisticated models in the region to predict catastrophic events, challenges are still experienced with skill as well as confidence. This chapter evaluates the performance of CAM and SPCAM in simulating the most intense El Niño events which occurred during the period of 1991/92, 1997/98 and 2015/16 whereas on a high amount of rainfall the study focus on the period of 1999/2000, 2010/2011 and 2011/2012 events.

5.2 Phases of El Niño Southern Oscillation

5.2.1 Evolution of Canonical El Niño and El Niño Modoki

Figure 5.1a shows observed monthly Nino 3.4 time series of sea surface temperature (SSTs) anomalies associated with the El Niño Southern Oscillation (ENSO). The occurrence of El Niño and La Niña may be determined using many indices such as Nino 3.4 Index., El Niño Modoki Index (EMI) and Dipole mode index (DMI) which is used to measure the strength of the Indian Ocean Dipole (IOD). The time series of Nino 3.4 index indicates a strong positive phase of SST anomalies during the period of 1982/83; 1997/98 and 2015/16 due to El Niño induced drought which have affected the South African region. However, moderate El Niño is observed during the period of 1991/92 and 2002/2003 Table 5.1.

A strong positive phase of SSTs and strong positive phase of DMI are associated with drought over the subcontinent (Richards et al., 2000). The DMI shows a strong positive phase of SST during the period of 1991/92 and 1997/98 (Figure 5.2a). However, not all strong positive phase of DMI results in droughts over the subcontinent (Chikoore, 2016).

Figure 5.5a indicates global SSTs of canonical El Niño symbolized by above average SSTs over the eastern equatorial Pacific with cold waters on the western part of the basin. El Niño Modoki is associated with above usually ocean temperatures in the central Pacific flanked by cold waters west and east respectively creating a tripolar pattern (Figure 5.5b). ENSO is known to be the main

climate driver of seasonal rainfall over the subcontinent (Phakula, 2017). PCA for SSTs over the Indian Ocean indicate a distinct dominant mode of variability. PC4 clearly indicates El Niño Modoki explained by 14.29 % of the variance in much of the Indian Ocean whilst PC1 explain Canonical El Niño is explained by 82.19% of the variance in much of the Indian Ocean (PC4 and PC2) Table 5.3. Table 5.2.

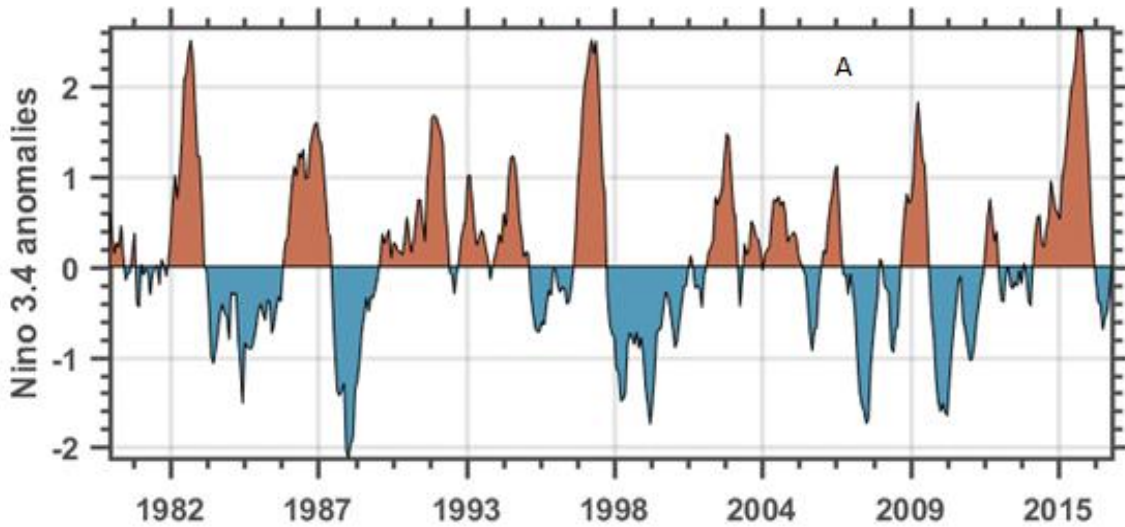


Figure 5.1 : Global sea surface temperatures over the south Indian Ocean for Nino 3.4 anomalies for the period 1987 to 2016

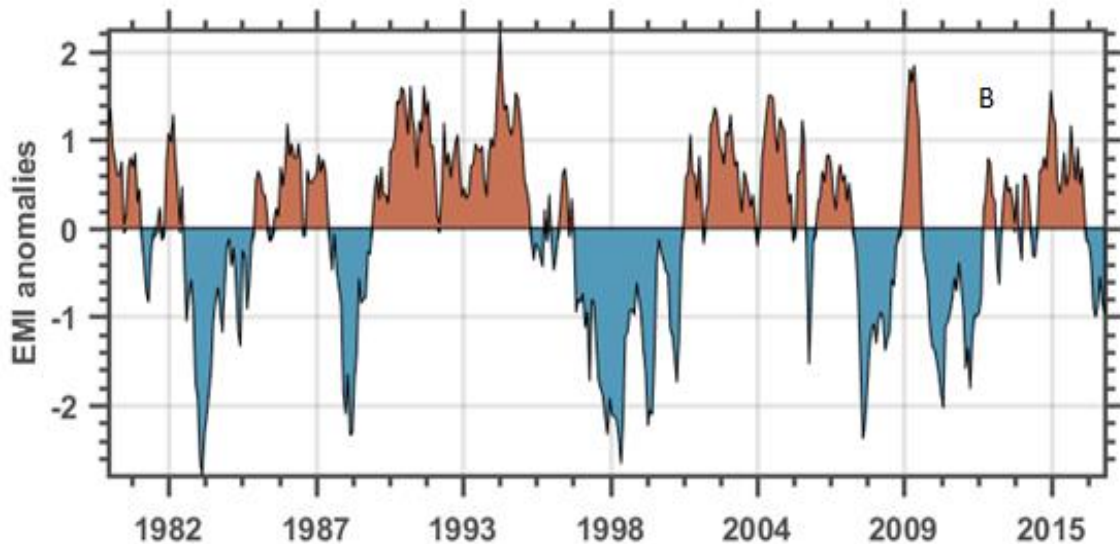


Figure 5.2 : Global sea surface temperatures over the south Indian Ocean for El Niño Mode Index for the period 1987 to 2016.

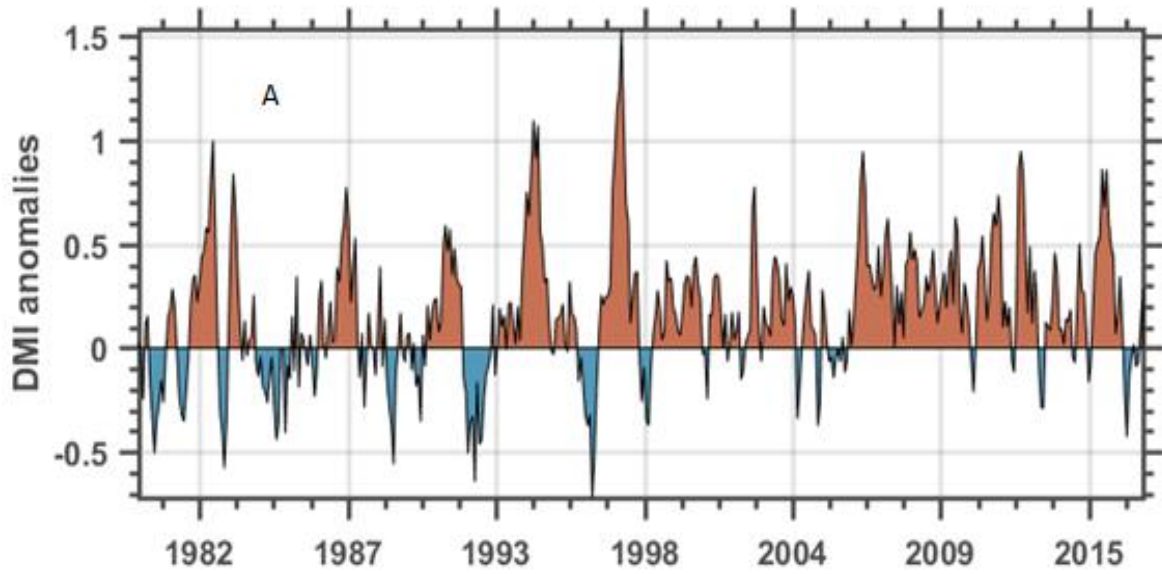


Figure 5.3 : Global sea surface temperatures over the south Indian Ocean for Dipole Modoki Index for the period 1987 to 2016

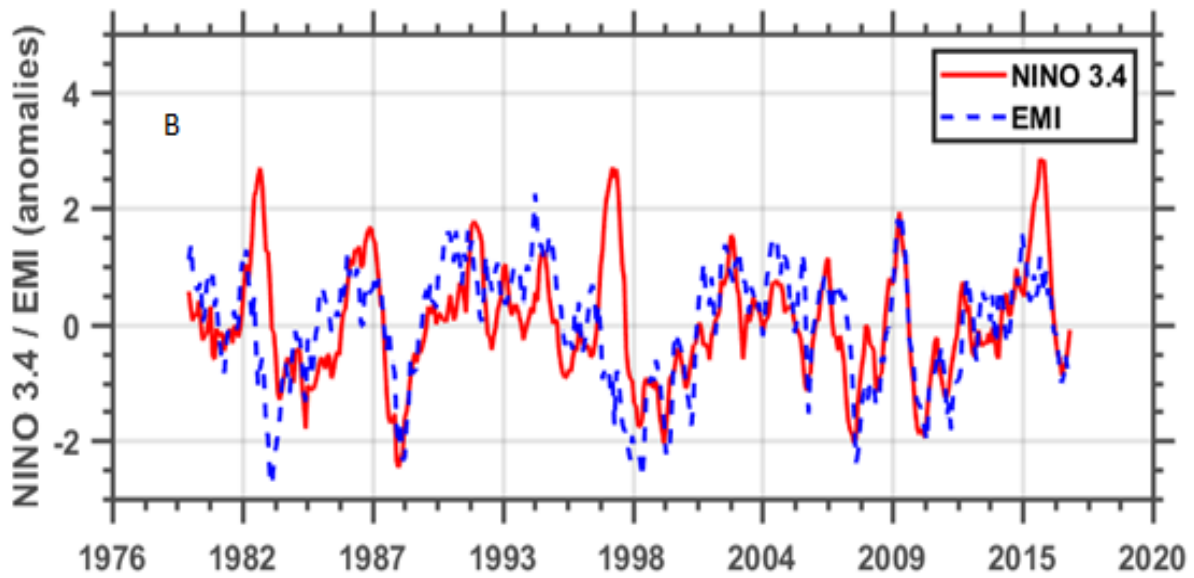


Figure 5.4 : Nino 3.4 Index and Modoki index anomalies.

Table 5.1: El Niño and La Niña seasons for the period 1987-2016 based on Nino 3.4 anomalies

R4re5tyf	La Niña
1986/87 (moderate)	1988/89 (strong)
1987/88 (moderate)	1995/96 (weak)
1991/92 (moderate)	1999/00 (strong)
1997/98 (strong)	2004/05 (weak)
2002/03 (moderate)	2006/07 (weak)
2009/10 (moderate)	2007/08 (moderate)
2015/16 (strong)	2011/12 (weak)

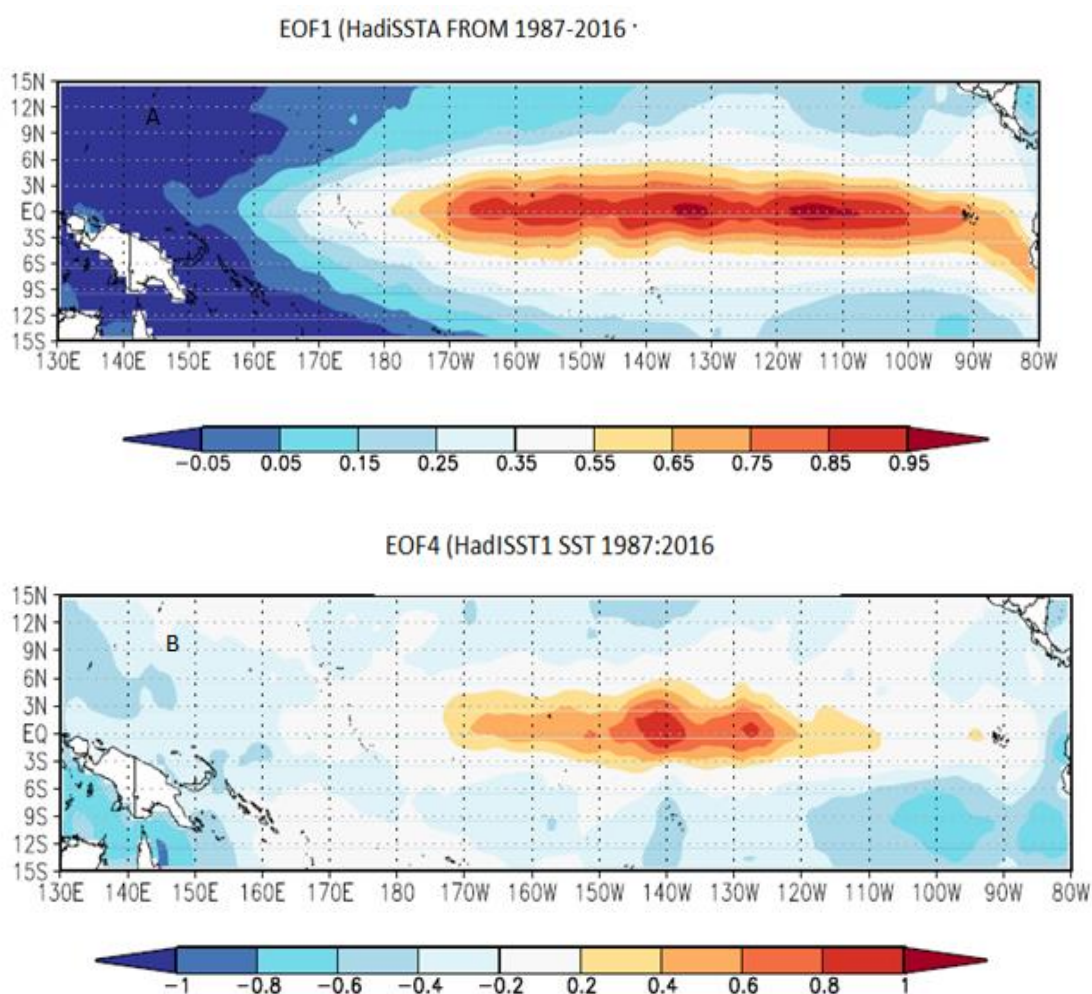


Figure 5.5 : Global sea surface temperatures of a) canonical El Niño and b) El Niño Modoki

Table 5.2: Austral summer PCA variance and cumulative percentage sea surface temperature showing canonical El Niño

PCA NO	Explain variance	Cumulative %
PC1	82.19%	82.19%
PC2	8.67%	90.85%

Table 5.3: Austral summer PCA variance and cumulative percentage sea surface temperature showing canonical El Niño Modoki

PCA NO	Explain variance	Cumulative %
PC3	64.12%	64.12%
PC4	14.29%	78.40%

5.3 Drought cases

5.3.1 Rainfall anomalies (1991/92; 1997/98; 2015/16)

The CAM was not able to detect the drought events which occurred during 1991/92 and in 1997/98 (Figure 5.6b and e). However, the CAM was able to depict drought over much of southern Africa region which occurred during 2015/16 which is an exaggeration of the actual observation (Figure 5.6h). SPCAM shows much greater skill in simulating drought over South African region such that it justifies the use of SPCAM simulation best compared to the CAM. The 1991/92 and 2015/16 events are interesting in the sense that they rank as the most severe droughts. The 1991/92 event was the worst drought to have affected the region in terms of rainfall anomalies and its impacts on agriculture due to the failure of the cloud bands (Chikoore, 2016). The worst El Niño events were in 1997/98 and 2015/16 droughts, tied up as the strongest El Niños in the equatorial Pacific, but their impacts were different. The 2015/16 remains the worst drought in terms of temperature anomalies characterized by repeated heat waves and high temperatures. The 2015/16 was recorded as the warmest year over the past 50 years in the record and this could be as a result of the earth warming and climate change. Several seasonal climate forecasts made during 1997/98 indicated enhanced below-normal precipitation but the predicted drought failed to materialize (Buizer et al, 2000). The South African region experienced near-normal rainfall during 1997/98 as a result of an unusually strong Angola Low which strengthens during January-March 1998 (Reason and Jagadeesha, 2005). During strong ENSO events, the Angola low is typically weakened and therefore supplies less moisture to the cloud bands over southern Africa resulting in drier-than-average conditions (Mulenga et al., 2003; Reason and Jagadheesha, 2005).

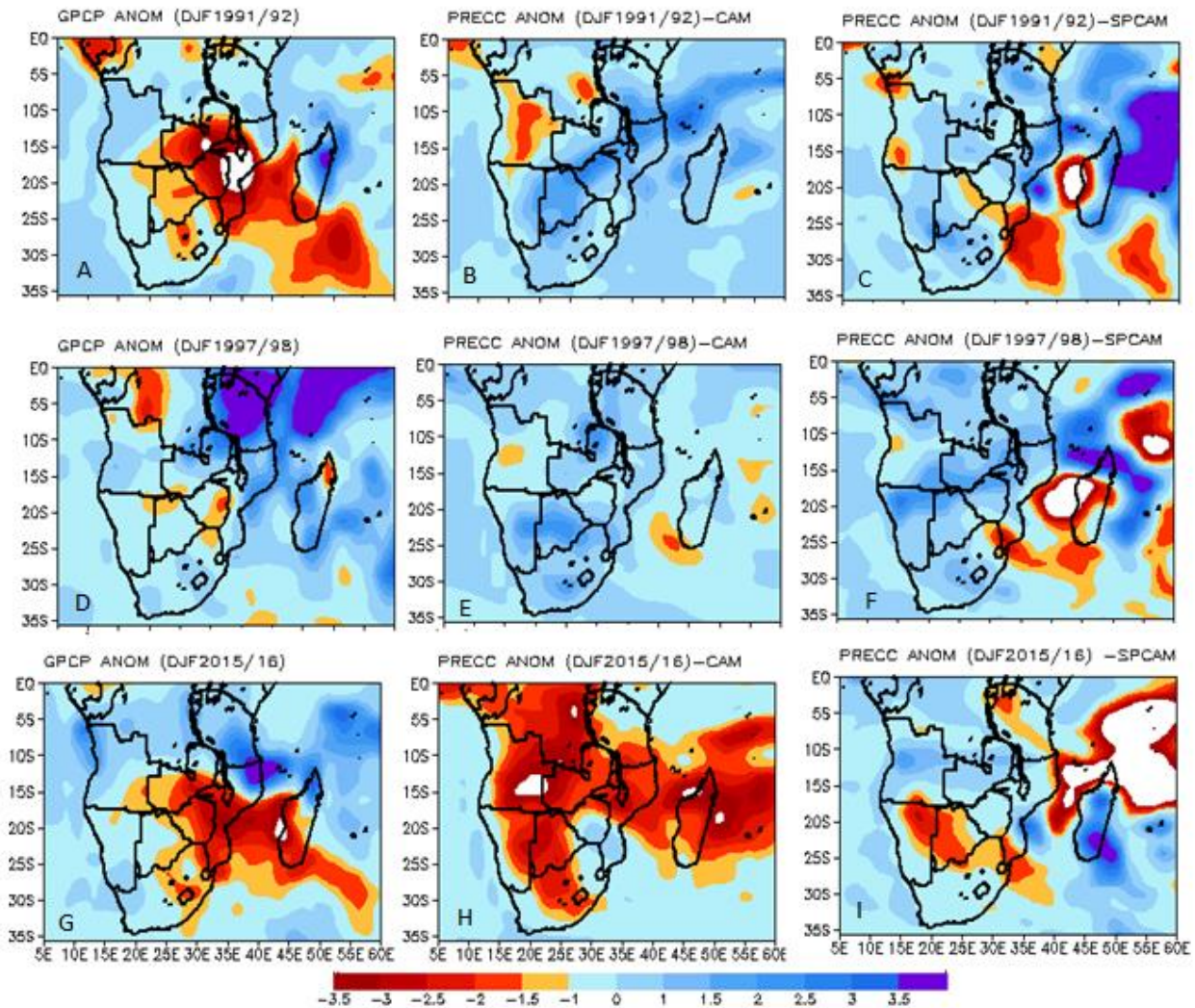


Figure 5.6 : DJF rainfall (mm/day) anomalies as simulated by CAM, SPCAM and observation for the period 1991/92 (first row); 1997/98 (second row) and 2015/16 (third row).

5.3.2 Geopotential height anomalies and wind vectors (1991/92; 1997/98; 2015/16)

Both configurations (CAM and SPCAM) poorly resolved the geopotential height when compared with the observation (Figure 5.7). The 1997/98 event exhibits an unusually strong Angola Low which is not there in both CAM and SPCAM simulations over Namibia and Angola (Figure 5.7a). However, in terms of the wind field, the SPCAM exhibited a greater skill than CAM simulation and such was observed during 2015/16 event particularly over the south West Indian Ocean, there is a south Indian subtropical anticyclone with offshore westerly wind in SPCAM results which is more similar to the observation. During drought wind tend to be offshore westerly (no transport of moisture over the interior) even if a tropical cyclone develop it won't form. In addition, during the period of 1991/92 and 2015/16 SPCAM show positive anomalous of geopotential height over much of South African region. Meanwhile, in 1997/98 positive geopotential height is observed

over the Limpopo region and southwestern Cape. CAM depict negative geopotential height anomalous over the South African region particularly during 2015/16 over South Western Cape. Positive geopotential height is characterized by subsidence and less rainfall whist negative geopotential height may indicate uplift and high amount of rainfall over South African region.

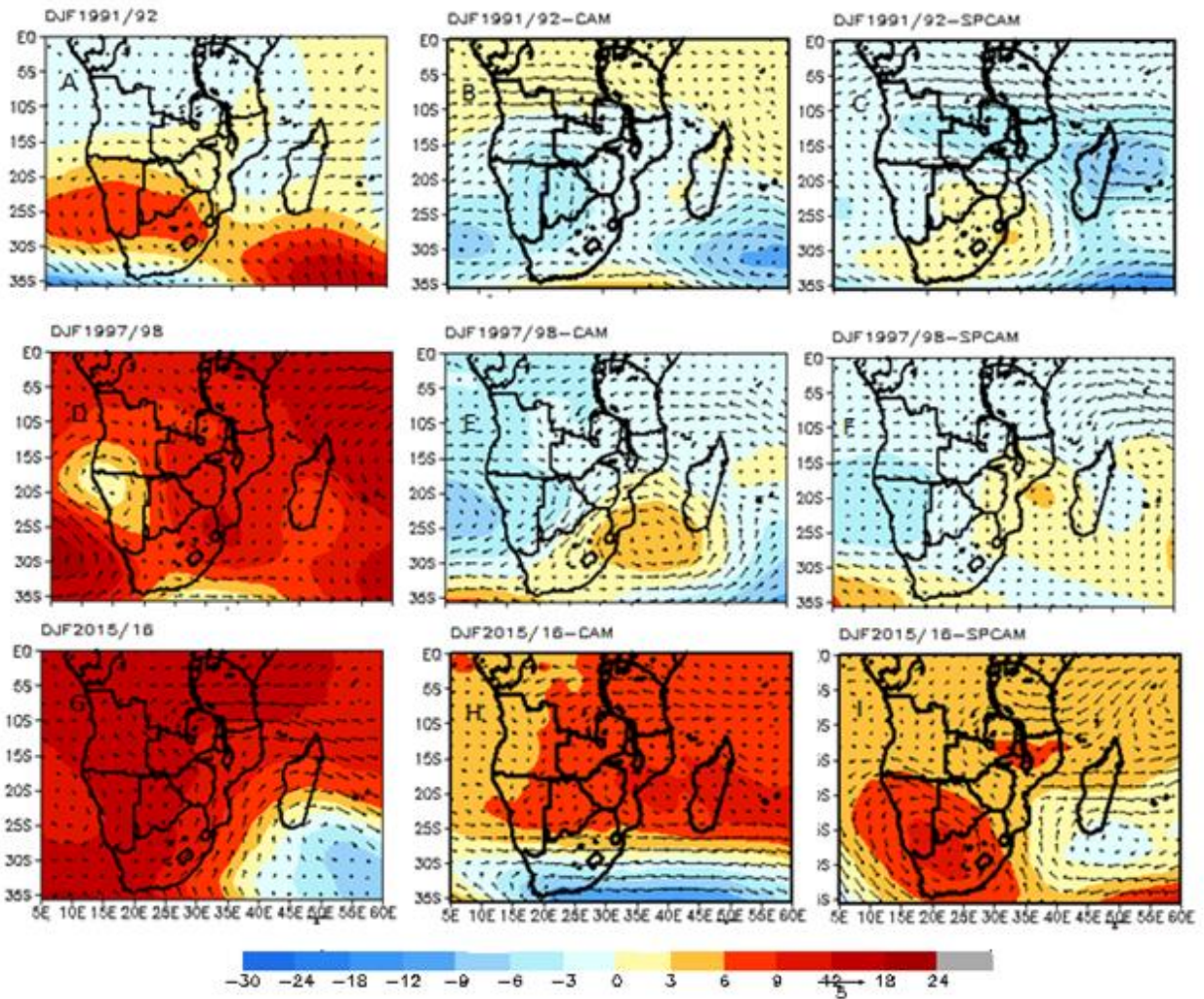


Figure 5.7 : 500 hPa geopotential height and wind vectors (m/s) anomaly as simulated by CAM; SPCAM and observation for the period of 1991/92 (first row), 1997/98 (second row) and (third row) 2015/16 (a scale vector is shown)

5.3.3 Omega (500hPa) and Relative humidity % (1991/92; 1997/98 and 2015/16)

CAM depicts negative values of omega during period of 1991/92, 1997/98 and 2015/16 over the Limpopo region and in most parts of South African continent (Figure 5.9a, 5.9e and 5.9h). However, the SPCAM results shows much greater skill in simulating omega over the subcontinent with positive values of omega during the drought of 1991/92, 1997/98 and 2015/16 particularly

over the Limpopo region when compared against observation. Negative omega represents uplift whilst positive omega depicts subsidence over the region. In terms of relative humidity SPCAM show results which are close to the reanalysis and was able to simulate the large-scale features but struggled to provide detailed information of the local features more especially in the year of 2015/16 droughts.

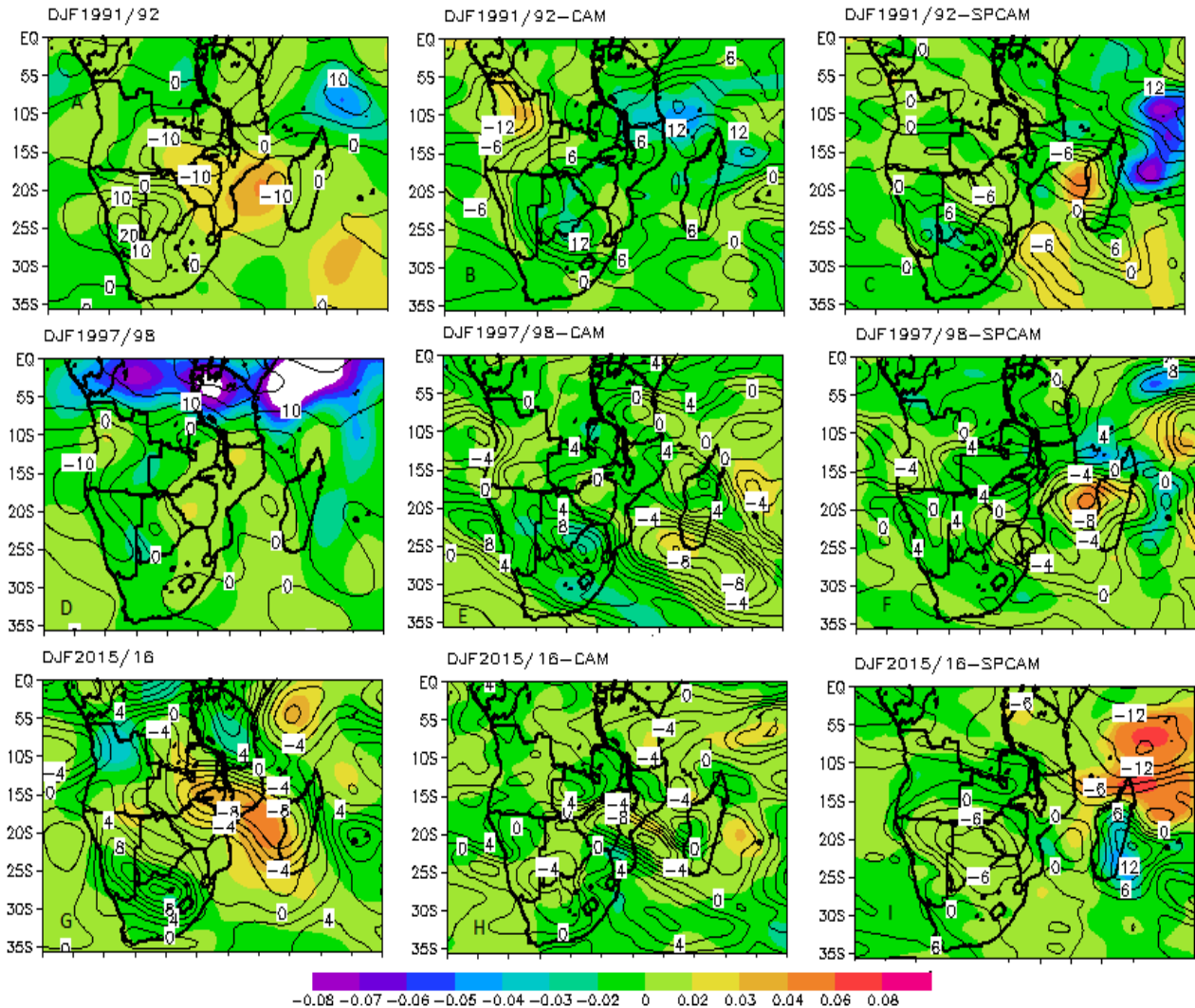


Figure 5.8 : 500hPa omega (Pa/s) and Relative humidity (%) anomaly as simulated by CAM; SPCAM and observation for the period of 1991/92 (first row), 1997/98 (second row) and (third row) 2015/16

5.4 Wet seasons

5.4.1 Rainfall anomalies (1999/00; 2010/11 and 2011/12)

La Niña events caused excessive seasonal flooding during the period of 1999/00 and 2010/2011 over South Africa. In 1999/00, high amount of rainfall was caused by tropical cyclone (TC) Eline which made a landfall over Mozambique and killed thousands of people while multitudes were left homeless (Bopape, 2013). TC Eline started on 1 February to 29 February 2000. Nevertheless, CAM was not able to depict the wet season of 1999/00 and 2010/11. The standard CAM depicts below normal rainfall over Mozambique and the north eastern part of Zimbabwe during the period of 1999/00 whilst in 2010/11 (Figure 5.9b and 5.9e) CAM show below normal rainfall over Mozambique, Botswana and some part of the Limpopo region which is dissimilar to the reanalysis. SPCAM was able to depict the wet season of 1999/00, 2010/2011 and 2011/2012 when compared the simulation with observation (Figure 5.9c; 5.9f and 5.9k). The results are consistent with a study done by Li et al, (2012) who found that SPCAM had skill in simulating the distribution of extreme precipitation events more than the CAM over the continental United States. In addition, SPCAM successfully depicted the drought which occurred in the late summer of 2011/2012 and affected some parts of Limpopo and North West regions of South Africa.

In February 2012 TC Giovanna took the lives of more than 35 individuals (Chikoore et al 2015). In addition, below normal rainfall which occurred in the 2011/12 summer season was more observed over much of the central parts of the South African region whilst large parts in the west, south and some areas in the east received above-average rainfall (Chikoore et al., 2015). The 2010/2011 summer rainfall was characterized by a series of floods in South Africa linked to La Niña event resulting in a thousand people being displaced. In January 2011 more than 141 people died including 88 in KwaZulu Natal. The major flooding episode of this period devastated Mozambique and killed many individuals while 200 000 were left homeless.

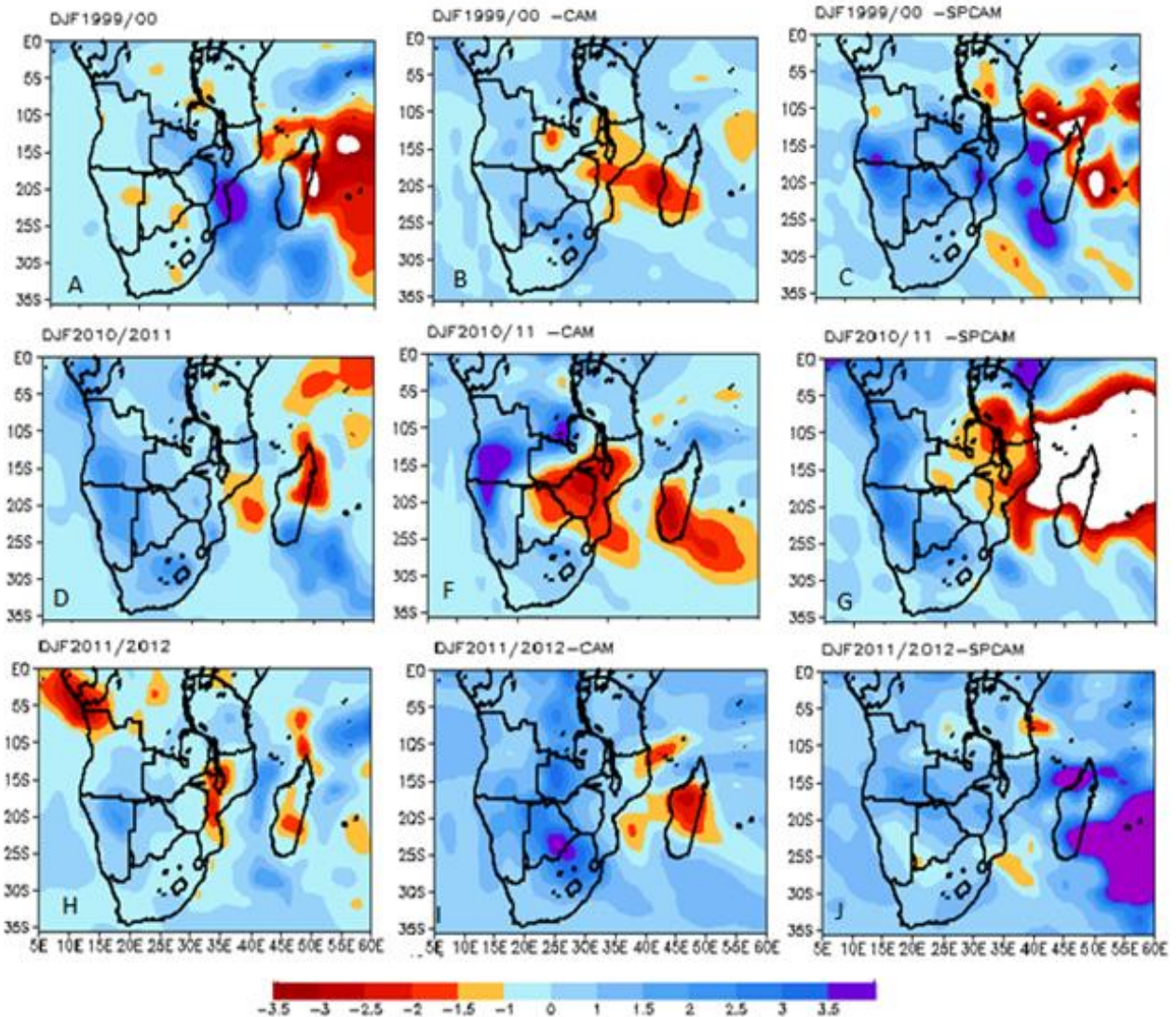


Figure 5.9 : Rainfall (mm/day) anomalies as simulated by CAM; SPCAM and observation for the period of 1999/00 (first row), 2010/11 (second row) and (third row) 2011/12 Over southern Africa.

5.4.2 Geopotential height (500hPa) and wind anomalies (1999/00; 2010/11; 2011/12)

Both CAM and SPCAM poorly resolve the geopotential height of 1999/00, 2010/11 and 2011/2012 when compared with the reanalysis (Figure 5.10). The 1999/00 and 2010/11 simulation by CAM and SPCAM depict strong anticyclones which are not there in the observation. However, in terms of the wind patterns, SPCAM depicts a greater skill than CAM simulation with onshore wind that brings moisture over land (Figure 510 G and I) particularly over the south West Indian Ocean. During La Niña event wind blow from east to west carrying moisture from the Indian Ocean to the subcontinent.

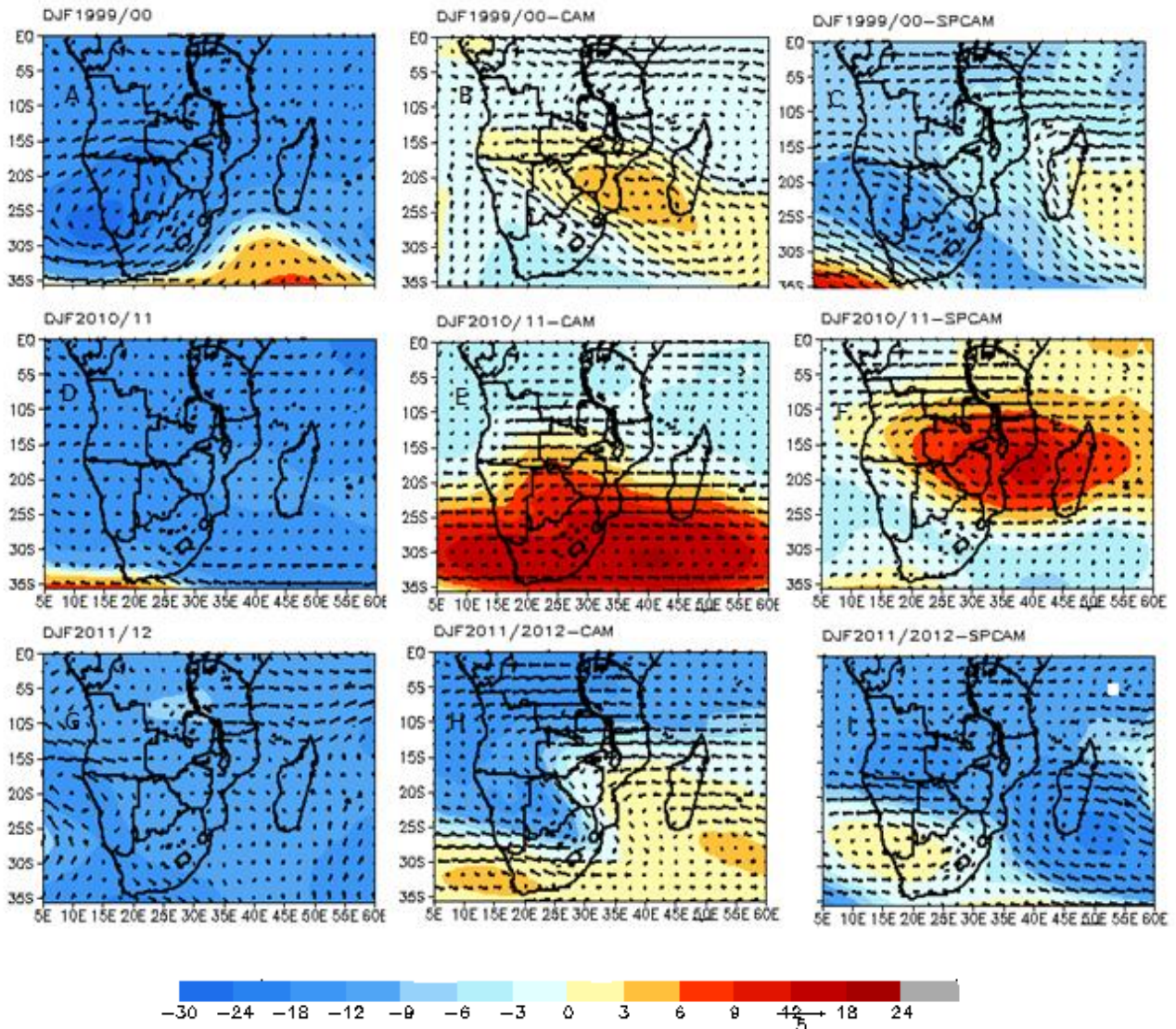


Figure 5.10 : 500 hPa geopotential height and wind (m/s) anomaly as simulated by CAM; SPCAM and observation for the period of 1999/00 (first row), 2010/11 (second row) and (third row) 2011/12 over southern Africa (a scale vector is shown)

5.4.3 Omega (500 hPa) and Relative humidity (1999/00; 2010/1 and 2011/12)

CAM showed positive anomalies of omega over Mozambique and some part of Zimbabwe during the period of 1999/00 wet season (Figure 5.10). CAM also depicts positive anomalies of omega over some part of Limpopo, Mozambique, Zimbabwe as well as Botswana during the period of 2010/11, which could be the reason for CAM inability to realistically simulate rainfall anomalies during this period. During 2011/12 CAM indicates negative anomalies of omega over the northern part of the subcontinent. SPCAM depicts negative anomalies of omega over the Mozambique,

Channel, Mozambique extending to the northern parts of Botswana and Namibia for 1999/00 summer season. It can be concluded that SPCAM has a higher accuracy than CAM in simulating wet summer season over the subcontinent. Positive anomalies of Omega are associated with subsidence and dry condition while negative anomalies of omega are associated with uplift. During positive anomalies of omega, the region experiences below normal rainfall whilst during negative omega the subcontinent experience above normal rainfall.

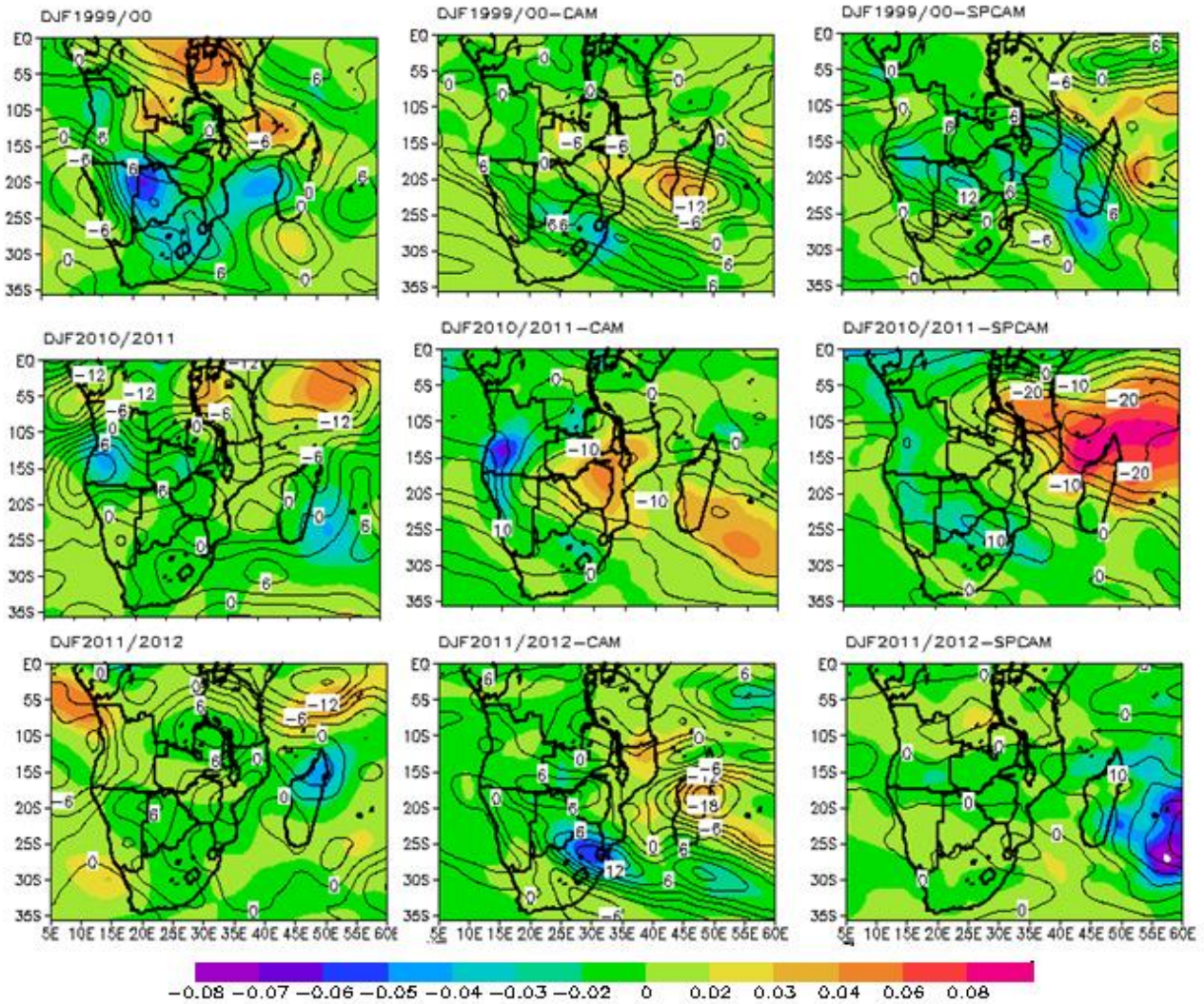


Figure 5.11 : 500 hPa omega (Pa/s) and relative humidity (%) anomaly as simulated by CAM; SPCAM and observation for the period of 1999/00 (first row), 2010/11 (second row) and (third row) 2011/12 over southern Africa.

5.5 Summary

The SPCAM configuration was found to outperform the standard CAM in simulating drought over South Africa. CAM was found to poorly resolved the drought of 1991/92, 1997/98. However CAM was able to simulate the drought of 2015/16, which is an exaggeration when comparing the observation with simulation. Whilst SPCAM exhibited much greater skill than the CAM in simulating wind pattern, particularly over the south West Indian Ocean. In addition, both CAM and SPCAM poorly resolved geopotential height during drought and wet seasons but SPCAM exhibited better skill than the CAM.

CHAPTER SIX: DISCUSSION AND CONCLUSION

6.1 Introduction

Climate models are simplification of the climate system and the large -scale grid cell that the model use does not provide adequate information at local scales. Climate models tend to overestimate rainfall over most of South Africa basically making the whole country wet. The models also struggle to provide realistic rainfall simulations over areas characterized by complex topography due to the low resolution used in climate models. Meteorologists are restricted to the low resolution in models by a limitation in computational resources. In order to represent small scale processes that the models are not able to capture explicitly, parametrization schemes are used. The IPCC (2007 and 2013) stated that the use of parameterization schemes in climate models is thought to be the reason for most of the uncertainties found in simulations of climate variability and change. It is documented that the southern African region is prone to floods and drought which have a negative impact on sectors such as agriculture, water resource management and disaster risk management. The study examined a climatology of key variables such as rainfall and temperature patterns and circulation variables from low levels and middle levels as simulated by Community Atmosphere Model (CAM) and Super Parameterized Community Atmosphere Model (SPCAM) for the period of 1987 to 2016. The study further analyzed the inter-annual variability of rainfall and temperature for different homogenous regions across the whole of South Africa using both configurations of the CAM. Further, ENSO cases - three El Niños and three La Niña seasons as simulated by CAM and SPCAM were also studied. This chapter provides a summary of the work done in the study, results obtained and also provides conclusions and recommendations.

6.2 Discussion and synthesis of key findings

6.2.1 South African climate as simulated by SPCAM

The study found that SPCAM simulated the climate of South Africa better than CAM. CAM was found to overestimate rainfall over the interior of South Africa and the eastern part of the region. This result was consistent for all the seasons considered in the study where SPCAM was found to be better generally compared to CAM in simulating rainfall at seasonal time scale. During the winter season both configurations did not produce winter rainfall over the south Western Cape, they had a dry bias. In addition, SPCAM proved to be more realistic in terms of simulating temperatures at seasonal timescales compared to the CAM over South Africa. CAM was found

to underestimate temperatures over the western part of the region in the North West, Namibia and Kalahari whilst SPCAM simulated temperatures which are more comparable to the reanalysis during summer season. The configurations inability to realistically simulate temperatures affected the simulation of certain variables such as relative humidity, boundary layer height (PBLH) and geopotential height as they are the function of temperature. CAM underestimated whilst SPCAM simulation was comparable with the reanalysis. Further, SPCAM simulations were also found to improve the short comings of the CAM simulation in simulating geopotential height for all seasons. Last but not least, SPCAM was found to be more skillful than the CAM in simulating inter annual variability of rainfall over the summer rainfall regions except over Limpopo and KwaZulu Natal from the period of 1987 to 2016. It was also found that there is much skill in simulating inter annual variability of rainfall in the winter rainfall regions in the SPCAM results than CAM.

6.2.2 ENSO cases as simulated by SPCAM

The study investigated ENSO cases -three El Niño and three La Niña season for the period of 1987 to 2016. It was found that SPCAM had a greater skill in simulating droughts over South Africa compared to the CAM. CAM was not able to depict the drought which occurred during 1991/92, 1997/98. However, CAM was able to depict the drought which occurred in 2015/16 which is an exaggeration of the actual results. Both CAM and SPCAM poorly resolved geopotential height at 500hPa levels during drought and wet season. In addition, SPCAM was also found to outperform the standard CAM in simulating the wind field and omega anomalies when simulations were compared to the reanalysis particularly over the south West Indian Ocean. The study also focusses on La Niña seasons which occurred during 1999/00, 2010/2011 and 2011/12 in order to test the capability of SPCAM and found that SPCAM outperformed the standard CAM in simulating three wet seasons which affected South African region. SPCAM was also found to be better than the standard CAM in simulating wind patterns and omega during the wet seasons.

6.3 Implications and future work

The results from the study suggest that the climate community in South Africa should consider the use of SPCAM as an alternative for operational seasonal forecasting. This result can be used to improve the predictability and current modelling efforts and therefore agricultural management and save the economic sector of South Africa. Future studies can break down the summer into early summer (OND) and late summer (JFM). South African institutions such as the South African Weather Service (SAWS), University of Cape Town, CSIR and University of Pretoria (UP) should consider the use of SPCAM to improve the climate information or seasonal climate forecasting. It is also worthwhile to consider the use of 3D (Cloud resolving model) SP than 2 D CRM to simulate

winter rainfall over the south Western Cape region as informed by the available computational resources.

6.4 Conclusions

The study contributed new knowledge to the climate community by comparing simulations made with a super-parametrized GCM versus one that uses conventional parameterization schemes over South Africa. The study has shown that the South African climate community should consider the use of super-parametrized models as they outperform those with conventional schemes. Further studies on super-parametrization are needed over the country and questions need to be asked if SPCAM can't be used for operational seasonal forecasting. While super-parametrization outperforms conventional schemes, there were still some shortcomings with SPCAM. More research should be undertaken to further understand the source of the still remaining issues in the model, so that the models can be improved further.

References

- Archer, E.R.M., Landman, W.A., Tadross, M.A., et al., 2017. Understanding the evolution of the 2014–2016 summer rainfall seasons in southern Africa: Key lessons. *Climate risk management*, 16, 22-28.
- Available at: https://www.pmel.noaa.gov/el_nino/schematic_diagrams (Accessed 04 november 2017).
- Ashok, K., Behera, S.K., S.A Rao, et al., 2007. El Niño Modoki and its possible teleconnection. *J. Geophys. Res: Oceans*, 112(C11), 1978-2012.
- Baldwin, M.E., Kain, J.S. and Kay, M.P., 2002. Properties of the convection scheme in NCEP's Eta model that affect forecast sounding interpretation. *Weather and forecasting*, 17(5), 1063-1079.
- Benedict, J.J. and Randall, D.A., 2009. Structure of the Madden–Julian oscillation in the super parameterized CAM. *J. Atmos. Sci*, 66(11), 3277-3296.
- Beraki, A.F., Landman, W.A. and DeWitt, D., 2015. On the comparison between seasonal predictive skill of global circulation models: Coupled versus uncoupled. *J. Geophys. Res: Atmospheres*, 120(21), 11-151.
- Beraki, A.F., Landman, W.A., DeWitt, D. et al., 2016. Global dynamical forecasting system conditioned to robust initial and boundary forcings: seasonal context. *Int. J. Climatol*, 36(14), 4455-4474.
- Bopape, M.M., 2013. Simulations of moist convection using the quasi-elastic equations, Doctoral dissertation, University of Pretoria, South Africa.
- Browne, N.A.K., 2011. Model evaluation for seasonal forecasting over southern Africa, Doctoral dissertation, University of Cape Town, South Africa.
- Buckle, C., 1996. *Weather and climate in Africa*. Longman. Malaysia. 312pp.

- Buizer, J.L., Foster, J. and Lund, D., 2000. Global impacts and regional actions: Preparing for the 1997–98 El Niño. *B. A. Meteorol Soc*, 81(9), 2121-2140.
- Busuioc, A., Chen, D. and Hellström, C., 2001. Performance of statistical downscaling models in GCM validation and regional climate change estimates: application for Swedish precipitation. *Int J Climatol: J. Royal Meteorol Soc*, 21(5), 557-578.
- Chai, T. and Draxler, R.R., 2014. Root mean square error (RMSE) or mean absolute error (MAE)—Arguments against avoiding RMSE in the literature. *Geoscientific model development*, 7(3), 1247-1250.
- Charney, J.G. and Eliassen, A., 1964. On the growth of the hurricane depression. *Journal of the Atmospheric Sciences*, 21(1), 68-75.
- Chikoore, H. and Jury, M.R., 2010. Intraseasonal variability of satellite-derived rainfall and vegetation over Southern Africa. *Earth Interactions*, 14(3), 1-26.
- Chikoore, H., 2005. Vegetation feedback on the boundary layer climate of South Africa, Masters Dissertation, University of Zululand, South Africa.
- Chikoore, H., 2016. Droughts in Southern Africa: Structure, characteristics and impacts, Doctoral Dissertation, University of Zululand, South Africa.
- Cocke, S., LaRow, T.E. and Shin, D.W., 2007. Seasonal rainfall predictions over the southeast United States using the Florida State University nested regional spectral model. *J Geophys Res: Atmospheres*, 112(D4).
- Collins, W.D., Bitz, C.M., Blackmon, M.L., et al., 2006. The community climate system model version 3 (CCSM3). *J. Climate*, 19(11), 2122-2143.
- Crétat, J., Pohl, B., Richard, Y. et al., 2012. Uncertainties in simulating regional climate of Southern Africa: sensitivity to physical parameterizations using WRF. *Clim dynam*, 38(3-4), 613-634.

- Daron, J.D (2014) "Regional Climate Messages: Southern Africa". Scientific report from the CARIAA Adaptation at Scale in Semi-Arid Regions (ASSAR) Project, December 2014.
- Davis, C.L., 2011. Climate risk and vulnerability: a handbook for Southern Africa. Council for Scientific and Industrial Research, Pretoria, South Africa, 25.
- Donner, L.J., 1993. A cumulus parameterization including mass fluxes, vertical momentum dynamics, and mesoscale effects. *J. Atmos. science*, 50(6), 889-906.
- Donner, L.J., Seman, C.J., Hemler, R.S. and Fan, S., 2001. A cumulus parameterization including mass fluxes, convective vertical velocities, and mesoscale effects: Thermodynamic and hydrological aspects in a general circulation model. *J. Climat*, 14(16), 3444-3463.
- Donner, L.J., Wyman, B.L., Hemler, R.S., et al., 2011. The dynamical core, physical parameterizations, and basic simulation characteristics of the atmospheric component AM3 of the GFDL global coupled model CM3. *J. Climat*, 24(13), 3484-3519.
- Driver, P.M., 2014. Rainfall variability over southern Africa, Doctoral Dissertation, University of Cape Town, South Africa.
- Eaton, B., 2011. User's Guide to the Community Atmosphere Model CAM-5.1
- Gerard, L., 2007. An integrated package for subgrid convection, clouds and precipitation compatible with meso-gamma scales. *Q. J. Royal Meteorol. Soc*, 133(624), 711-730.
- Goswami, B.N., Wheeler, M.C., Gottschalck, J.C. et al., 2011. Intraseasonal variability and forecasting: A review of recent research. In *The global monsoon system: Research and forecast* (pp. 389-407).

- Grabowski, W.W. and Smolarkiewicz, P.K., 1999. CRCP: A cloud resolving convection parameterization for modeling the tropical convecting atmosphere. *Physica D: Nonlinear Phenomena*, 133(1), .171-178.
- Grabowski, W.W., 2001. Coupling cloud processes with the large-scale dynamics using the cloud-resolving convection parameterization (CRCP). *J. Atmos. Sci*, 58(9), 978-99.
- Grabowski, W.W., 2004. An improved framework for super parameterization. *J. Atmos. Sci*, 61(15), 1940-1952.
- Grabowski, W.W., Bechtold, P., Cheng, A., et al., 2006. Daytime convective development over land: A model intercomparison based on LBA observations. *Q. J. Royal Meteorol Soc*, 132(615), 317-344.
- Grabowski, W.W., Yano, J.I. and Moncrieff, M.W., 2000. Cloud resolving modeling of tropical circulations driven by large-scale SST gradients. *Journal of the atmospheric sciences*, 57(13), 2022-2040.
- Guilyardi, E., Wittenberg, A., Fedorov, A., et al., 2009. Understanding El Niño in ocean-atmosphere general circulation models: Progress and challenges. *B. A. Meteorol Soc*, 90(3), 325-340.
- Hansingo, K. and Reason, C.J.C., 2008. Modelling the atmospheric response to SST dipole patterns in the South Indian Ocean with a regional climate model. *Meteorol Atmos Phys* 100: 37-52.
- Harrison, M.S.J., 1984. A generalized classification of South African summer rain-bearing synoptic systems. *J. Climatol*, 4(5), 547-560.
- Hart, N.C., Reason, C.J. and Fauchereau, N., 2013. Cloud bands over southern Africa: seasonality, contribution to rainfall variability and modulation by the MJO. *Climat dynam*, 41(5-6), 1199-1212.

- Hart, N.C., Reason, C.J. and Fauchereau, N., 2013. Cloud bands over southern Africa: seasonality, contribution to rainfall variability and modulation by the MJO. *Clim dynam*, 41(5-6), 1199-1212.
- Hart, N.C.G., Reason, C.J.C. and Fauchereau, N., 2010. Tropical–extratropical interactions over southern Africa: Three cases of heavy summer season rainfall. *Mon Weather Rev*, 138(7), 2608-2623.
- Hernandez, C.A., 2008. The Quasi-Biennial Oscillation's influence on lightning production and deep convection in the tropics. Master's thesis, Texas A (&) M University.
- Hu, Q., 1997. A cumulus parameterization based on a cloud model of intermittently rising thermals. *J Atmos sciences*, 54(18), 2292-2307.
- Huffman, G.J., Adler, R.F., Bolvin, D.T. and Gu, G. 2009. Improving the Global Precipitation Record: GPCP Version 2.1. *Geophys. Res. Lett.*, 36, L17808, doi: 10.1029/2009GL040000.
- IPCC (Intergovernmental Panel on Climate Change). 2007. Climate change 2007: the physical science basis. Contribution of Working Group I to the Fourth Assessment Report of the Intergovernmental Panel on Climate Change, Solomon S, Qin D, Manning M, Chen Z, Marquis M, Averyt KB, Tignor M, Miller HL (eds). CAM-5.1bridge University Press: Cambridge, UK/New York, NY, 996 pp.
- IPCC (Intergovernmental Panel on Climate Change). 2013: Summary for Policymakers. In: Climate Change 2013: The Physical Science Basis. Contribution of Working Group I to the Fifth Assessment Report of the Intergovernmental Panel on Climate Change [Stocker TF, Qin D, Plattner G-K, Tignor M, Allen SK, Boschung J, Nauels A, Xia Y, Bex V, Midgley PM (eds.)]. Cambridge University Press, Cambridge, United Kingdom and New York, NY, USA.
- Jakob Themeßl, M., Gobiet, A. and Leuprecht, A., 2011. Empirical-statistical downscaling and error correction of daily precipitation from regional climate models. *Int J. Climatol*, 31(10), 1530-1544.

- Jan van Oldenborgh, G., Balmaseda, M.A., Ferranti, L., et al. 2005. Evaluation of atmospheric fields from the ECMWF seasonal forecasts over a 15-year period. *Journal of Climate*, 18(16), 3250-3269.
- Johnson, N.C., 2013. How many ENSO flavors can we distinguish? *J. Climate*, 26(13), 4816-4827
- Kain, J.S. and Fritsch, J.M., 1993. Convective parameterization for mesoscale models: The Kain-Fritsch scheme. In *The representation of cumulus convection in numerical models* (pp. 165-170). American Meteorological Society, Boston, MA.
- Kanamitsu, M., Ebisuzaki, W., Woollen, J., et al., 2002. Ncep–doe amip-ii reanalysis (r-2). *Bull Am Meteorol Soc*, 83(11), 1631-1643.
- Kgatuke, M.M., Landman, W.A., Beraki, A. et al., 2008. The internal variability of the RegCM3 over South Africa. *Int J Climatol*, 28(4), 505-520.
- Khairoutdinov, M., Randall, D. and DeMott, C., 2005. Simulations of the atmospheric general circulation using a cloud-resolving model as a super parameterization of physical processes. *J. Atmos. Sci.*, 62(7), 2136-2154.
- Khairoutdinov, M.F. and Randall, D.A., 2001. A cloud resolving model as a cloud parameterization in the NCAR Community Climate System Model: Preliminary results. *Geophys. Res. Lett*, 28(18), 3617-3620.
- Khairoutdinov, M.F. and Randall, D.A., 2003. Cloud resolving modeling of the ARM summer 1997 IOP: Model formulation, results, uncertainties, and sensitivities. *J Atmos Sci*, 60(4), 607-625.
- Khairoutdinov, R.F., Doubova, L.V., Haddon, R.C. et al., 2004. Persistent photoconductivity in chemically modified single-wall carbon nanotubes. *J. Physic Chemistry B*, 108(52), 19976-19981.

- Kiehl, J.T., 1994. Clouds and their effects on the climate system. *Physics Today*, 47, 36-42
- Kim, D., Sperber, K., Stern, W., et al., 2009. Application of MJO simulation diagnostics to climate models. *J Climate*, 22(23), 6413-6436.
- Kooperman, G.J., Pritchard, M.S. and Somerville, R.C., 2014. The response of US summer rainfall to quadrupled CO₂ climate change in conventional and super parameterized versions of the NCAR community atmosphere model. *J. Adv. Modeling Earth Systems*, 6(3), 859-882.
- Kooperman, G.J., Pritchard, M.S., Burt, M.A., et al., 2016. Robust effects of cloud super parameterization on simulated daily rainfall intensity statistics across multiple versions of the Community Earth System Model. *J. Adv. Modeling Earth Systems*, 8(1), 140-165.
- Kruger, A.C. and Shongwe, S., 2004. Temperature trends in South Africa: 1960–2003. *Int. J. Climatol*, 24(15), 1929-1945.
- Landman, W.A. and Beraki, A., 2012. Multi-model forecast skill for mid-summer rainfall over southern Africa. *Int J Climatol*, 32(2), 303-314.
- Landman, W.A., 2014. How the International Research Institute for Climate and Society has contributed towards seasonal climate forecast modelling and operations in South Africa. *Earth Perspectives*, 1(1), p.22.
- Landman, W.A., DeWitt, D., Lee, D.E., et al., 2012b. Seasonal rainfall prediction skill over South Africa: one-versus two-tiered forecasting systems. *Weather and Forecasting*, 27(2), 489-501.
- Landman, W.A., Engelbrecht, F.A., Beraki, A., et al., (2009). Model output statistics applied to multi-model ensemble long-range forecasts over South Africa. *Water Research Commission Report*, (1492/1), p.08.

- Landman, W.A., Kgatuke, M.J., Mbedzi, M., et al., 2009. Performance comparison of some dynamical and empirical downscaling methods for South Africa from a seasonal climate modelling perspective. *Int J Climatol: J Royal Meteorol Soc*, 29(11), 1535-1549.
- Landman, W.A., Mason, S.J., Tyson, P.D. et al., 2001. Retro-active skill of multi-tiered forecasts of summer rainfall over southern Africa. *Int J Climatol*, 21(1), 1-19.
- Lawal, K.A., 2015. Understanding the variability and predictability of seasonal climates over West and Southern Africa using climate models, Doctoral dissertation, University of Cape Town.
- Li, F., Rosa, D., Collins, W.D. and Wehner, M.F., 2012. "Super-parameterization": A better way to simulate regional extreme precipitation? *J Adv Model Earth Syst*, 4(2).
- Lindesay, J.A., Hobbs, J., Lindesay, J. et al., 1998. Present climates of southern Africa. *Climates of the Southern Continents: Present, Past and Future*. Wiley press, Ed. JE Hobbs, JA Lindesay y HA Bridgman, 297.
- Liniger, M.A., Mathis, H., Appenzeller, C. and Doblus-Reyes, F.J., 2007. Realistic greenhouse gas forcing and seasonal forecasts. *Geophys Res Lett*, 34(4).
- Liu, Y. and Ding, Y., 2001. Modified mass flux cumulus parameterization scheme and its simulation experiment. Part I: Mass Flux Scheme and its simulation of the flooding in 1991. *Acta Meteorologica Sinica*, 59, 10-22.
- Lyon, B. and Mason, S.J., 2007. The 1997–98 summer rainfall season in southern Africa. Part I: Observations. *J Climat*, 20(20), 5134-5148.
- Mackellar, N., New, M. and Jack, C., 2014. Observed and modelled trends in rainfall and temperature for South Africa: 1960-2010. *S. Afr. J. Sci.*, 110(7-8), 1-13.
- Mahala, B.K., Nayak, B.K. and Mohanty, P.K., 2015. Impacts of ENSO and IOD on tropical cyclone activity in the Bay of Bengal. *Nat Hazards*, 75(2), 1105-1125.

- Malan, N., Reason, C.J.C. and Loveday, B.R., 2013. Variability in tropical cyclone heat potential over the Southwest Indian Ocean. *J Geophys Res: Oceans*, 118(12), pp.6734-6746.
- Malherbe, J., Engelbrecht, F.A., Landman, W.A. et al., 2012. Tropical systems from the southwest Indian Ocean making landfall over the Limpopo River Basin, southern Africa: a historical perspective. *Intl J Climatol*, 32(7), 1018-1032.
- Manabe, S., Smagorinsky, J. and Strickler, R.F., 1965. Simulated climatology of a general circulation model with a hydrologic cycle. *Mon. Wea. Rev*, 93(12), 769-798.
- Mbokodo, I.L., 2017. *Heat waves in South Africa: Observed variability, structure and trends*
Master's Dissertation, University of Venda, South Africa.
- McCrary, R.R., 2012. Seasonal, synoptic, and intraseasonal variability of the West African monsoon, Doctoral dissertation, Colorado State University. Libraries.
- Moatshe, P.S., 2008. Verification of South African Weather Service operational seasonal forecasts, Doctoral dissertation, University of Pretoria.
- Molekwa, S., 2013. Cut-off lows over South Africa and their contribution to the total rainfall of the Eastern Cape Province, Doctoral dissertation, University of Pretoria.
- Molinari, J. and Dudek, M., 1992. Parameterization of convective precipitation in mesoscale numerical models: A critical review. *Monthly Weather Review*, 120(2), 326-344.
- Morrison, H., 2010, June. An overview of cloud and precipitation microphysics and its parameterization in models. In *WRF Workshop* (pp. 21-25).
- Mulenga, H.M. 1998. Southern African Anomalies, Summer Rainfall and the Angola Low. PhD thesis, University of Cape Town, 231pp.

- Mulenga, H.M., 1999. *Southern African climate anomalies, summer rainfall and the Angola low*, Doctoral dissertation, University of Cape Town.
- Mulenga, H.M., Rouault, M. and Reason, C.J.C., 2003. Dry summers over northeastern South Africa and associated circulation anomalies. *Climat Res*, 25(1), 29-41.
- Mwafhulirwa, N.D., 1999. Climate variability and predictability in tropical southern Africa with a focus on dry spells over Malawi. Doctoral dissertation.
- Neale, R.B., Chen, C.C., Gettelman, A., et al., 2010. Description of the NCAR community atmosphere model (CAM 5.0). NCAR Tech. Note NCAR/TN-486+ STR.
- National oceanic and atmospheric administration (NOAA), n.d. *El Niño theme page*. [Online] Available at: <https://www.pmel.noaa.gov/elnino/schematic-diagrams> [Accessed 04 november 2017].
- New, M., Hewitson, B., Stephenson, D.B., et al., 2006. Evidence of trends in daily climate extremes over southern and West Africa. *J. Geophys. Res: Atmospheres*, 111(D14).
- New, M., Hulme, M. and Jones, P., 2000. Representing twentieth-century space–time climate variability. Part II: Development of 1901–96 monthly grids of terrestrial surface climate. *J. Clim* , 13(13),2217-2238.
- Oliver, M.A. and Webster, R., 1990. Kriging: a method of interpolation for geographical information systems. *Int J Geogr Inf System*, 4(3), 313-332.
- Ooyama, K., 1964. A dynamical model for the study of tropical cyclone development. *Geofisica Internacional (Mexico)*, 4, 187-198.
- Pennell, C. and Reichler, T., 2011. On the effective number of climate models. *J Climat*, 24(9), 2358-2367.

- Phakula, S., 2017. Modelling intra-seasonal rainfall characteristics over South Africa Masters dissertation, University of Pretoria, South Africa.
- Pielke Sr, R.A., Matsui, T., Leoncini, et al., 2006. A new paradigm for parameterizations in numerical weather prediction and other atmospheric models. *National Weather Digest*, 30, 93-99.
- Pohl, B., Fauchereau, N., Reason, C.J.C. et al., 2010. Relationships between the Antarctic Oscillation, the Madden–Julian Oscillation, and ENSO, and consequences for rainfall analysis. *J. Clim*, 23:238-254.
- Pohl, B., Fauchereau, N., Richard, Y., et al 2009. Interactions between synoptic, intraseasonal and inter-annual convective variability over Southern Africa. *Climat Dynam*, 33(7-8), p.1033.
- Pohl, B., Richard, Y. and Fauchereau, N., 2007. Influence of the Madden–Julian oscillation on southern African summer rainfall. *J. Clim*, 20: 4227-4242.
- Randall, D., Khairoutdinov, M., Arakawa, A. et al., 2003. Breaking the cloud parameterization deadlock. *B. A Meteorol Soc*, 84(11), 1547-1564.
- Randall, D.A., 2013. Beyond deadlock. *Geophys. Res. Lett.*, 40(22), 5970-5976.
- Randall, D.A., Xu, K.M., Somerville, R.J. and Iacobellis, S., 1996. Single-column models and cloud ensemble models as links between observations and climate models. *J Climate*, 9(8), 1683-1697.
- Reason, C.J.C. and Jagadheesha, D., 2005. A model investigation of recent ENSO impacts over southern Africa. *Meteorology and Atmospheric Physics*, 89(1-4),181-205.
- Reason, C.J.C. 2001. Subtropical Indian Ocean SST dipole events and southern African rainfall. *Geophys. Res. Lett.*, 28: 11, 2225-2227.

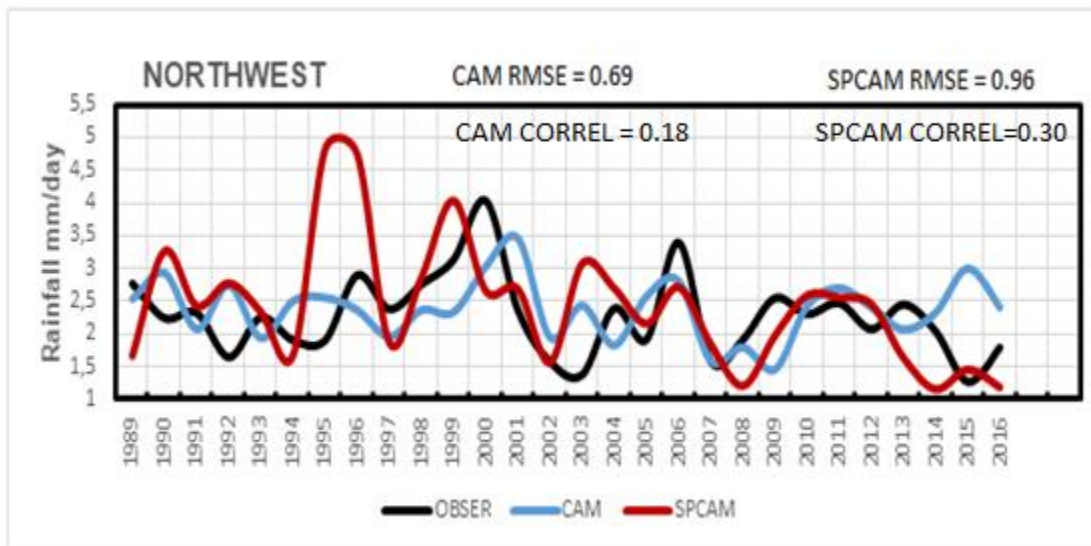
- Reynolds, R.W., Rayner, N.A., Smith, T.M., et al., 2002. An improved in situ and satellite SST analysis for climate. *J Climat*, 15(13), 1609-1625.
- Richard, Y., Fauchereau, N., Pocard, I., et al., 2001. 20th century droughts in southern Africa: spatial and temporal variability, teleconnections with oceanic and atmospheric conditions. *Int J Climatol*, 21(7), 873-885.
- Richard, Y., Trzaska, S., Roucou, P. et al., 2000. Modification of the southern African rainfall variability/ENSO relationship since the late 1960s. *Clim Dyna*, 16: 883-895.
- Rouault, M. and Richard, Y., 2003. Intensity and spatial extension of drought in South Africa at different time scales. *Water SA*, 29(4), 489-500.
- Rouault, M. and Richard, Y., 2005. Intensity and spatial extent of droughts in southern Africa. *Geophys Res Lett*, 32(15).
- Royle, A.G., Clausen, F.L. and Frederiksen, P., 1981. Practical universal kriging and automatic contouring. *Geoprocessing*, 1, 377-394.
- Saltfleetbyweather, 2017. *clouds*. Available at: <http://www.saltfleetbyweather.co.uk/clouds.html>
- Shin, D.W., LaRow, T.E. and Cocke, S., 2003. Convective scheme and resolution impacts on seasonal precipitation forecasts. *Geophysical research letters*, 30(20).
- Singh, A., Delcroix, T. and Cravatte, S., 2011. Contrasting the flavors of El Niño-Southern Oscillation using sea surface salinity observations. *J. Geophys Res: Oceans*, 116(C6).
- Singleton, A.T. and Reason, C.J.C., 2007. *Variability in the characteristics of cut-off low pressure systems over subtropical southern Africa. International Journal of Climatology: A Journal of the Royal Meteorological Society*, 27(3), 295-310.
- Singleton, A.T. and Reason, C.J.C., 2007b. A numerical model study of an intense cutoff low-pressure system over South Africa. *Mon. Weather Rev.*, 135(3), 1128-1150.

- Söhne, N., Chaboureau, J.P. and Guichard, F., 2008. Verification of cloud cover forecast with satellite observation over West Africa. *Mon. Weather Rev*, 136(11), 4421-4434.
- Solomon, S., Qin, D., Manning, M., et al., 2007. Climate change 2007-the physical science basis: Working group I contribution to the fourth assessment report of the IPCC (Vol. 4). Cambridge university press.
- Song, X. and Zhang, G.J., 2011. Microphysics parameterization for convective clouds in a global climate model: Description and single-column model tests. *J. Geophys Res: Atmospheres*, 116(D2).
- Stan, C., Khairoutdinov, M., DeMott, C.A., et al., 2010. An ocean-atmosphere climate simulation with an embedded cloud resolving model. *Geophys. Res. Lett*, 37(1).
- Sylla, M.B., Gaye, A.T., Pal, J.S., Jenkins, G.S. and Bi, X.Q., 2009. High-resolution simulations of West African climate using regional climate model (RegCM3) with different lateral boundary conditions. *Theoretical and Applied Climatology*, 98(3-4), 293-314.
- Tennant, W., 1999. Numerical forecasting of monthly climate in southern Africa. *Int. J. Climatol.*, 19(12), 1319-1336.
- Thayer-Calder, Katherine, and David A. Randall. "The role of convective moistening in the Madden-Julian oscillation." *J. Atmos Sciences* 66, no. 11 (2009): 3297-3312.
- Tiedtke, M., 1993. Representation of clouds in large-scale models. *Monthly Weather Review*, 121(11), 3040-3061.
- Tomczak, M. and Godfrey, J.S., 2003. *Regional Oceanography, an Introduction*, 2nd. Daya, Delhi.
- Tomita, H., Miura, H., Iga, S., Nasuno, T. and Satoh, M., 2005. A global cloud-resolving simulation: Preliminary results from an aqua planet experiment. *Geophys Res Lett*, 32(8).

- Tyson, P.D. and Preston-Whyte, R.A., 2000. Weather and climate of southern Africa. Oxford University Press, 396pp.
- Usman, M.T. and Reason, C.J.C., 2004. Dry spell frequencies and their variability over southern Africa. *Climat Res*, 26(3), 199-211.
- Wang, J. and Kotamarthi, V.R., 2013. Assessment of dynamical downscaling in near-surface fields with different spectral nudging approaches using the nested regional climate model (NRCM). *J. A. Meteorol Climatol*, 52(7), 1576-1591.
- Washington, R. and Preston, A., 2006. Extreme wet years over southern Africa: Role of Indian Ocean sea surface temperatures. *J. Geophys Res. Atmos*, 111(D15).
- Washington, R. and Todd, M., 1999. Tropical–temperate links in southern African and Southwest Indian Ocean satellite-derived daily rainfall. *Int J Climatol*: 19(14), 1601-1616.
- Xu, Y. and Yang, Z.L., 2012. A method to study the impact of climate change on variability of river flow: an example from the Guadalupe River in Texas. *Climatic change*, 113(3-4), pp.965-979.
- Xulu, N.G., 2017. Impact of spatio-temporal variability of the Mascarene High on weather and climate over southern Africa, Masters Dissertation, University of Venda.
- Yu, E., Wang, H., Gao, Y. and Sun, J., 2011. Impacts of cumulus convective parameterization schemes on summer monsoon precipitation simulation over China. *Acta Meteorological Sinica*, 25(5), 581-592.
- Zhang, G.J. and Song, X., 2016. Parameterization of microphysical processes in convective clouds in global climate models. *Meteorological Monographs*, 56, 12-1.

Zhao, S. and Sun, J., 2007. Study on cut-off low-pressure systems with floods over Northeast Asia. *Meteor Atmos Phys*, 96(1-2), 159-180.

Appendix 1



Inter annual variability of rainfall over the North west Province of South Africa from the period of 1987 to 2016.

